

ANODIC OXIDATION OF PHENOLICS FOUND IN
COAL CONVERSION EFFLUENTS

by

MEENAKSHI CHETTIAR

(M.Sc., University of Madras, India 1978)

A THESIS SUBMITTED IN PARTIAL FULFILMENT OF
THE REQUIREMENTS FOR THE DEGREE OF
MASTER OF APPLIED SCIENCE

in

THE FACULTY OF GRADUATE STUDIES
(Chemical Engineering Department)

We accept this thesis as conforming
to the required standard

THE UNIVERSITY OF BRITISH COLUMBIA

December 1981



Meenakshi Chettiar, 1981

In presenting this thesis in partial fulfilment of the requirements for an advanced degree at the University of British Columbia, I agree that the Library shall make it freely available for reference and study. I further agree that permission for extensive copying of this thesis for scholarly purposes may be granted by the head of my department or by his or her representatives. It is understood that copying or publication of this thesis for financial gain shall not be allowed without my written permission.

Department of Chemical Engineering

The University of British Columbia
2075 Wesbrook Place
Vancouver, Canada
V6T 1W5

Date 22nd Dec '81

ABSTRACT

Anodic oxidation of the major phenolics that arise in coal conversion effluents was investigated. Experiments were performed in a packed bed anode of electrodeposited lead dioxide. The phenolics were treated individually in concentrations ranging up to 1 gpl in aqueous solutions in a batch recirculation system. Compounds studied were phenol, O-cresol, p-cresol, 2,3-Xylenol, 3,4-Xylenol, resorcinol and catechol.

The effects of variation in initial concentration and applied current were studied. Solutions were analyzed primarily by gas chromatography and by total organic carbon analyzer. The effect of the oxidation process on the removal of chemical oxygen demand (C.O.D.) and biological oxygen demand (B.O.D.) was determined in a few cases.

Oxidation of the phenolics was favoured by increasing the current density and decreasing the initial concentration. Complete oxidation of the organic carbon in the phenolics was found to be difficult although complete removal of the phenolic compound was achieved in several cases. No direct correlation was found between the rate of anodic oxidation on PbO_2 and the structure of the phenolic compounds. A mixture of five monohydric phenols which were present at concentrations reported as typical for coal conversion wastewaters was also oxidized. Up to 95% oxidation of the phenolics was obtained.

A gas chromatograph/mass spectrometer analyzer was used to examine the products of anodic oxidation in typical runs. Reaction routes were postulated for the oxidation process. Comparisons of the experimental results with a mass transfer model are presented for a few experiments.

TABLE OF CONTENTS

	<u>Page</u>
ABSTRACT	ii
LIST OF TABLES	vi
LIST OF FIGURES	vii
ACKNOWLEDGEMENTS	x
CHAPTER	
1 INTRODUCTION	1
1.1 Phenolics in coal processing effluents	1
1.2 Typical composition of coal conversion wastes	1
1.3 Available methods of treatment of phenolic wastes and interest for this study	3
2 LITERATURE SURVEY	5
2.1 General concepts	5
2.2 Literature review on the electrochemical oxidation of selected phenolics	8
2.2.1 Anodic oxidation of phenol	9
2.2.2 Electrolytic oxidation of cresols	9
2.2.3 Anodic oxidation of Xylenols	12
2.2.4 Anodic oxidation of dihydric phenols	13
2.2.5 Oxidation of phenolic mixtures	14
2.3 Importance of choice of experimental conditions ...	15
2.3.1 Nature of electrode materials	15
2.3.2 Current density-anode potential	16
2.3.3 Nature of the electrolyte	18
2.3.4 Effect of pH	18
2.3.5 Cell configuration	19
3 BASIS AND EXTENT OF EXPERIMENTAL STUDY	21

CHAPTER		Page
4	EXPERIMENTAL APPARATUS AND METHODS	23
4.1	Apparatus	23
4.1.1	Description of equipment	23
4.1.2	Flow diagram of the apparatus	27
4.2	Experimental methods	27
4.2.1	Anodization process	27
4.2.2	Electrochemical oxidation of individual phenolics	30
4.2.3	Experimental modifications made with certain phenolics	31
4.2.4	Anodic oxidation of phenolic mixtures	33
4.3	Analytical techniques	33
4.3.1	Analysis of phenols	33
4.3.2	Total organic carbon analysis	34
4.3.3	Biological oxygen demand analysis	35
4.3.4	Chemical oxygen demand analysis	35
4.3.5	GC/MS Analysis	36
4.3.6	Accuracy and reproducibility	37
5	RESULTS AND DISCUSSION	39
5.1	Oxidation of individual phenolics	39
5.1.1	Anodic oxidation of phenol	39
5.1.2	Oxidation of p-cresol	42
5.1.3	Oxidation of O-cresol	46
5.1.4	Oxidation of 2,3-Xylenol	48
5.1.5	Oxidation of 3,4-Xylenol	52
5.1.6	Oxidation of resorcinol	56
5.1.7	Oxidation of catechol	62
5.2	Comparison of performance of different phenolics ..	66
5.2.1	Effect of variation of initial concentration	66
5.2.2	Effect of variation of applied current	69
5.2.3	Substituent effects	69
5.2.4	Effect of diffusivity	72
5.3	Oxidation of phenolic mixtures	74
5.4	Reaction efficiency for a typical run	79

CHAPTER		<u>Page</u>
	5.5 Cell voltage	80
	5.6 Comparison of experimental results with mathematical models	82
6	CONCLUSIONS	86
7	FURTHER WORK	88
NOMENCLATURE		90
BIBLIOGRAPHY		93
APPENDIX		
1	Specification of auxilliary equipment and materials ...	97
2	Experimental data	105
3	Mathematical model	162
4	Calculations	169
5	Relevant data	176

LIST OF TABLES

<u>TABLE</u>		<u>Page</u>
I	Composition of synthetic coal conversion wastewater	2
II	Comparison of half wave potential values	10
III	Effect of current density and type of electrolyte on C.O.D. removal using PbO ₂ anode	17
IV	Fundamental specifications of the electrolytic cell ...	25
V	Diffusivities of the phenolic compounds in water	73
VI	Results obtained from the oxidation of mixture of monohydric phenols (run 8-3)	78
VII	Variation of ΔV	81

Appendix-2 Experimental data tables for:

Run 1-1 to Run 1-5	Anodic oxidation of phenol	105-111
Run 2-1 to Run 2-5	Anodic oxidation of p-cresol	112-116
Run 3-1 to Run 3-5	Anodic oxidation of O-cresol	117-121
Run 4-1 to Run 4-5	Anodic oxidation of 2,3-Xylenol	122-126
Run 5-1 to Run 5-5	Anodic oxidation of 3,4-Xylenol	127-131
Run 6-1 to Run 6-5	Anodic oxidation of resorcinol	132-136
Run 7-1 to Run 7-5	Anodic oxidation of catechol	137-145
Run 8-1 to Run 8-3	Anodic oxidation of mixture of monohydric phenols of interest	146-151
Run 9-1 to Run 9-8	Anodic oxidation for GC/MS analysis	152

Appendix-3

A-1	Theoretical 2,3-Xylenol fractional conversion vs time for a mass transfer controlled batch system	167
A-2	Theoretical resorcinol fractional conversion vs time for a mass transfer controlled batch system	168

LIST OF FIGURES

FIGURE		<u>Page</u>
1	Components of a simple electrolytic cell	5
2	Side view of the general undivided cell arrangement (N.T.S.) Components of the electrolytic cell	24
3	Experimental set-up for anodic oxidation	26
4	Various components of the cell	26
5	Flow diagram of the apparatus	28
6	Deposition of condensation product during the oxidation of catechol	32
7	Conc. effect on % phenol oxidized at 10 A	40
8	Current effect on % phenol oxidized (1 g/l runs)	40
9	Effect of conc. on rate of oxidation of organic carbon in phenol at 10 A	43
10	Conc. effect on % p-cresol oxidized at 10 A	44
11	Current effect on % p-cresol oxidized (1 g/l runs)	44
12	Effect of conc. on rate of oxidation of organic carbon in p-cresol	45
13	Conc. effect on % o-cresol oxidized at 10 A	47
14	Current effect on % o-cresol oxidized (1 g/l runs)	47
15	Effect of conc. on rate of oxidation of organic carbon in o-cresol	49
16	Conc. effect on % 2,3-Xylenol oxidized at 10 A	50
17	Current effect on 2,3-Xylenol oxidized (1 g/l run)	51
18	Effect of conc. on rate of oxidation of organic carbon in 2,3-Xylenol at 10 A	53
19	Effect of current on rate of oxidation of organic carbon in 2,3-Xylenol (1 g/l runs)	54
20	Conc. effect on % 3,4-Xylenol oxidized at 10 A	55

FIGURE		<u>Page</u>
21	Current effect on % 3,4-Xylenol oxidized (1 g/l runs) ..	55
22	Conc. effect on % resorcinol oxidized at 10 A	58
23	Current effect on % resorcinol oxidized (1 g/l runs) ..	59
24	Effect of conc. on rate of oxidation of organic carbon in resorcinol at 10 A	60
25	Effect of current on rate of oxidation of organic carbon in resorcinol (1 g/l runs)	61
26	Effect of conc. on rate of oxidation of organic carbon in catechol at 10 A	63
27	Effect of current on rate of oxidation of organic carbon in catechol (1 g/l runs)	64
28	Variation of final % oxidized with initial concentration of phenolics at 10 A	67
29	Variation of initial rate with initial concentration at 10 A	68
30	Variation of final % oxidized with applied current (1 g/l runs)	70
31	Variation of initial rate of oxidation with applied current (1 g/l runs)	71
32	Effect of nature of phenolics on % oxidation (10 A, 2 hrs; run 8-1)	75
33	Effect of nature of phenolics on % oxidation (10 A, 3 hrs; run 8-2)	76
34	Effect of nature of phenolics on % oxidation (10 A, 5 hrs; run 8-3)	77
35	GC/MS analysis of final product from phenol oxidation (run 9-1)	154
36	GC/MS analysis of final product from p-cresol oxidation (run 9-3)	155
37	Mass spectrum showing the presence of 4-Hydroxy-4-Methyl-2,5-Cyclohexadiene-1-one	156
38	GC/MS analysis of final product from o-cresol oxidation (run 9-2)	157

FIGURE		<u>Page</u>
39	GC/MS analysis of final product from 2,3-Xylenol oxidation (run 9-4)	158
40	GC/MS analysis of final product from 3,4-Xylenol oxidation (run 9-5)	159
41	MS confirmation of traces of 2,3-Dimethyl hydroquinone or isomer	160
42	GC/MS analysis of final product of oxidation of mixture and Xylenols (run 9-8)	161
<u>Appendix 3</u>		
A-1	Schematic representation of a multiple pass system	162

ACKNOWLEDGEMENTS

I wish to place on record my sincere gratitude to Prof. Paul Watkinson, under whose guidance and encouragement this work was carried out.

My grateful acknowledgement is due to my husband, Mohan Chettiar for his suggestions and thoughtfulness. Thanks are due to our parents for their cooperation, patience and sacrifices.

I would like to express my appreciation for the assistance of Prof. Colin Oloman and for his sincere interest.

Also acknowledged are the staff of the Chemical Engineering department and Environmental Engineering Laboratory for their enthusiastic assistance.

Further thanks are due to Tim Ma for helping with GC/MS analysis, Mrs. Christine Lee for typing the manuscript, Mrs. Bea Kirzsan and my husband for the drafting of figures.

CHAPTER 1

INTRODUCTION

1.1 Phenolics in coal processing effluents

The term "phenols" in waste water includes not only phenol (C_6H_5OH) but an assortment of organic compounds containing one or more hydroxyl groups attached to an aromatic ring.

Phenols have a high pollution potential due to their toxicity. Permissible levels of phenols in industrial wastes have been established by the U.S. Environmental Protection Agency (EPA). These guidelines establish phenol levels of 0.1 mg/l for the Best Practical Control Technology Currently Available for 1977, and 0.02 mg/l for the Best Available Control Technology Economically Achievable for 1983 [1].


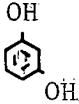
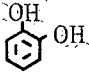
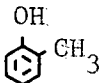
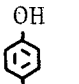
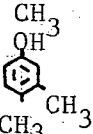
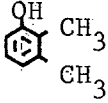


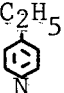
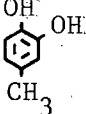
Coal gasification, coal liquefaction and coke oven plants have phenolic-waste problems. It has been reported that 60 to 80 percent of the total organic carbon (TOC) in the organic contaminants from coal conversion systems is phenolic in nature [2].

1.2 Typical composition of coal conversion wastes

Wastewater composition appears to be relatively independent of process technology and coal feed in the case of phenolic constituents [2]. For pollution control studies, it is convenient to define a simulated wastewater which approaches the composition of real coal conversion wastewaters from various processes. Table I provides a typical composition of such a synthetic wastewater [3] as might arise from the condensate (gas

TABLE I *

COMPOSITION OF SYNTHETIC COAL CONVERSION WASTEWATER

COMPOUND	STRUCTURAL FORMULA	CONCENTRATION mg/l
1. Phenol		2000
2. Resorcinol		1000
3. Catechol		1000
4. Acetic Acid	CH_3COOH	400
5. O-Cresol		400
6. P-Cresol		250
7. 3,4-Xylenol		250
8. 2,3-Xylenol		250
9. Pyridine		120
10. Benzoic Acid		100
11. 4-Ethylpyridine		100
12. 4-Methylcatechol		100

* Only the list of compounds present in concentrations of 100 mg/l or above is presented here. The actual composition of the synthetic waste can be found in Appendix 5.

liquor) of a coal gasifier. For example, the Synthane process produces about 0.4 - 0.6 tons of condensate water of this approximate composition per ton of coal gasified [3].

1.3 Available methods of treatment of phenolic wastes and interest for this study

The choice between recovery or destruction of phenolics can be made on the basis of economics. The value of the recovered product should be balanced against both the cost of recovery and the cost of pollution control systems required for the destruction of the chemicals. Recovery is applicable only to concentrations in the percentage range and to flows in excess of about 50 G.P.M. [1]. Although recovery becomes less costly as the concentration increases, recovery processes may produce streams which require effluent treatment.

Treatment processes include incineration techniques, adsorption on activated carbon, various chemical oxidation methods, biological oxidation and ion exchange resin processes. A review of alternative methods of phenol wastewater control [4] and cost comparison between various treatment processes currently being used [5], reveals that biological treatment is the best available choice to degrade these wastes. However, even in an ideal biological environment, many operating problems have been associated. Besides, the ability of this process to produce effluent phenol concentrations of less than 500 ppb on a consistent basis is questionable and hence is not recommended if phenol removal is the primary concern [4]. For example, in a series of test runs with phenol inlet concentrations ranging from 450 to 4800 ppm [3], it was found that as the phenol inlet concentration was increased, a breakthrough point was reached where

additional inlet phenol resulted in a significant increase in the effluent phenol concentration.

New methods for treating phenolic effluents have been attempted [6,7] because of the intensity of the pollution problem and the highly restrictive future pollution control standards expected.

Dephenolization of these effluents by electro-oxidative methods has been attempted [8]. Investigation of the feasibility of anodic oxidation of the major phenolics in Table I is the subject of the present study. The work is restricted to the oxidation of the phenolics present in concentrations equal to or greater than 250 mg/l in the synthetic waste. This research was motivated by the results of previous work [9] that revealed the possibility of essentially complete removal of phenol by electro-oxidation under certain conditions.

CHAPTER 2

LITERATURE SURVEY

2.1 General concepts

An electrochemical reactor is a device in which chemical reactions can be performed directly by the input of electrical energy. The basic components and fundamental operation of an electrochemical process can be visualized from Fig. 1.

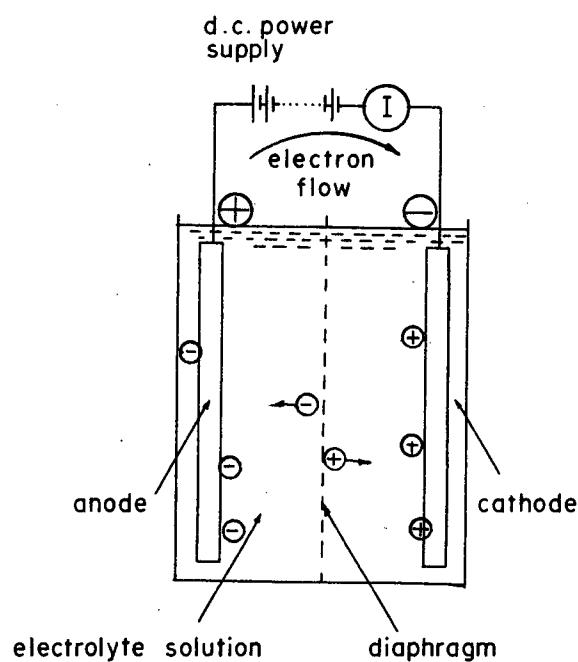


Fig. 1. Components of a simple electrochemical reactor

The anode and cathode are immersed in the electrically conducting electrolyte. The electrodes are connected outside the bath to the terminals of a d.c. power supply. When an emf of sufficient magnitude is applied, electron transfer occurs between the electrodes and the electrolyte. This results in a flow of electricity in the external circuit and chemical reaction at each electrode. In a chemical sense, oxidation occurs at the anode and reduction at the cathode. The diaphragm in its simple form acts as a kind of filter.

Consider a general reversible electrode reaction at equilibrium



O represents the oxidised form and R represents the reduced form of the same substance. In the case, when $r_r = r_o$, there is no net current flow. The rate of the forward reaction, r_r is given by

$$r_r = \frac{i_c}{zF} = k_c C_o$$

where i_c is the partial current density for the cathodic reaction, k_c is the electrochemical rate constant and C_o is the concentration of O at the point of discharge. Similarly,

$$r_o = \frac{i_a}{zF} = k_a C_r$$

where r_o is the rate of oxidation, i_a is the partial current density for the anodic reaction, k_a and C_r are the corresponding electrochemical rate constant and concentration of R respectively.

The current density, i is given by the modulus of the difference between i_c and i_a . The rate constants k_c and k_a can be expressed in terms of the electrode potential [10], by the formulae

$$k_c = k_c^0 \exp \frac{\alpha z F |V^*|}{RT} \quad (2)$$

$$k_a = k_a^0 \exp \frac{(1-\alpha) z F |V^*|}{RT} \quad (3)$$

where k_c^0 and k_a^0 are rate constants referenced to a particular electrode potential under standard conditions and α is a constant known as the charge transfer coefficient. Equations (2) and (3) imply that a fraction of the electrode potential $|V^*|$ drives the forward reaction and the remainder $(1-\alpha)|V^*|$ drives the reverse reaction. As the electrochemical rate constant depends exponentially on the electrode potential as well as the temperature, adjustment of the potential would lead to a wide variation of reaction rate.

The total electrolysing voltage, ΔV which is the sum of V_a^* and V_c^* and the total ohmic drop is easier to measure than the anode potential V_a^* or cathode potential V_c^* . In order to measure V_a^* or V_c^* , a reference electrode has to be connected at the surface of the anode or cathode and the difference in potential between the electrode under consideration and the solution should be measured. The total electrolysing voltage is of importance because the operating cost of the electrolytic process will depend on its power requirement, which is directly related to the voltage drop through the cell at a given current density. Besides, if the potential of the electrode is in the right range, many side reactions such as the anodic formation of oxygen and cathodic formation of hydrogen can occur

in aqueous solutions, resulting in the loss of current efficiency.

The concentration of a reactant A, at the surface of the electrode is related to both the rate of the electrochemical reaction and the rate of mass transfer from the bulk of the solution to the electrode surface,

$$\text{Mass transfer flux} = k_m(C_{A_b} - C_{A_s}) \quad (4)$$

where k_m is the mass transfer-coefficient. For a given species, k_m is a function of the electrode configuration and fluid dynamics. For design purposes, empirical and theoretical expressions for transfer coefficients can be obtained from standard texts [11]. In very dilute systems, it might be expected that the rate of electrochemical reaction is dictated by mass transfer processes. At this limiting current condition, the current efficiency will tend to be low. There must therefore be a practical limit of concentrations below which electrochemical oxidation would become very inefficient. Some coupling of electrochemical and chemical or biochemical processes might be of interest in these situations.

2.2 Literature review on the electrochemical oxidation of selected phenolics

A substantial literature exists in this field. This literature covers a variety of anodes, current densities, electrolytes and other operating conditions. And not unexpectedly, a wide range of oxidation products have been obtained.

The available information concerning the last stages of the anodic oxidation of phenolics to open chain compounds or eventually to carbon dioxide is very limited because most oxidation studies were aimed at

synthesis of compounds and elucidation of the reaction mechanisms rather than at destruction of the organics for waste treatment.

2.2.1 Anodic oxidation of phenol

Early studies of the anodic oxidation of phenol were done by Fichter and co-workers [12-16]. They reported that phenol oxidation at a lead dioxide electrode in sulphuric acid media results in the formation of hydroquinone, p-benzoquinone, catechol, maleic acid, monophenyl ether of pyrocatechol, 2,4' dihydroxy diphenyl and 4,4' dihydroxy diphenyl. The final products obtained were oxalic acid, formic acid, carbon monoxide and carbon dioxide. A few suggestions have been made about the mechanism of the oxidation [12]. In more recent publications [15-20] the presence of diphenyl derivatives has not been reported.

2.2.2 Electrolytic oxidation of cresols

The relative ease of oxidation of various phenolic compounds depends on the substituents present on the ring. The half wave potential value is an indication of the effect of adding different substituent groups to the phenolic ring. The half wave potential, ($E_{1/2}$) is defined as the potential on the polarographic curve when the current is equal to one half the mass transfer limiting current. When electron-donating substituents like OH and alkyl groups are present, the $E_{1/2}$ is shifted towards more negative values and this should be accompanied by an increase in the ease of oxidation. The effect of the substituents is greatest at the ortho and para positions. The $E_{1/2}$ values for the phenols of interest are presented in Table II. Based on the half-wave potential values,


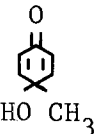

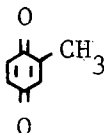
TABLE II
COMPARISON OF HALF WAVE POTENTIAL VALUES

Name of phenolic compound	$E_{1/2}$ volt	Conditions of measurement	Reference
Phenol	0.633	Acetate buffer pH 5.6; graphite electrode	[21]
p-Cresol	0.543	" "	[21]
O-Cresol	0.556	" "	[21]
Catechol	0.139	wax-impregnated graphite anode	[25]
Resorcinol	0.490	" "	[25]
Hydroquinone	0.018	" "	[25]
2,4-Xylenol	0.459	Acetate buffer pH 5.6; graphite electrode	[21]
3,4-Xylenol	0.513	" "	[21]
3,5-Xylenol	0.587	" "	[21]

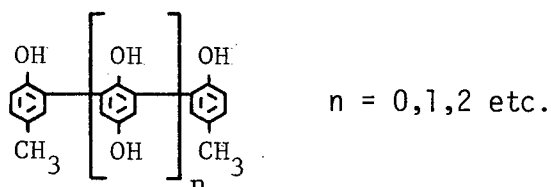
Note: All half-wave potentials are reported with reference to the S.C.E.

p-cresol should be more susceptible to anodic oxidation than phenol [22].

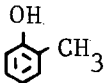
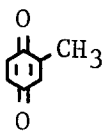
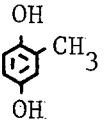
p-cresol oxidation at polished lead electrodes (PLE) in sulphuric acid media in a cell with a diaphragm [23] resulted in the following products detected by n.m.r analysis.

p-cresol		40%
4-Hydroxy-4methylcyclohexa-2,5-dienone		20%
p-Benzoquinone		33%
Methyl-p-benzoquinone		7%

Extraction of the lead anode with hot methylene chloride yielded after evaporating a mixture of coupling products of the type:



Similar electrolysis of o-cresol [23] yielded

o-cresol		12%
Methyl-p-benzoquinone		75%
Methyl hydroquinone		13%

Extraction of the anode with hot methylene chloride yielded tars which n.m.r indicated to be coupling products of 0-cresol.

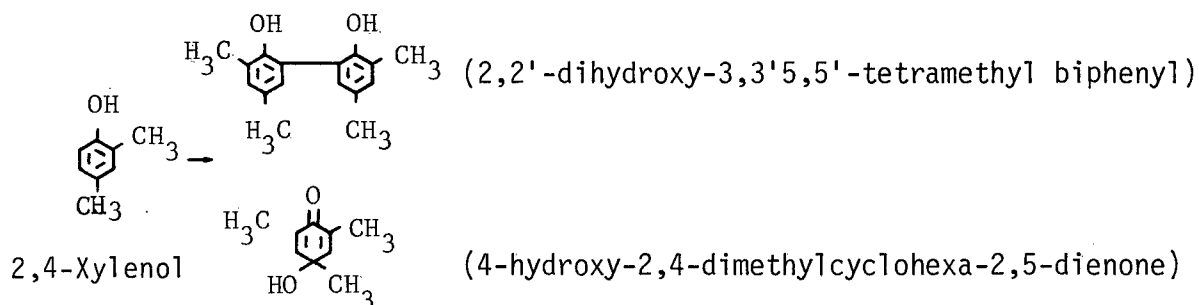
In a study of the effect of anode material, $\text{PbO}_2\text{-C}$ anode (prepared by anodic precipitation of lead dioxide on a carbon rod) is reported to behave in a similar manner to the PLE with respect to the rate of conversion and % yield of certain products. An increase in initial concentration of p-cresol resulted in the production of larger percentages of coupling products on a PLE [23].

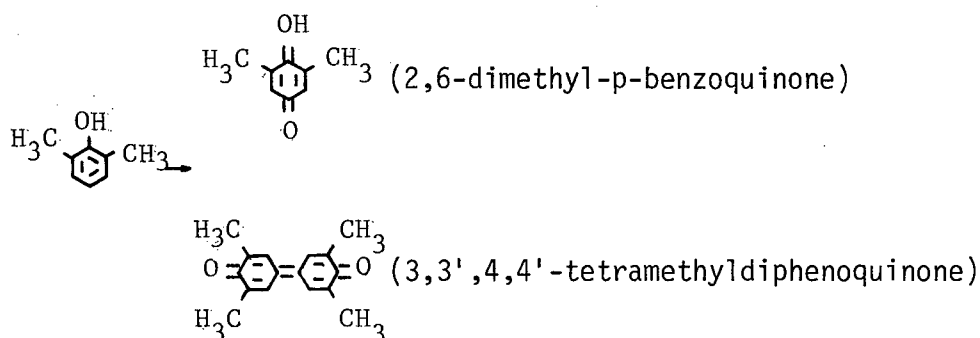
In a comparison of anodic oxidation of cresols [24], p-cresol is reported to have a larger % conversion (96%) than 0-cresol (90%) under similar conditions.

On the basis of cyclic voltammetric studies on a lead dioxide anode [23] it was concluded that the phenol is oxidised chemically by lead dioxide on the anode surface, and the reduced lead species thus formed is oxidised (via direct charge transfer) rapidly back to Pb (IV), as it is part of the anode itself.

2.2.3 Anodic oxidation of Xylenols

Electrooxidation of 2,4-Xylenol and 2,6-Xylenol under conditions reported for the cresols with a PLE has been reported [23]. The following products were obtained from 2,4-Xylenol and 2,6-Xylenol.





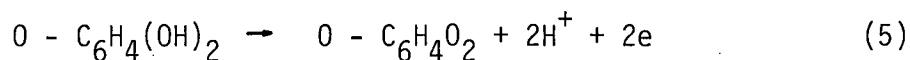
Although 2,3-Xylenol and 3,4-Xylenol are the Xylenols of greatest importance in coal wastewaters, no data are available on anodic oxidation of these compounds. However, corresponding products analogous to the above mentioned ones can be expected.

2.2.4 Anodic oxidation of dihydric phenols

As evidenced by their half-wave potentials [Table II], the dihydric phenols, resorcinol and catechol are easier to oxidise than phenol itself. Nash, Skauen and Purdy [25] report a similar trend in half-wave potential values of dihydric phenols as obtained in reference 26.

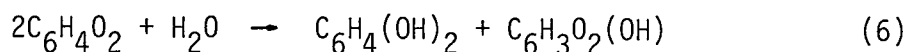
It has been suggested [26] that during the oxidation of resorcinol, radicals are generated which then may polymerize and deposit on the electrode.

The kinetics and mechanism of coulometric oxidation of catechol at controlled potential have been investigated [27]. The oxidation is said to proceed as a two-electron process:



It has been pointed out by several investigators [28,29] that O-benzoquinone in aqueous solutions decomposes giving catechol and

2-hydroxyquinone or 4-hydroxyquinone, the stoichiometric course of which is given by Eq. (6).



The latter product (2-hydroxyquinone or 4-hydroxyquinone) is said to condense rapidly giving a substance of high molecular weight and unknown chemical composition. The reaction is reported [28,29] to be accelerated both by hydroxyl ions and excess amounts of catechol at pH values from 5 to 8. However, at low pH conditions, the catalytic effect of catechol is negligible [27].

2.2.5 Oxidation of phenolic mixtures

A number of electrode reactions are possible when several phenolics are present in the reactant solution or, when different phenols are produced as intermediates during the oxidation. It is of interest to know which electrode reactions are favoured. An analysis of the effect of potential and electrode kinetic parameters on reaction selectivity and on current and rate distribution has been made for plug-flow and back mixed electrochemical reactors [30] in which a sequence of reactions takes place, however application of such an analysis to the present case is a complex mathematical problem.

In an attempt [8] to oxidise a phenol and trichlorophenol mixture it was found that both constituents were attacked at about the same rate. Otherwise there is little information on the oxidation of phenolic mixtures such as those arising in coal conversion effluents.

2.3 Importance of choice of experimental conditions

The factors which determine the rate and product distribution of the anodic oxidation of phenolics at a given temperature and flowrate are as follows.

- (i) nature of anode material
- (ii) current density - anode potential
- (iii) nature of the electrolyte
- (iv) effect of pH
- (v) cell configuration

The effects of these factors are as follows.

2.3.1 Nature of electrode materials

Gladisheva and Lavrenchuk [15] have compared the performance of different anode materials such as nickel, smooth platinum, graphite and electro deposited lead dioxide. Their experiments showed that under the same operating conditions, the highest oxidation rate occurred on the lead dioxide electrode. The lead dioxide anode was found to be superior to others in terms of stability and ease of operation.

The same result was obtained by Fioshin et al [20] when comparing platinum and lead dioxide electrodes in the study of electrochemical oxidation of phenol to quinone. It has been suggested that the adsorptive powers of the electrodes towards the organic substrate plays a major role in addition to the overpotential of the electrodes.

Sucre and Watkinson [31] reported that electrodeposited lead dioxide is a better anode than anodised lead shot in terms of phenol oxidation and corrosion resistance for phenolic waste treatment applications.

A packed bed anode is a good choice for oxidation of dilute phenolic solutions because it provides larger electrode surface areas per unit cell

volume compared to simple flat plate electrode [32]. However, the use of very fine particles which would give large external surface areas might lead to cell blockage in applications where solids are present in the wastewater or are produced by the oxidation. Also spatial electrode potential variations in packed bed cells can be so large that loss of reaction selectivity will result.

Considering the nature of electrodeposited lead dioxide, methods used for the electrodeposition of PbO_2 on inert substrate from electrolytes containing lead have been summarized in reference [33]. Electrodeposited PbO_2 , uniformly coated on a graphite substrate has been recommended [19,31] for this case. These anodes are being commercially made by Pacific Engineering and Production Co. of Nevada.

2.3.2 Current density - anode potential

From a study of the effect of different variables on phenol oxidation, it was concluded that in the range of $50-2000 \text{ A/m}^2$, the current density was the strongest rate determining factor [15]. The results are given in Table III.

From the table it can be seen that, starting with 466 mg/l of chemical oxygen demand (C.O.D.) at a current density of 50 A/m^2 , the final C.O.D. was 420 mg/l after 5 h, whereas at 2000 A/m^2 the C.O.D. dropped to 30 mg/l in 1 hour. Similar effects of current density have been reported elsewhere [31]. Experiments may be performed under a constant anode potential using a potentiostat. But it appears to be much easier to control the current density.

TABLE III
EFFECT OF CURRENT DENSITY AND TYPE OF
ELECTROLYTE ON C.O.D. REMOVAL USING PbO_2 ANODE

Current density A/m^2	Electrolyte	Time of Electrolysis (h)	Final C.O.D. (mg/l of O_2)
50	I	5	307
	II	5	420
500	I	3	90
	II	5	120
1000	I	1	30
	II	2	75
2000	I	0.5	0
	II	1.0	30

Notes: Initial phenol concentration = 200 mg/l
 Initial C.O.D. concentration = 466 mg/l of O_2
 Electrolyte I - 1 g/l NaCl , 1.5 g/l Na_2SO_4
 Electrolyte II - 3 g/l Na_2SO_4

2.3.3 Nature of the electrolyte

Chloride salts have been used as electrolytes in phenolic waste treatment studies [Table III]. This electrolyte gives rise to undesirable chlorination products. As chlorinated phenols are more objectionable than phenol itself, it appears desirable to use an inert supporting electrolyte such as sodium sulphate. From the point of view of reduction in C.O.D., however sodium chloride would be preferable as seen in Table III.

Other electrolytes, such as $\text{Na}_2\text{B}_4\text{O}_7$, NH_3 and H_2SO_4 have also been tested using a packed bed graphite electrode [16].

Sucre [31] showed that the rate of phenol oxidised is unchanged by increasing the conductivity of the electrolyte.

2.3.4 Effect of pH

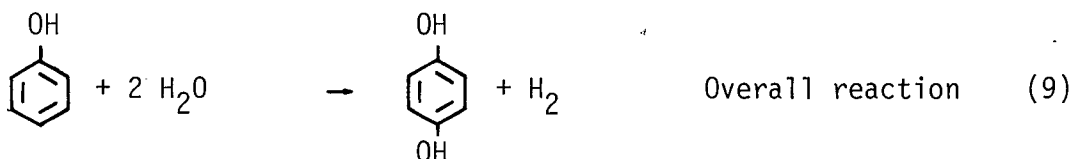
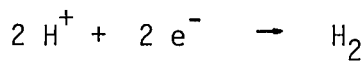
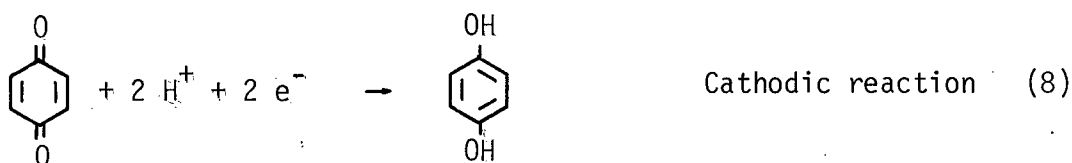
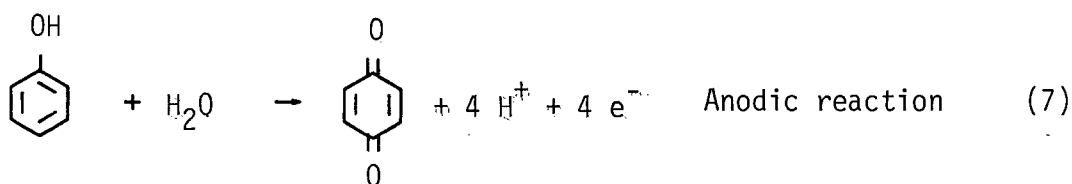
From the relationship between half wave potential and pH for the oxidation of phenol [34] it can be expected that a high pH would make phenol more easily oxidizable.

Due to the ability of phenols to exist in the ionized or unionized form depending on the pH of the solution, pH is believed to play a major role in the mechanism of electron transfer during the oxidation process.

No definitive results could be found in the reviewed literature about the effect of pH on further oxidation of intermediate products. However Sucre and Watkinson [31] report that oxidation of phenol was more rapid under acidic conditions but the oxidation of the total organic carbon was favoured by alkaline conditions.

2.3.5 Cell configuration

In the study of electrochemical oxidation of phenol for hydroquinone production, Covitz [17] reported that the reaction can be controlled to produce hydroquinone at over 90% yield in an undivided cell in acid media. The mechanism proposed for the electrolytic process is as follows [35].



From this reaction scheme, it is obvious that in an undivided cell p-benzoquinone can be reduced at the cathode to produce hydroquinone. If the process is carried out in a divided cell, p-benzoquinone would not contact the cathode and therefore no hydroquinone would be produced.

Another interesting possible reaction in an undivided cell is the oxidation of hydroquinone back to p-benzoquinone, which would compete with the phenol for oxidation at the anode, thus lowering the current efficiency for phenol oxidation. Reference [31] provides valuable information in this connection. Rates of phenol oxidation were reportedly similar

in divided and undivided cells. Even in terms of T.O.C. removal, no improvement was obtained with the divided cell even under optimum pH controlled conditions provided by an anionic membrane. Thus it appears that there would be no particular advantage in choosing divided cell operation.

Due to the lack of available information about the effect of cell configuration factors on the anodic oxidation of other phenolics of interest, these effects have been discussed for phenol (C_6H_5OH) alone. Similar effects may be expected for other phenolics.

CHAPTER 3

BASIS AND EXTENT OF EXPERIMENTAL STUDY

The aim of this work was to study the feasibility of electrochemical oxidation of the major phenolics in coal processing effluents. Experimental studies of the anodic oxidation of phenol, ortho cresol, para cresol, 2,3-Xylenol, 3,4-Xylenol, resorcinol, and catechol are reported. For each of the phenolics, the effect of variation of initial concentration and applied current was studied by recirculating solution from a feed tank through a packed bed cell.

The effects of the above variables are reported in terms of the fractional oxidation of both the phenolics and the total organic carbon (T.O.C.) versus time.

As this work is oriented towards waste treatment, the effects of the oxidation on chemical oxygen demand (C.O.D.) and biological oxygen demand (B.O.D.) have been reported in selected cases. Gas chromatograph/Mass spectrometer analysis was used to identify the products of oxidation and to obtain the percentages of the oxidation products from each of the phenolics studied.

Synthetic mixtures of phenolics of interest made up by mixing the monohydric phenolics in proportions outlined in Table I were oxidized under chosen conditions to study their susceptibility to oxidation in the mixture. The nature and quantities of oxidation products from the mixture are reported.

Comparisons have been made among the various phenolics to correlate their behaviour in response to variations in applied current density and initial concentration. Finally, the data from a few of the experimental

runs have been analyzed by comparison with mathematical models to understand the controlling factors governing the process.

On the basis of a prior study on phenol [31] the following operating conditions were fixed during this work.

Anode	Packed bed of electrodeposited lead dioxide, packing particle size - 0.7-1.1 m.m
Cell configuration	Undivided
Supporting electrolyte	Sodium sulphate, 5g/l + H_2SO_4 [electrical conductivity $8 \times 10^{-3} (\Omega \text{ c.m})^{-1}$]
Operating mode	Batch-recirculation system
pH	2-3
Period of oxidation	2 hours

CHAPTER 4

EXPERIMENTAL APPARATUS AND METHODS

4.1 Apparatus4.1.1 Description of equipment

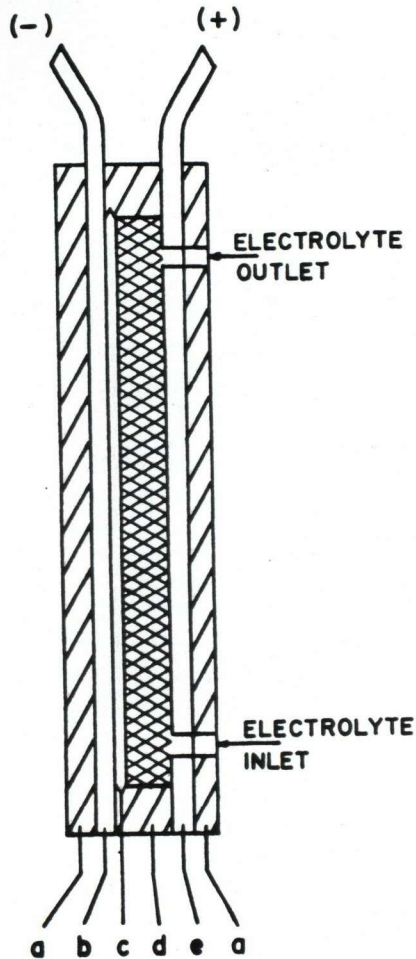
The apparatus of Sucre [31] was retained with relatively minor alterations. The side view of the general divided-cell arrangement is represented in Fig. 2. Basically, the cell consists of two flat plates, the anode and cathode current feeders. The anode current feeder is in contact with the anodic packing, which is contained in a 3 mm thick slotted neoprene gasket separated from the cathode by a saran screen.

The anolyte inlet is located at the bottom of the cell and the outlet is at the top. This facilitates the exit of any gases produced during the electrolysis. A commercial anode consisting of an electrodeposited lead dioxide coating on a graphite plate is used as the anode current feeder. To prevent corrosion and eventual deterioration of the lead dioxide layer, suitable precautions were taken at the point of introduction of the electrolyte through the graphite coated plate. The details of the inlet and outlet connections adapted for this purpose can be obtained from reference [31].

Specifications of the different elements of the cell are provided in Table IV.

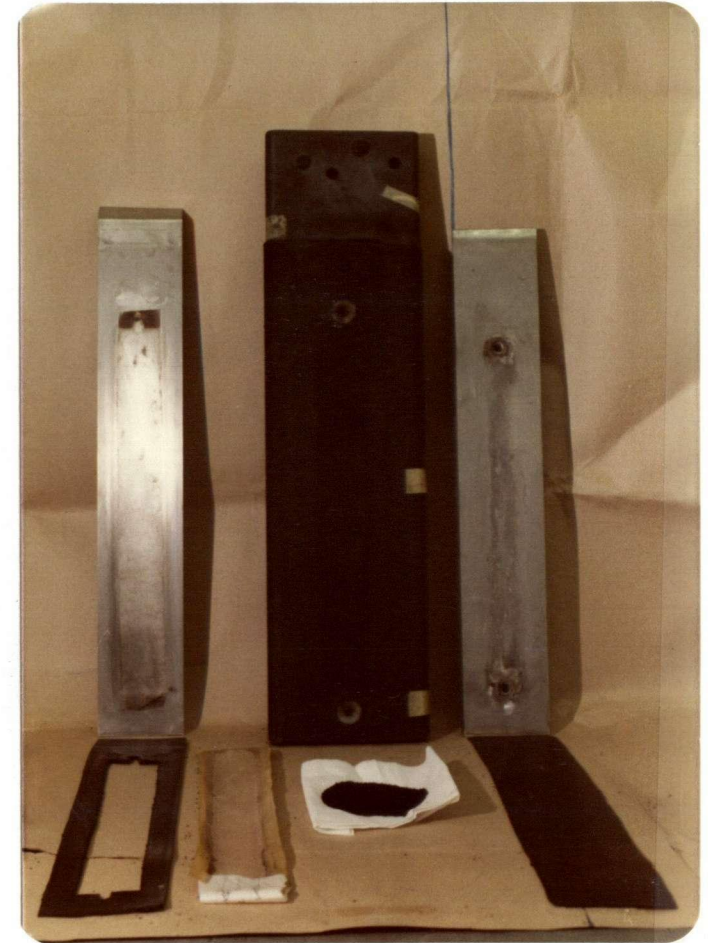
Fig. 3 shows the auxiliary equipment used in the process. The sequence of arrangement of the various layers in the cell displaying the various steps in cell assembly is shown in Fig. 4.

Fig. 2



- a = 1.6 mm THICK NEOPRENE INSULATOR
- b = 1.6 mm THICK CATHODIC FEEDER PLATE (S.S. 316)
- c = SARAN SCREEN TO HOLD ANODIC PACKING
- d = ANODIC PACKING — ELECTRODEPOSITED LEAD DIOXIDE PARTICLES SIZE $0.7 < d_p < 1.1 \text{ mm}$
- e = ANODIC CURRENT FEEDER : LEAD DIOXIDE COATED GRAPHITE PLATE 3 cm THICK

Side view of the general undivided cell arrangement
(N.T.S.)



Components of the electrolytic cell

TABLE IV
FUNDAMENTAL SPECIFICATIONS OF THE
ELECTROLYTIC CELL

Dimensions of the anode and cathode chambers:

Length = 38 cm

Width = 5 cm

Thickness = 3 mm

Anode particles - crushed PEPCON^{*} electrodeposited
PbO₂

particle size - 0.7-1.1 mm

weight - 250 gm

Anode backing plate - PEPCON PbO₂ coated graphite

Protective screen - saran

Cathode - 316 SS plate

* Pacific Engineering and Production Co. of Nevada

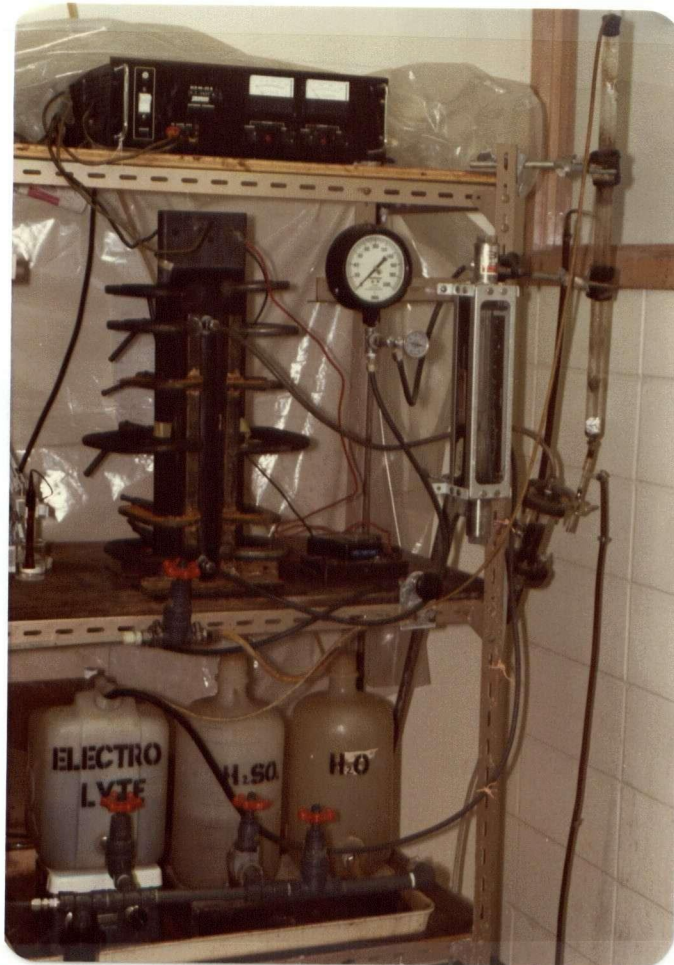


Fig. 3 Experimental set-up for anodic oxidation



Fig. 4 Various components of the cell

4.1.2 Flow diagram of the apparatus

A schematic flow diagram of the equipment is represented in Fig. 5.

Pump PU-1 delivers the electrolyte from tanks T-1, T-2 or T-3 to the cell. the liquid flow rate is controlled by adjusting valve V-4 and is measured with rotameter R-1. Pressure and temperature at the entrance are measured in P-1.

Filter F-1, located at the outlet of the cell is used to collect small particles that might be carried out of the cell and which might damage the flow circuit. This glass wool filter also facilitates the gas liquid separation in GL-1 by agglomerating small gas bubbles produced in the electrolysis.

In GL-1, a bed of glass beads provides extra agglomeration surface for the gas bubbles. If the gas bubbles are carried out with the liquid flow, the progressive accumulation of gas in the electrolyte would affect the results of the experiments. The gas is released at the top of GL-1 and the liquid flows to the heat exchanger, H.E., where the heat generated in the cell is removed by cooling water. From the heat exchanger, the liquid flows back to the feed tanks T-1 or T-2.

The cell was powered by a 1 KVA D.C power supply, P.S. (Appendix 1). The cell current was adjusted with the power-supply meter, and the voltage drop across the electrodes was measured by the voltmeter, V.

4.2 Experimental methods

4.2.1 Anodization process

Before each experiment, the PbO_2 was anodized by electrolysis in 20% H_2SO_4 [36], to minimize changes in activity over time. When the packing

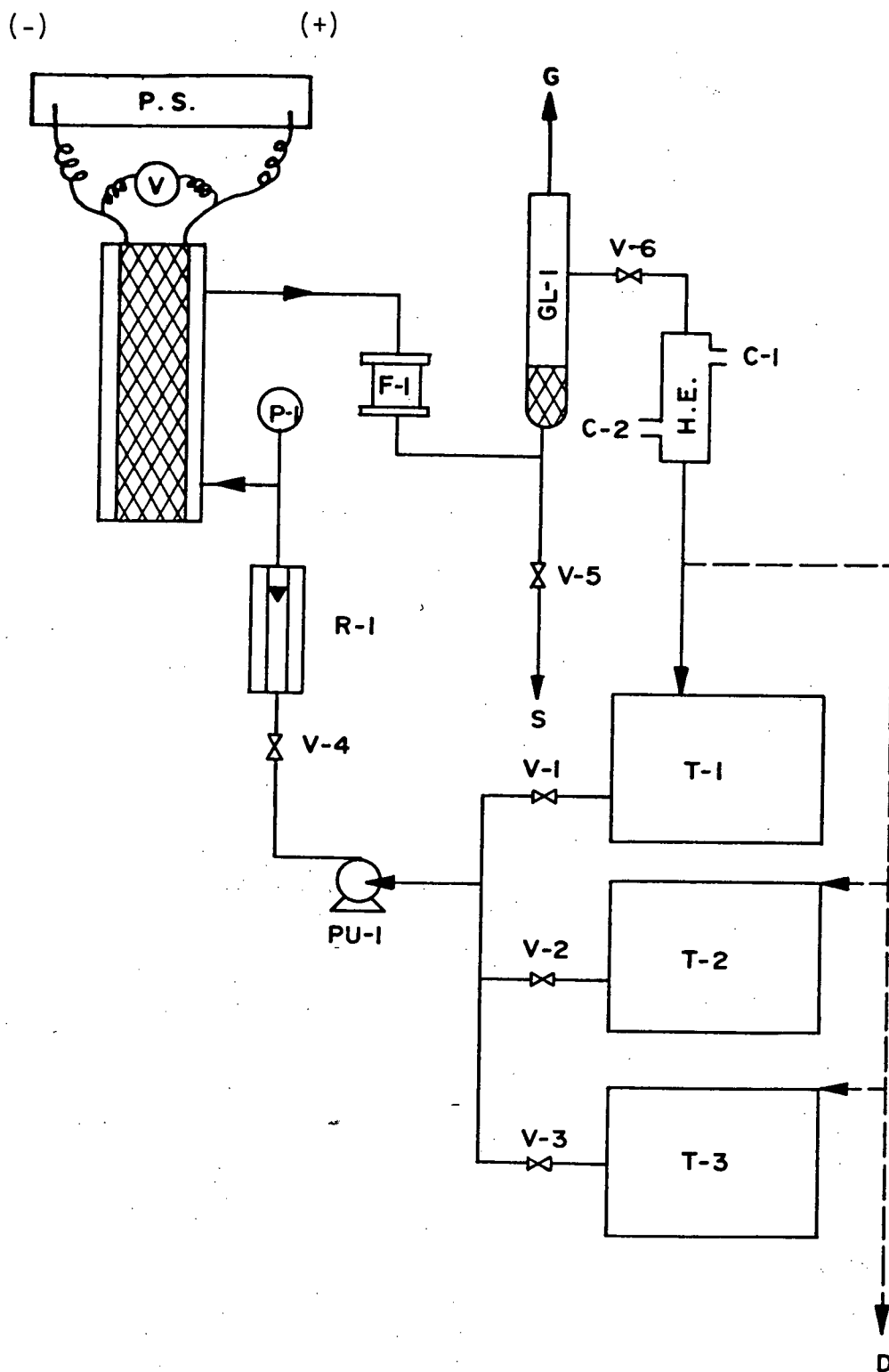


Fig. 5 Flow diagram of the apparatus

Legend for Fig. 5

- (P.S.) - POWER SUPPLY
- (V) - VOLTMETER
- (E.C.) - ELECTROLYTIC CELL
- (T-1) - ELECTROLYTE TANK
(CONTAINS PHENOLICS)
- (T-2) - ANODISATION TANK
- (T-3) - WATER TANK
- (PU-1) - PUMP
- (R-1) - ROTAMETER
- (P-1) - PRESS. & TEMP. GAUGE
- (F-1) - FILTER
- (GL-1) - GAS-LIQ. SEPARATOR
- (V-1) - ELECTROLYTE TANK
SHUT OFF VALVE
- (V-2) - ANODISATION TANK
SHUT OFF VALVE
- (V-3) - WATER TANK
SHUT OFF VALVE
- (V-4) - ELECTROLYTE FLOW
CONTROL VALVE
- (V-5) - LIQUID SAMPLE VALVE
- (V-6) - LIQUID LEVEL CONTROL VALVE
IN GL-1
- (H.E.) - HEAT EXCHANGER
- (C-1) - COOLING WATER INET
- (C-2) - COOLING WATER OUTLET
- (D) - DRAIN

was anodized for the first time, a 12 h anodization time was allowed, but for successive experiments the standard anodization time was 1 h as recommended by Sucre [31]. To carry out the anodization, valves V-1 and V-3 were shut off and tank T-2 was filled with 20% H_2SO_4 . The D.C. power supply was turned on. Valve V-2 was opened and Pump PU-1 was started up simultaneously. The current was adjusted to 10A ($\text{c.d} \approx 526.3 \text{ A/m}^2$). About 2ℓ of solution was drained off through D to purge the system and then recycling to tank T-2 was carried on for 1 h.

After anodization, the pump was shut off and simultaneously V-2 was shut off. Valve V-3 was opened and distilled water from T-3 was pumped through the cell. The cell was washed until the current dropped to practically zero and the potential difference through the cell increased indicating that essentially no electrolyte was contained in the cell.

4.2.2 Electrochemical oxidation of individual phenolics

Before each run, the cell was thoroughly washed in distilled water. In Tank T-1, the electrolyte was prepared by adding a constant quantity (5g/l) of sodium sulphate and sulphuric acid (0.44 g/l). The desired amount of the phenolic compound was then dissolved in distilled water, added to T-1, and the total volume was made up to 8 l. The tank was well agitated by means of a magnetic stirrer. The initial pH of the electrolyte was measured and readjusted if necessary with NaOH or H_2SO_4 . The actual quantities of the phenolic compound added in each of the runs are recorded in Appendix 2.

The valve V-1 was opened and the required flow rate was set by adjusting valve V-4. Immediately the current was set at the desired value.

In order to provide some time for the stabilization of flows and

current, 3 l of the electrolyte was discarded after passing through the cell, rather than recycling it to T-1. The electrolysis time was measured from the moment the electrolyte was recycled to tank T-1. Samples of about thirty ml were withdrawn through V-5 at intervals of 15 min for analytical purposes. The electrolysis was carried on for 2 h. Then the cell was washed with distilled water. In order to avoid the reduction of the PbO_2 anode, the current was on while the washing step proceeded.

4.2.3 Experimental modifications made with certain phenolics

Among the phenolics studied, the p-cresol was insoluble in distilled water. Therefore a few pellets of NaOH were added to obtain the p-cresol solution and a suitable quantity of H_2SO_4 was added to get the desired pH range.

The xlenols were soluble only in hot water ($\sim 50^\circ\text{C}$). Hence the electrolyte was made up to 8 l with hot water. The cooling water to the heat exchanger was carefully lowered during the anodic oxidation of the Xylenols because in the higher concentration runs (1 g/l runs), the Xylenols came out of the solution when the electrolyte was cooled during the run.

With the cresols, 2,3-Xylenol and catechol as there was excessive foaming, the electrolyte began to overflow from GL-1. To avoid the loss of electrolyte, a two-holed rubber stopper provided with an air vent was used to cover GL-1. From the stopper, a tube was connected to T-1, to recycle the overflowing liquid.

During experiments with catechol, in addition to excessive foaming, a brownish black, insoluble condensation product was formed in runs with initial concentrations equal to or greater than 0.5 g/l. This product blocked the glass wool in the filter, decreased the voidage in the packed

bed anode, caused problems in the gas-liquid separator and resulted in small values for maximum attainable flow rates. The saran screen was also blocked as can be seen in Fig. 6. Therefore, the screen had to be changed after the catechol runs. To overcome the problem of excessive foaming and pushing

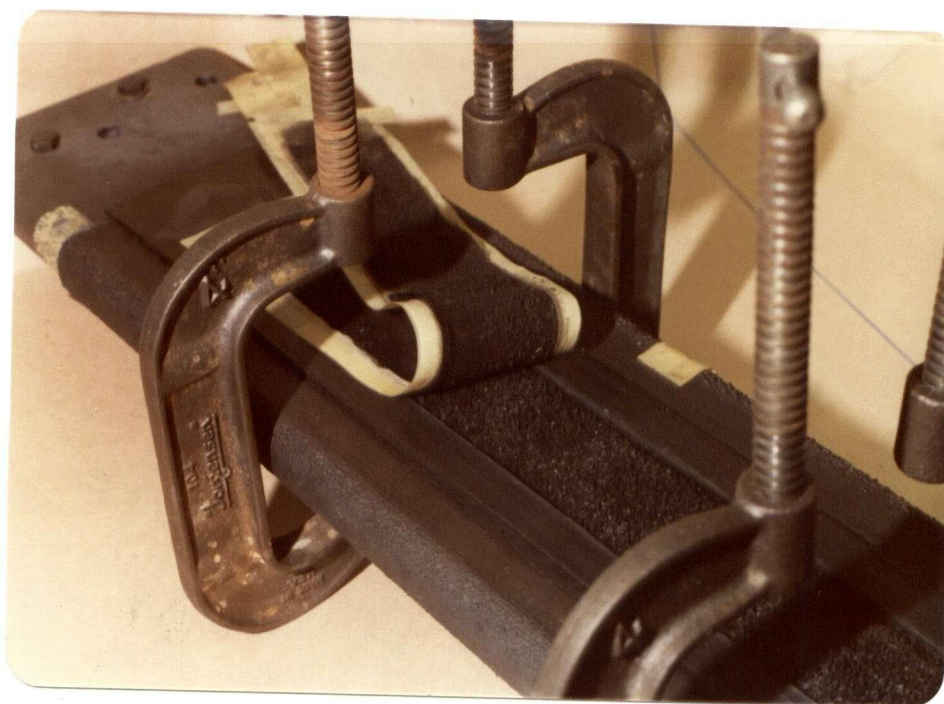


Fig. 6

Deposition of condensation product
during the oxidation of catechol

up of the glass beads from GL-1, glass beads were replaced by glass wool and the inlet and outlet of the electrolyte to GL-1 were interchanged.

4.2.4 Anodic oxidation of phenolic mixtures

Mixtures of phenol, cresols and xylenols were made up by weighing out the phenolics in the same proportions as they are found in synthetic coal conversion wastewaters (Table I) and dissolving them individually in distilled water. Addition of Na_2SO_4 , H_2SO_4 and adjustment of pH were made and all the steps elaborated in 4.2.2 were followed. In these runs, the total electrolysis time alone was varied. For one of these runs (run 8-3), in addition to the analysis of phenols and T.O.C., C.O.D. and B.O.D. analysis were performed on the initial and final sample. Wherever B.O.D. analysis results are reported, 1 ℓ samples were collected, both at the beginning of the run before recycling to T-1 was started and after the electrolysis was complete.

4.3 Analytical techniques

The samples collected were analyzed for phenols, total organic carbon and in some cases C.O.D. and B.O.D. Products of oxidation of typical runs were identified by GC/MS where possible.

4.3.1 Analysis of phenols

Concentration of the phenols was determined by gas chromatography using a flame ionization detector. Different columns were used for monohydric phenols and for dihydric phenols. Equipment specifications and operating conditions are given in Appendix 1.

Fresh standard solutions of the phenols in the desired range were prepared by accurately weighing out the phenols used to prepare the electrolyte for the experiments.

Before the injection of the samples, phenol standards were injected under the same conditions and the calibration curve of peak heights vs. phenol concentration was constructed. As the phenol peaks were narrow, the peak heights rather than peak areas were used directly. In a few cases, peaks of one or two oxidation products were observed. These peaks did not interfere with the analysis of the phenols, and they were not further identified. When mixtures of monohydric phenols were analysed, the column temperature was suitably adjusted to obtain retention times that had reasonable time intervals between the different peaks.

The samples were analysed within a day to avoid degradation [31].

For the analysis of resorcinol [37] the peaks were broad, but uniform. Hence the peak heights were again used. Large errors would be expected in this case at lower concentrations. In all cases, however, standards and samples were injected until the variation in peak heights was only 2-3%.

In the analysis of catechol attempts with the carbowax column used for resorcinol proved to be unsuitable even at conditions of maximum detectability with the flame ionization detector. Hence the catechol concentration could not be determined except in one case where a rough estimate was made. Attempts of methylating^{*} the samples with TMAH (Tri methyl anilinium hydroxide) followed by analysis of the methyl derivative of catechol with the column material OV-17 also proved futile.

4.3.2 Total organic carbon analysis

The total organic carbon analyzer contains two furnaces: one for total

* Catechol in the samples was extracted with ether followed by evaporation of the ether and addition of calculated quantities of the methylating agent.

carbon and one for inorganic carbon. The total carbon furnace operates at a temperature of 1000°C to convert all the carbon present in the sample to carbon dioxide. The inorganic carbon furnace operates at 150°C to convert only the inorganic carbon in the sample to carbon dioxide. The amount of carbon dioxide produced is detected in an infrared analyzer [38].

The total organic carbon (T.O.C.) in the sample is calculated by subtracting the inorganic carbon from the total carbon. Under the pH conditions used, it was found that the concentration and variation of inorganic carbon present in the samples was negligible. Hence in all cases only the total carbon has been reported as T.O.C.

The calibration procedure was similar to that used in gas chromatography. Variation in peak height in successive injection of a certain sample was <2%. For T.O.C. analysis, it was possible to use the same standards used in the analysis of the phenols knowing the fraction of organic carbon present in 1 g of the phenol. Specification and operating conditions of the T.O.C. analyzer are also given in Appendix 1.

4.3.3 Biological oxygen demand analysis

In cases where the biological oxygen demand (B.O.D.) is reported the analysis was performed by Wood Laboratory Ltd. The seed bacteria for B.O.D. analysis were grown by an enrichment process using B.O.D. water supplemented with phenolics.

4.3.4 Chemical oxygen demand analysis

The chemical oxygen demand (C.O.D.) determination provides a measure of the oxygen equivalent of that portion of the organic matter in a sample

that is susceptible to oxidation by a strong chemical oxidant [38]. Where the effluent contains only readily available organic bacterial food and no toxic matter, the C.O.D. value can be used to approximate the ultimate carbonaceous B.O.D. values.

C.O.D. was determined by the dichromate reflux method outlined in reference [39]. The test was repeated for each sample to test the reproducibility. The calculations are presented in Appendix 4.

4.3.5 GC/MS analysis

A Hewlett-Packard gas chromatograph/mass spectrometer combination equipped with a fully interactive data system (HP-1000 series computer) was used to analyse the composition and nature of the final sample from a few of the typical oxidation runs. For this purpose one run was performed with each of the phenolics studied at a current density of 526.3 A/m^{-2} , for 2 hrs with an initial concentration of 1g/l (Appendix 2). One similar run was performed with a mixture of monohydric phenols of composition similar to that used in run 8-3. The final sample from all of the above runs were given for the GC/MS analysis. This analysis was performed by Mr. Tim Ma. The results are reported in Appendix 2. The operating conditions and equipment specifications can be found in Appendix 1.

All the products were identified with standard data obtained for the compounds in the mass spectrometer. In cases where the possibility of two isomers has been reported, the mass spectrometer data was insufficient to distinguish between them. An example for such a case has been enclosed (Appendix 2).

The samples for the analysis were prepared by the following procedure. 10 ml samples of the final samples were individually extracted twice with

50 ml of methylene chloride. The organic phase was separated, dried with anhydrous MgSO_4 and evaporated in a rotary evaporator. The residue was dissolved in 10 ml of methylene chloride and given for GC/MS analysis.

In the case of resorcinol and catechol no products were detected. For catechol the clear layer and the suspended black product were separately extracted with methylene chloride. However in these cases the extraction in to the methylene chloride phase was inefficient. With the available column, the solvent choice was limited, and therefore other solvents were not tried. An alternative attempt was made with a solid probe in order to introduce the sample directly in to the mass spectrometer. No definite identifications were made in this attempt.

4.3.6 Accuracy and reproducibility

Care was taken to maintain accuracy in all the analyses. The reproducibility of results was checked. For the analysis of the phenolics and T.O.C., injections were repeated until the variations in peak heights were within 3%.

Reproducibility of the oxidation process was tested and found to be good. For example in repeated runs of phenol and resorcinol oxidation at 10 A with an initial concentration of 1 g/l, the following results were obtained after 2 hours of oxidation.

Name of Compound	% oxidised	
	Trial I	Trial II
phenol	89.6	89.2
resorcinol	71.6	68.2

The results obtained with a few of the phenol runs were compared with the corresponding results obtained by Sucre [31]. As seen below, there is a reasonable agreement.

% oxidation after 60 mins, working at 10 A with initial phenol concentration of 0.1 gm/l	Source	
	Ref [31]	Present study
	98 (Run 3-3)	100 (Run 1-4)
% oxidation after 120 mins, working at 10 A with initial phenol concentration of 1 gm/l	100 (Run 3-31)	89.6 (Run 1-1)

CHAPTER 5

RESULTS AND DISCUSSION

5.1 Oxidation of individual phenolics5.1.1 Anodic oxidation of phenol

A typical plot of results of the recirculating batch oxidation runs is shown in Fig. 7 where % phenol oxidized is plotted versus time for three different values of initial phenol concentration. As the initial phenol concentration was increased from 108 mg/l to 683 mg/l and to 910 mg/l, the % phenol oxidized after 30 minutes decreased from 88.9% to 55.3% to 30.2% although the absolute amount of phenol oxidized in a given time generally increased. However, in run 1-5, the % phenol oxidized levelled off after 1 hour. When the cell was opened, the cathode surface was found to be covered with a deposit of yellow tar-like material. This tar must have been formed primarily by the oligomerization and polymerization of p-benzoquinone and by its reaction with the phenolic compounds present. Tar formation has been encountered in literature [17,19] and an attempt to overcome this problem has been reported [19].

Fig. 8 shows the effect of increasing the applied current at a constant initial concentration of phenol. The effect of increasing the current is to raise the initial rate of phenol oxidation as shown by the slopes of the curves at the beginning of the runs. However, the initial rate is not proportional to the current since there is a larger increase in rate as the current is increased from 5A to 10A than from 10A to 15A. A possible reason for this is that with increasing currents more hydro-

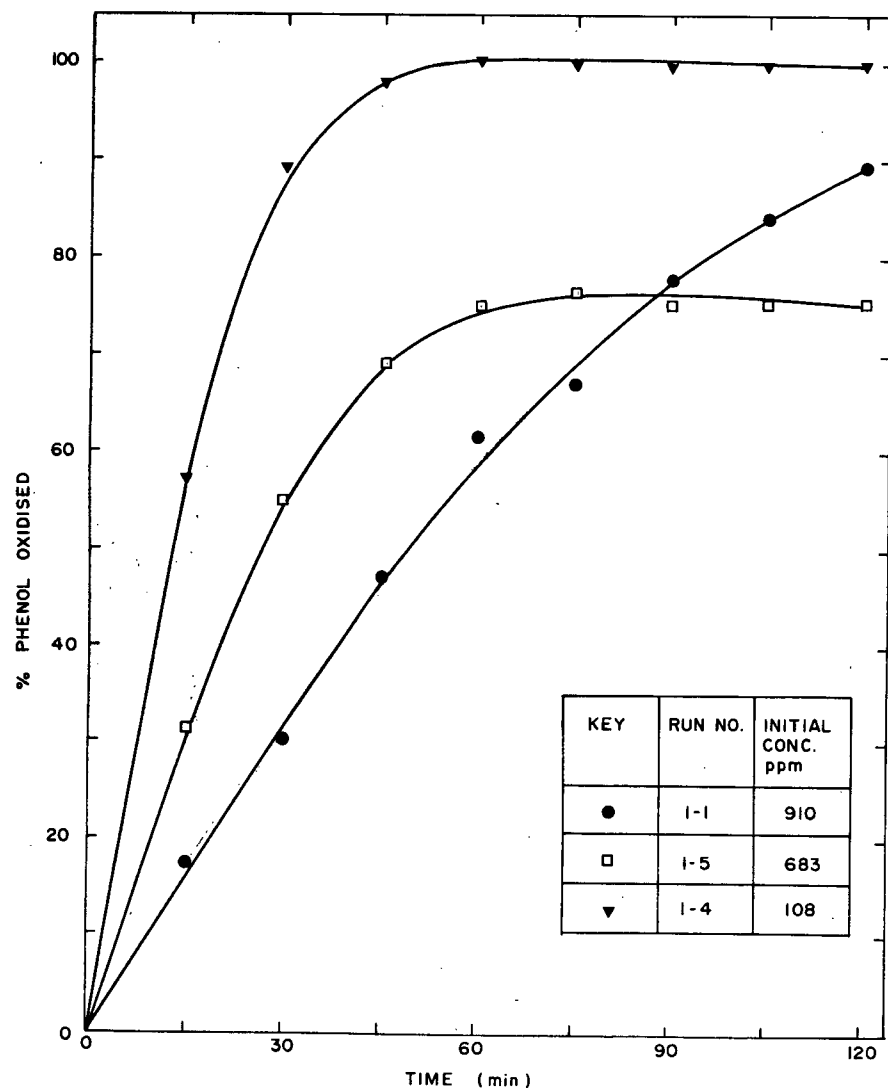


Fig. 7 Conc. effect on % phenol oxidized at 10 A.

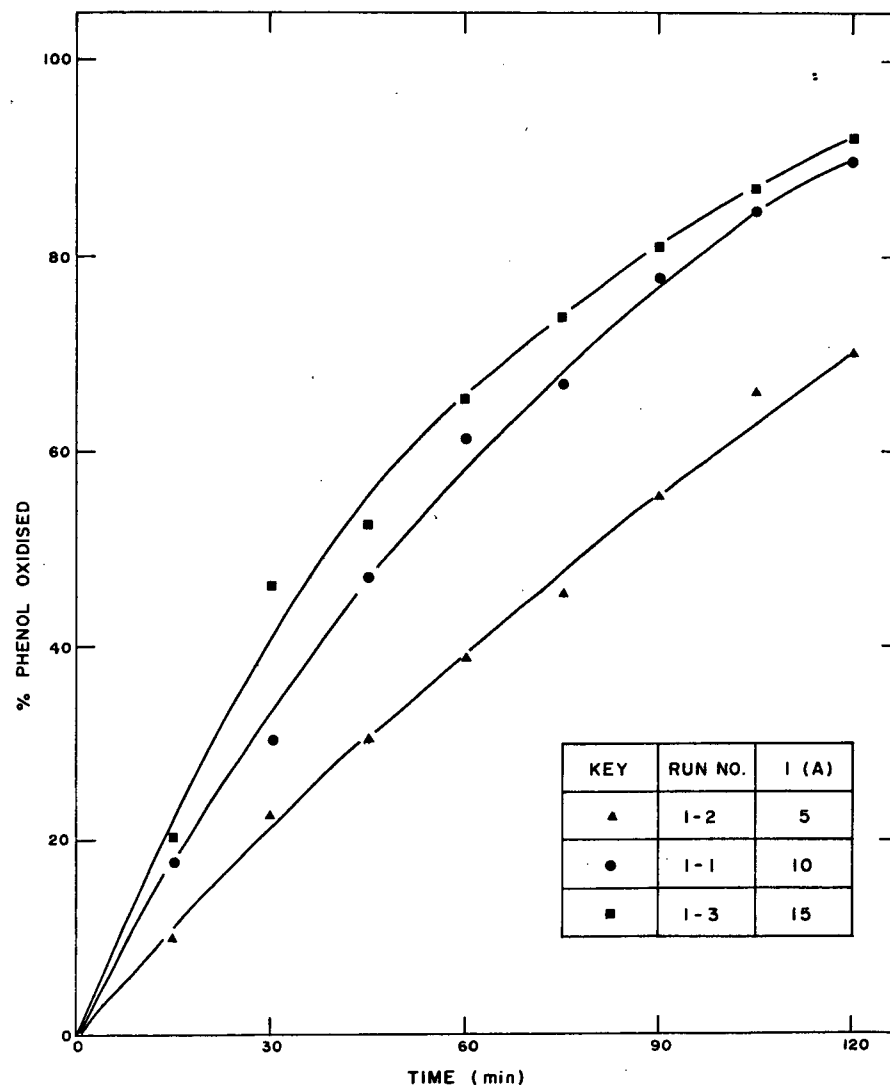
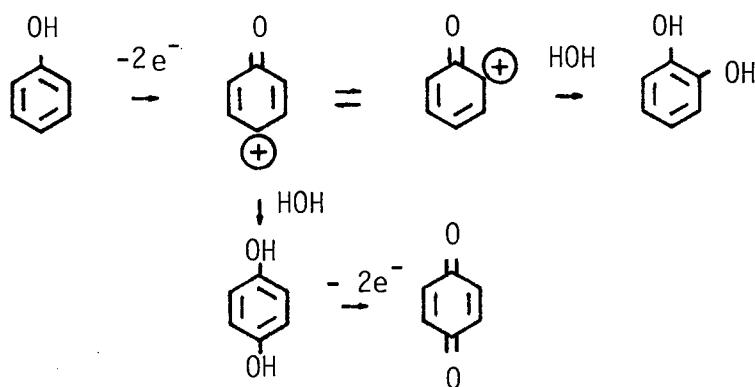


Fig. 8 Current effect on % phenol oxidized (1 g/l runs)

quinone is produced and its oxidation to p-benzoquinone may carry increasing fractions of the current. Stated in another way, the current efficiency for phenol oxidation falls off with increasing applied current and the production of p-benzoquinone probably increases. This postulate is perhaps supported by the observation that the intensity of the yellow colouration and smell due to p-benzoquinone appeared to increase in the treated solution as the applied current was increased.

The GC/MS analysis of the treated phenol solution however showed only (Appendix 2) the following constituents: unreacted phenol 12.6%, p-benzoquinone 69.5%, catechol 7% and hydroquinone 10.9%. No coupling products (dimers) were detected. The absence of such products rules out the radical mechanism for the reaction [40].

Based on the products obtained, the following reaction scheme is proposed. The first step is the formation of "phenoxonium ion" by electrophilic attack of the aromatic nucleus, followed by the formation of catechol or hydroquinone. Hydroquinone gets oxidized further by the loss of 2 electrons to form p-benzoquinone. The fact that 6 times more p-benzoquinone than hydroquinone is formed shows that under present conditions the oxidation of hydroquinone to p-benzoquinone is favoured. The cathodic reduction of p-benzoquinone is not as important. An explanation for this is presented in Section 5.4.



During the anodic oxidation of phenol under conditions chosen for the study, it is obvious that phenol goes through various oxidation states and results partly in the formation of carbon dioxide. As seen from Fig. 9, the actual quantity of phenol oxidized completely to carbon dioxide is about 22% and 18% in runs 1-4 and 1-5 respectively. [It should be noted that whenever % T.O.C. oxidized has not been reported, the net change in T.O.C. was practically undetectable due to the high concentration of carbon present in solutions].

5.1.2 Oxidation of p-cresol

Effects of variation of concentration and current shown in Fig. 10 and 11 are found to be similar to those observed in the case of phenol. However at every stage, the % p-cresol oxidized is lower than that observed with phenol itself. A similar result is observed in % total organic carbon (Fig. 12) oxidized. These trends are contrary to expectations based on the half-wave potential values. This might be either due to the unreactive nature of p-cresol under the conditions of present work or due to the retarding influence of the cathodic reduction of the oxidized product resulting in regeneration of p-cresol. In the GC/MS analysis a larger percentage (84.2) of unoxidized p-cresol was identified in comparison to the oxidation product (15.8). Besides the expected oxidation product, 4-hydroxy-4-methyl-cyclohexa-2,5, diene-1-one (which has been confirmed from the mass spectrum), no other oxidation product such as methyl-p-benzoquinone has been identified. Hence the required ideal conditions of time, potential or electrode activity for the complete anodic oxidation of p-cresol were not provided in this study.

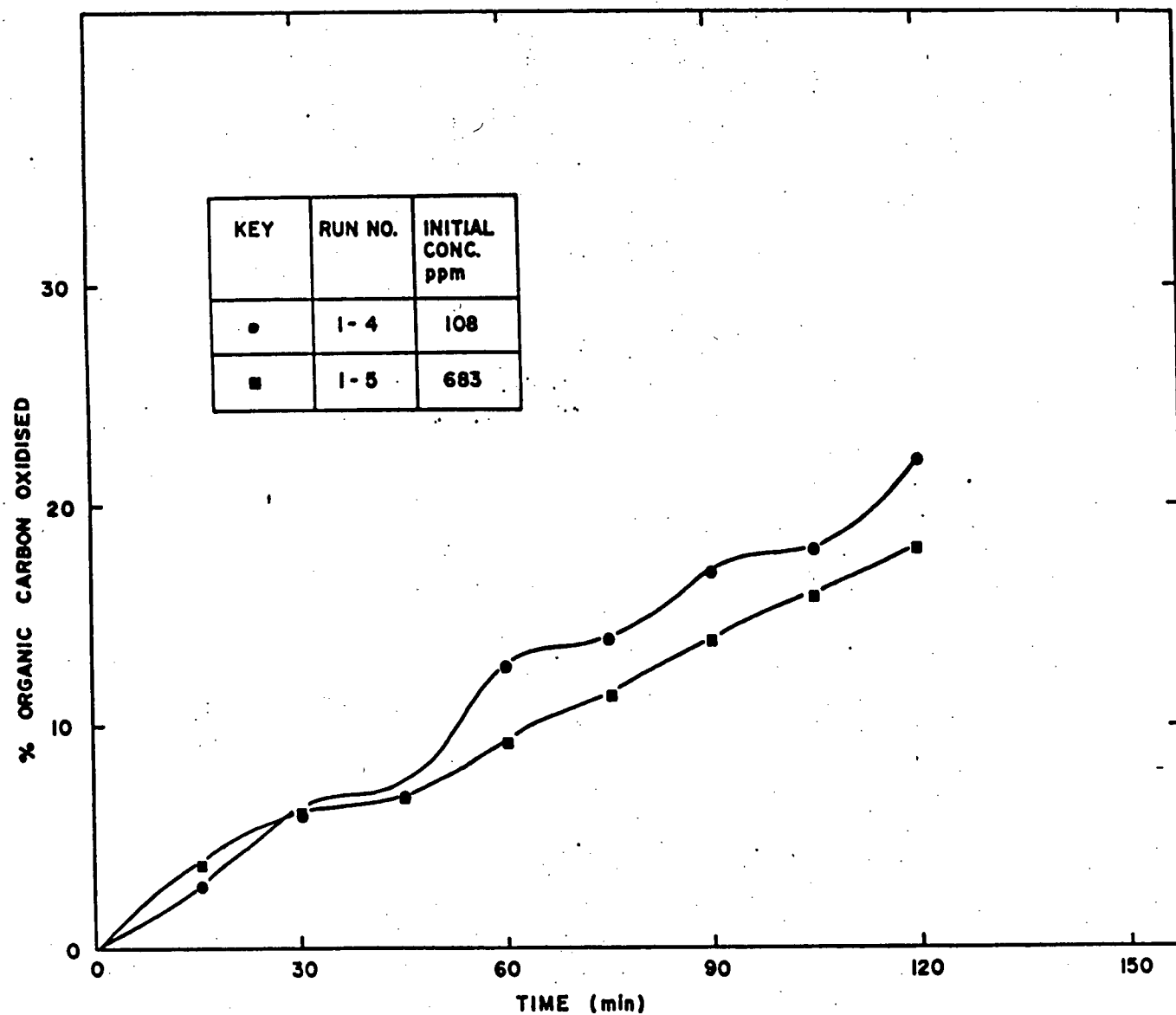


Fig. 9 Effect of conc. on rate of oxidation of organic carbon in phenol at 10 A.

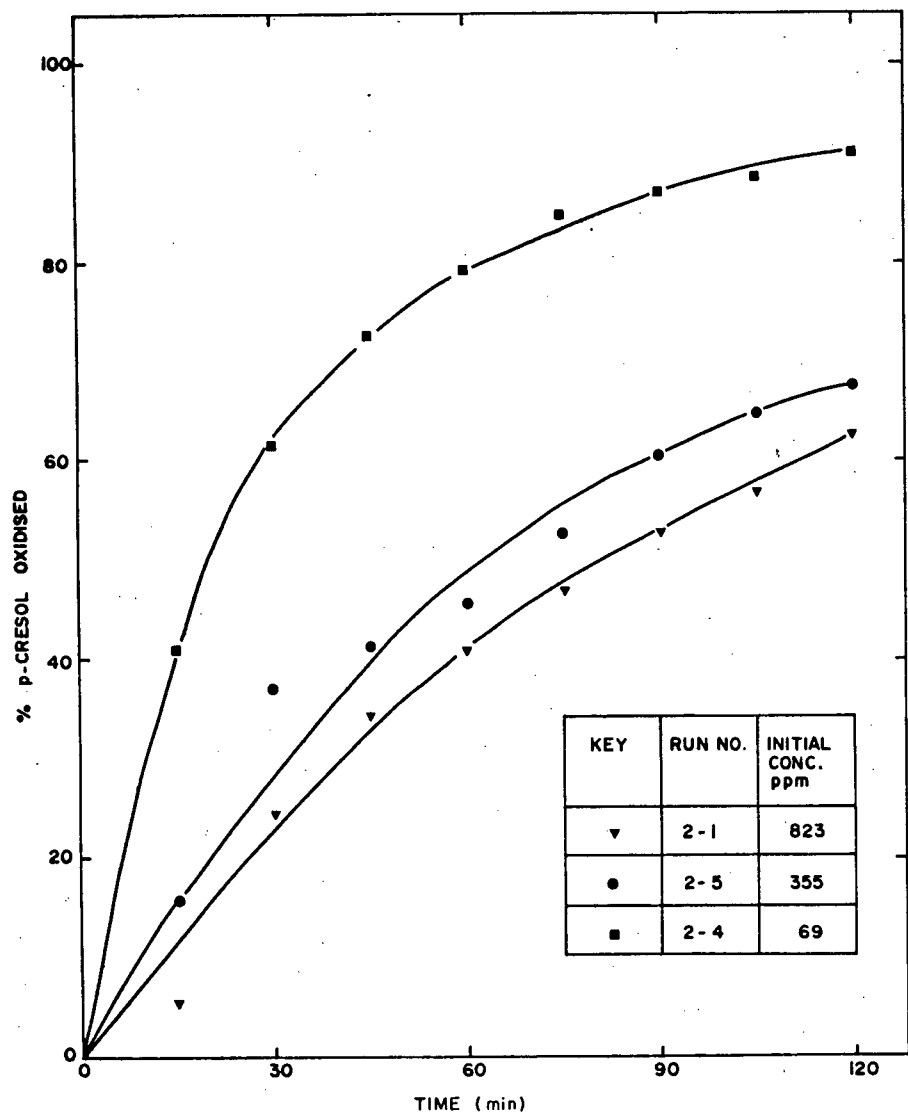


Fig. 10 Conc. effect on % p-cresol oxidized at 10 A

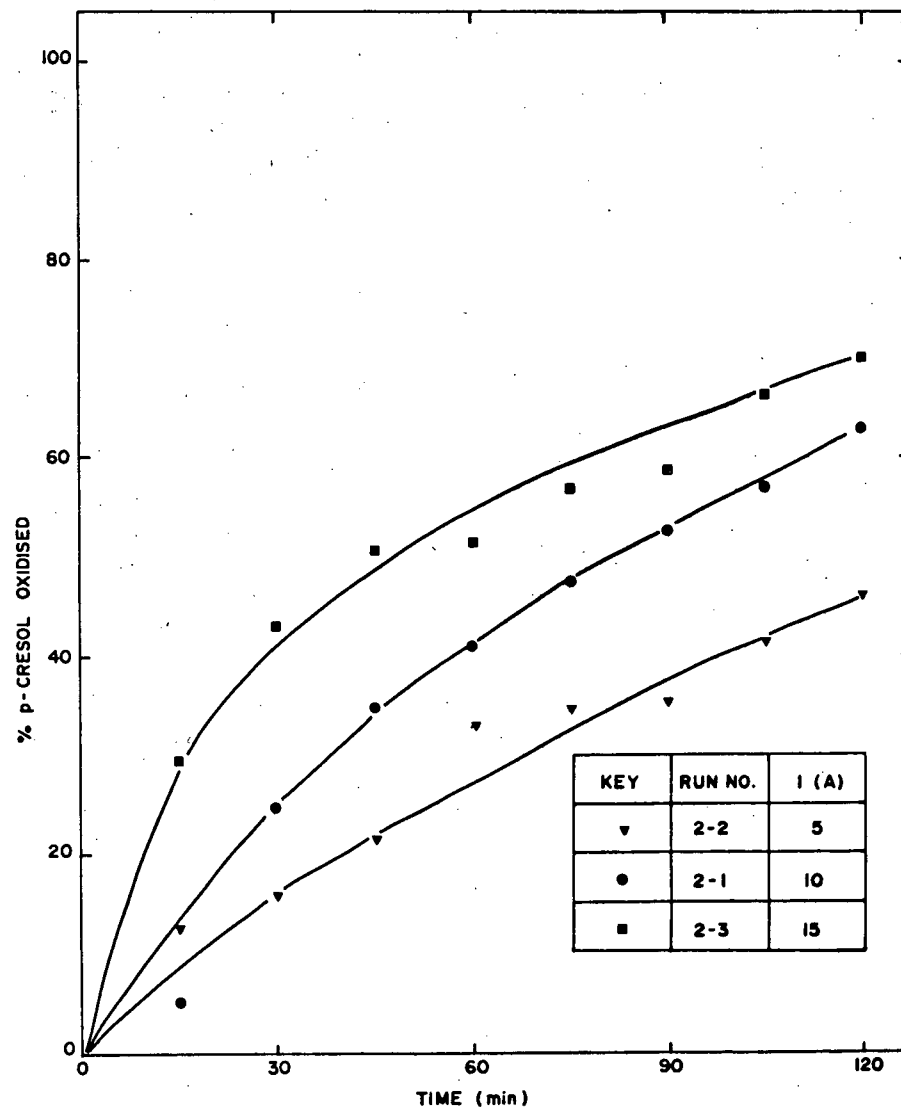


Fig. 11. Current effect on % p-cresol oxidized (1 g/l runs)

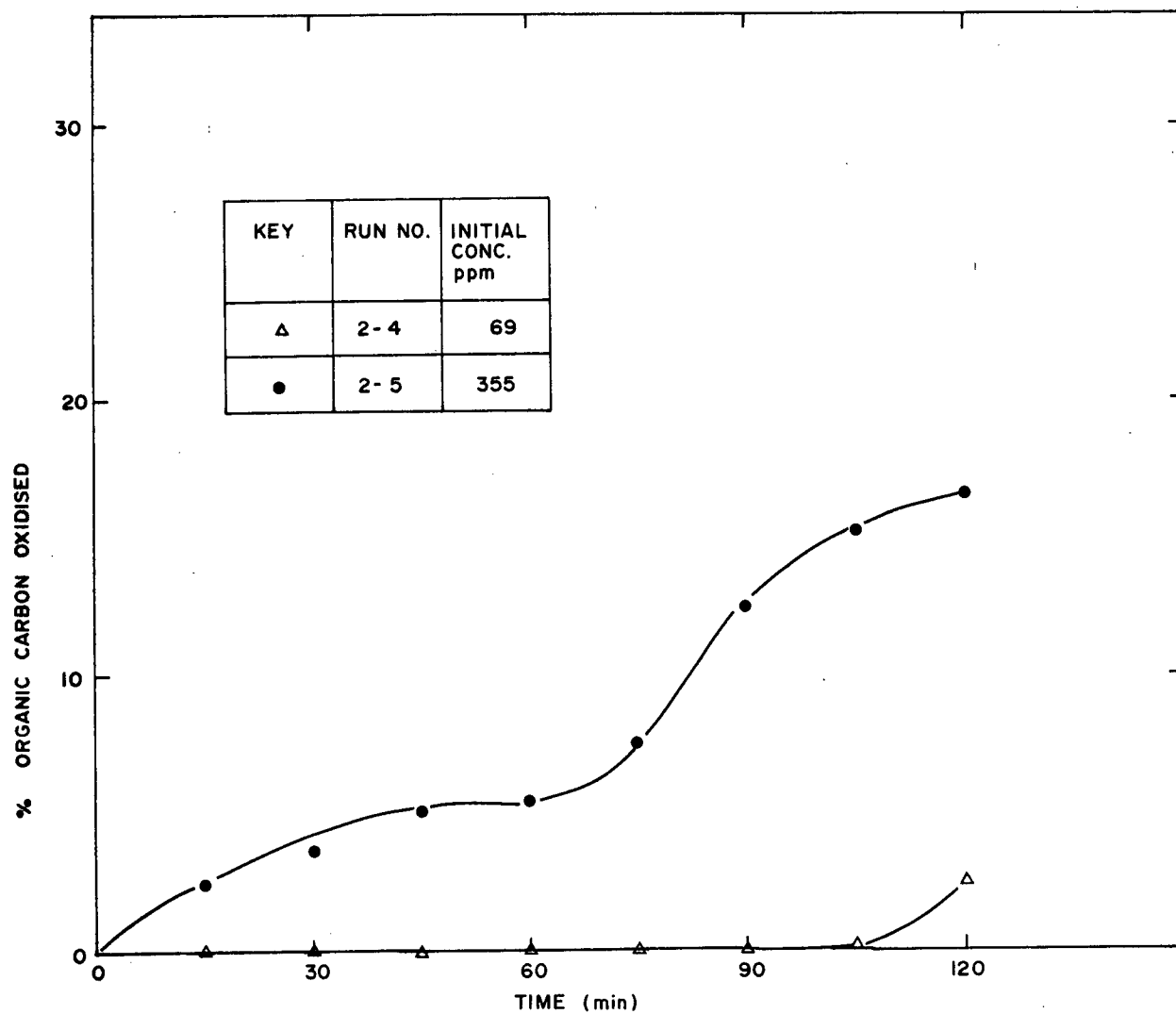


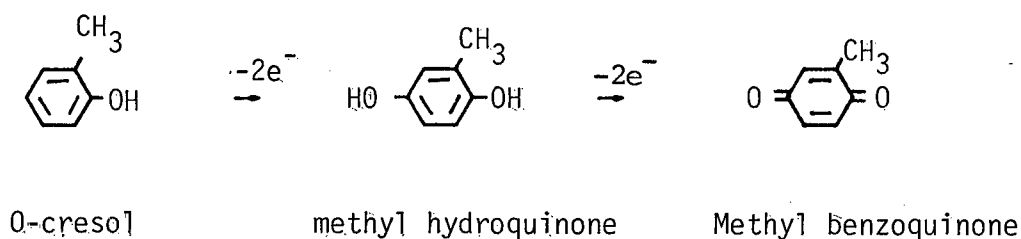
Fig. 12 Effect of conc. on rate of oxidation of organic carbon in p-cresol.

5.1.3 Oxidation of 0-cresol

In the study of the effect of initial concentration on the oxidation of 0-cresol (Fig. 13) it is observed that in run 3-4, the rate levels off after 96.8% oxidation showing the expected retarding influence due to a more favoured competitive reaction. This reaction is probably oxygen evolution.

In Fig. 14, where the initial concentration is about 1 gpl of 0-cresol, the percent oxidized is essentially linearly dependent on time. In addition, the % oxidation/unit time increases with applied current in a near linear manner unlike the trend observed with phenol and p-cresol. Products reported in the literature [23] (see Chapter 2) are detected in similar proportions in the present work, viz. 69.8% methyl benzoquinone 19.0% methyl hydroquinone and 11.3% starting compound, 0-cresol. Observation of intense yellow colouration is supported by the large concentration of methyl benzoquinone observed in the treated solution.

The anodic oxidation path appears to be similar to that reported for phenol by the formation of "phenoxonium ion". The formation of the reported products would be as follows:



No tar or coupling products formation was observed with 0-cresol.

As methyl benzoquinone, the main product of anodic oxidation has

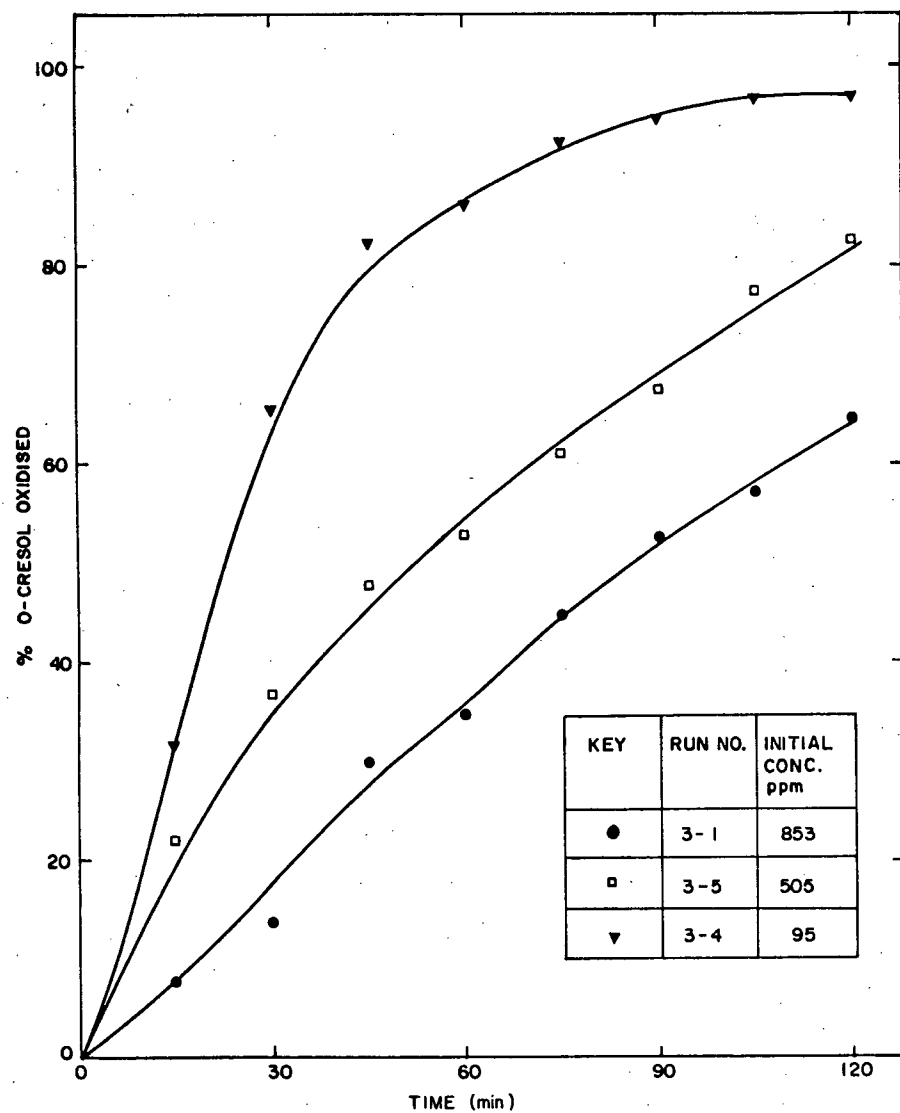


Fig. 13 Conc. effect on % o-cresol oxidized at 10 A

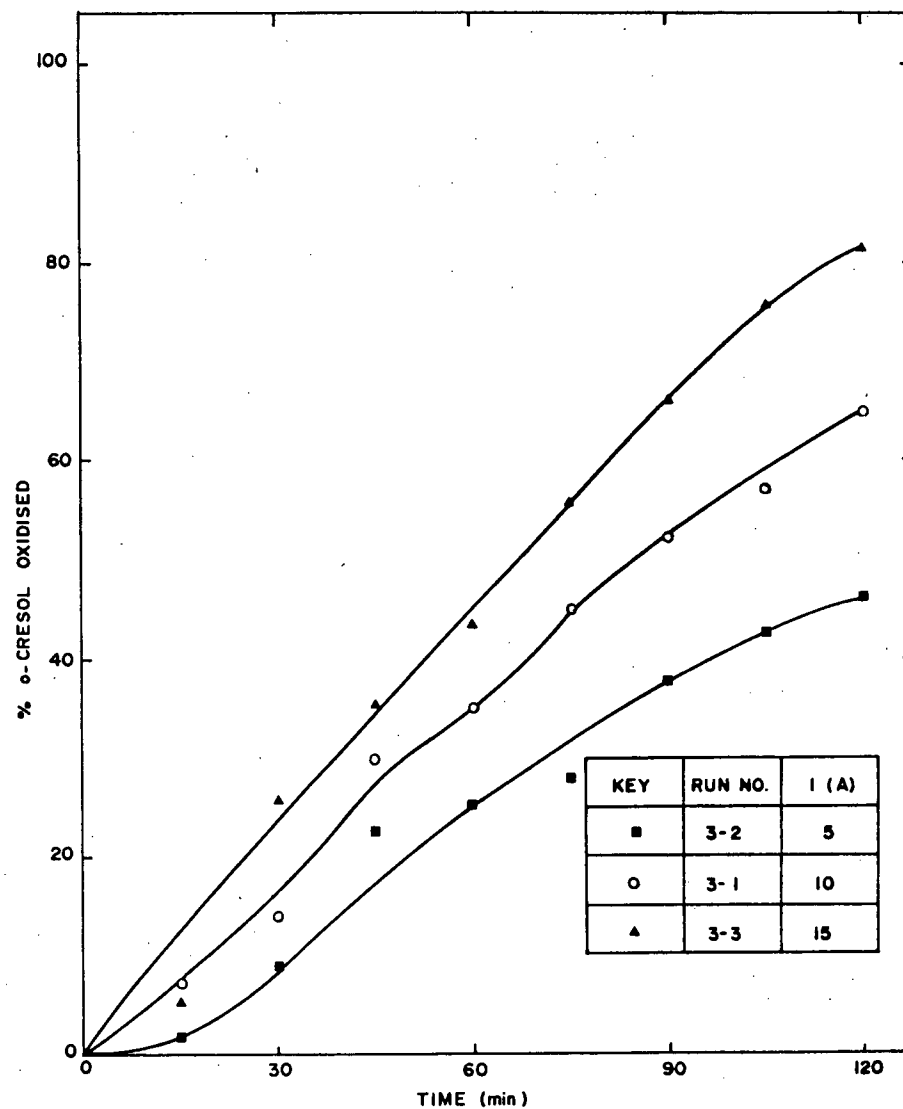


Fig. 14 Current effect on % o-cresol oxidized (1 g/l runs)

the same quantity of organic carbon as the starting material, the % organic carbon oxidized changes very little (Fig. 15) as the process is carried on.

5.1.4 Oxidation of 2,3-Xylenol

Based on the structure of 2,3-Xylenol, substitution of the methyl groups in the ring should increase the electron density at the carbon atom to which the hydroxyl group is attached, making it more susceptible to anodic oxidation than phenol and the cresols. Experiments with 2,3-Xylenol did show increased susceptibility. Fig. 16 shows that 2,3-Xylenol gets oxidized completely within two hours even at the higher initial concentrations of 380 and 625 mg/l.

The current effect (Fig. 17) is however more critical with the rate of oxidation being extremely slow in 5A run. Unlike the other runs with 2,3-Xylenol there was no excessive gas evolution and foaming in the above run (run 4-2). The lower voltage corresponding to the low applied current might have an important role in reducing the gas evolution and the rate of oxidation. It should be noted, however that the usual concentration effect also comes into play in Fig. 17. Although runs 4-1, 4-2 and 4-3 were intended to have the same initial concentration, equal initial concentrations were not achieved because of non-uniform dissolution and evaporation of 2,3-Xylenol in hot water. Otherwise the curve for run 4-1 would have been farther removed from that of run 4-3 in Fig. 17.

The % T.O.C. oxidized could be measured in all runs with 2,3-Xylenol. The initial concentrations from G.C. and T.O.C. analysis do not agree in this case. This could be due to the vigorous reaction which started

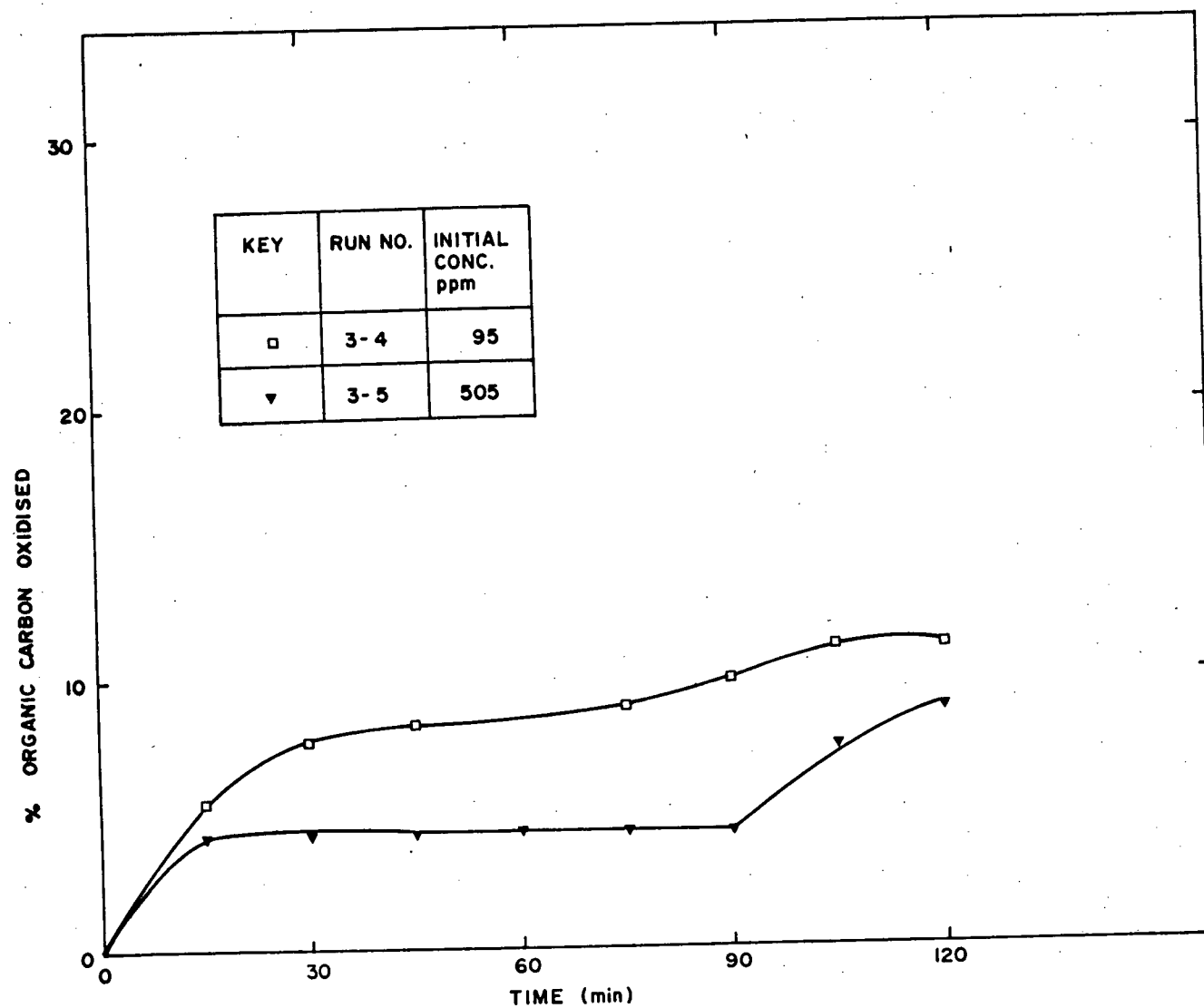


Fig. 15 Effect of conc. on rate of oxidation of organic carbon in o-cresol

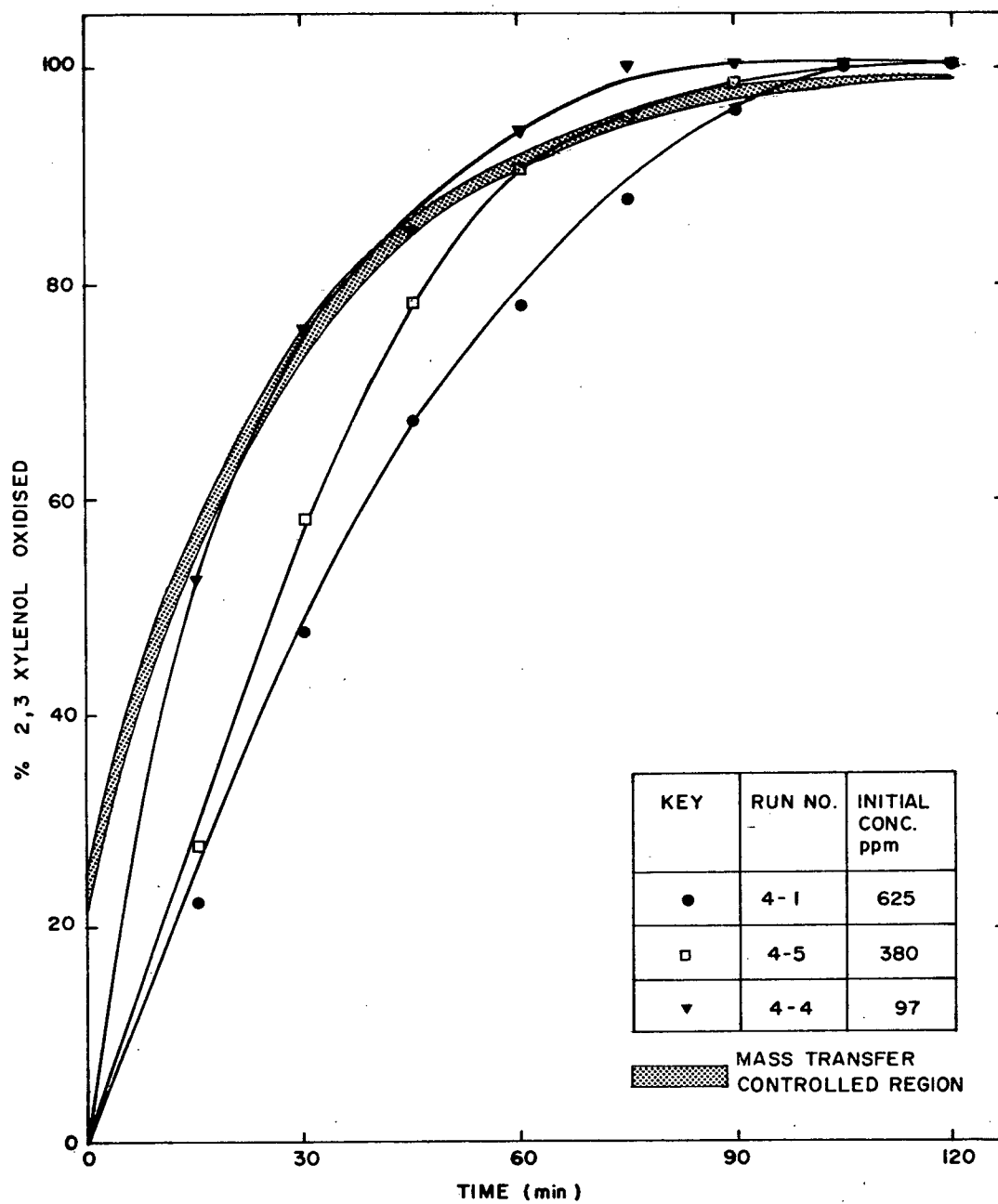


Fig. 16 Conc. effect on % 2,3-Xylenol oxidized at 10 A

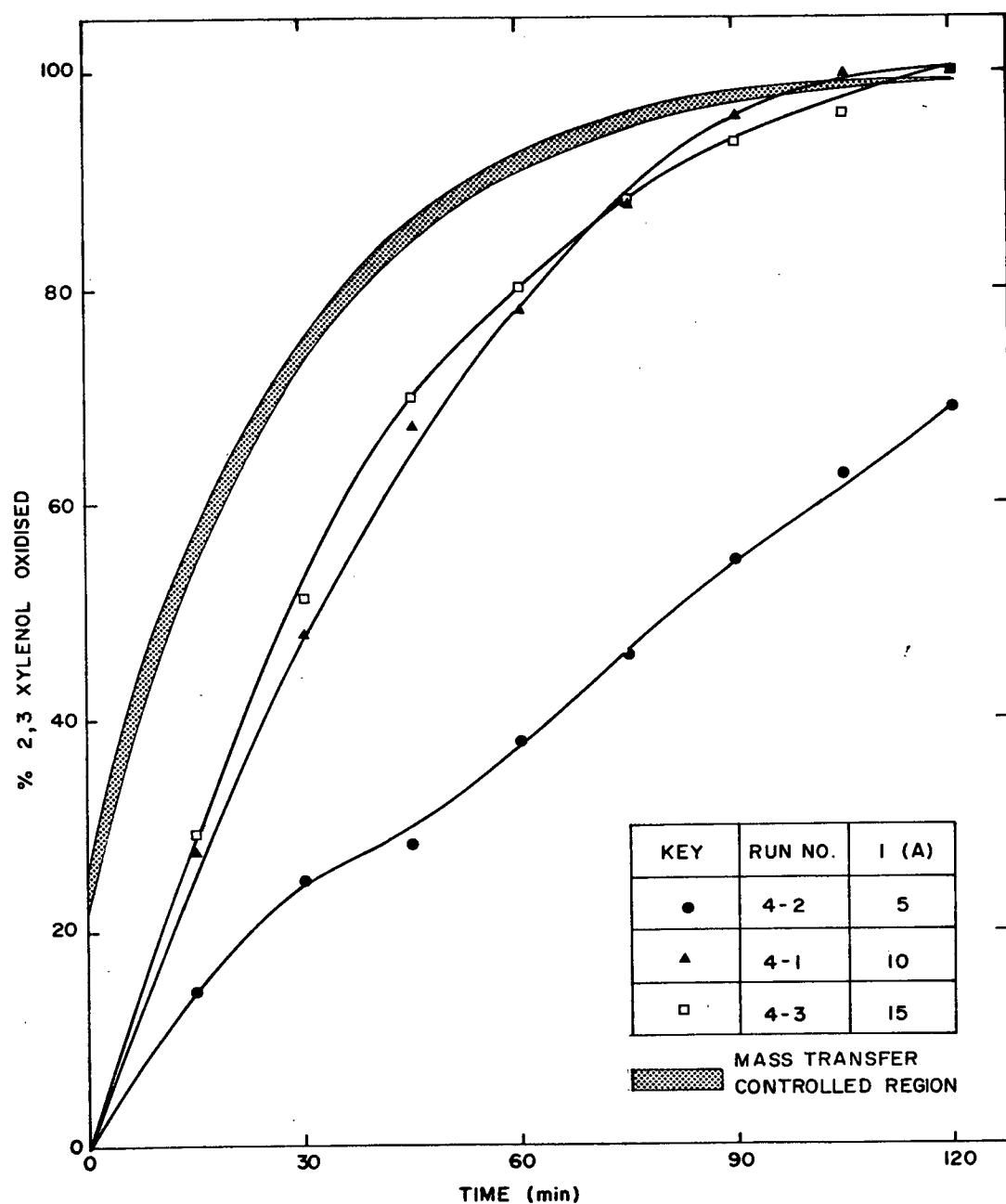
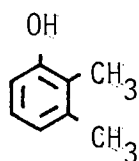


Fig. 17 Current effect on % 2,3-Xylenol oxidized (1 g/l run)

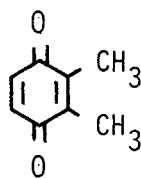
well before recycling was started. Besides, contrary to expectation, with an increase in initial concentration, a larger % T.O.C. is oxidized (Fig. 18). The effect of current on % T.O.C. oxidized can be observed in Fig. 19. There is a significant increase in % T.O.C. oxidized when the current is raised from 5A to 10A although the trend between 10A and 15A is not clear-cut.

The treated solution when subjected to GC/MS analysis showed the following compounds

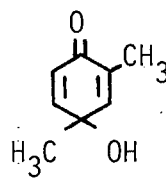


17.6%

2,3-Xylenol



79.8%

2,3-dimethyl
benzoquinone

2.6%

4-hydroxy-2,4-
dimethyl, 2,5-cyclo-
hexadiene-1-one

and traces of 2,3-dimethyl hydroquinone. Based on the products identified, the mechanism of the oxidation is probably similar to that outlined for phenol. The presence of only traces of 2,3-dimethyl hydroquinone shows that the loss of 2 electrons from 2,3-dimethyl hydroquinone is rapid, with the equilibrium shifted in such a way as to make this reaction almost irreversible.

5.1.5 Oxidation of 3,4-Xylenol

Based on its structure, 3,4-Xylenol should be as reactive as 2,3-Xylenol. The $E_{1/2}$ of 3,4-Xylenol (0.513 V) is much lower [21] than that of phenol. The usual well marked trends are observed in the plots of the concentration effect (Fig. 20) and the current effect (Fig. 21).

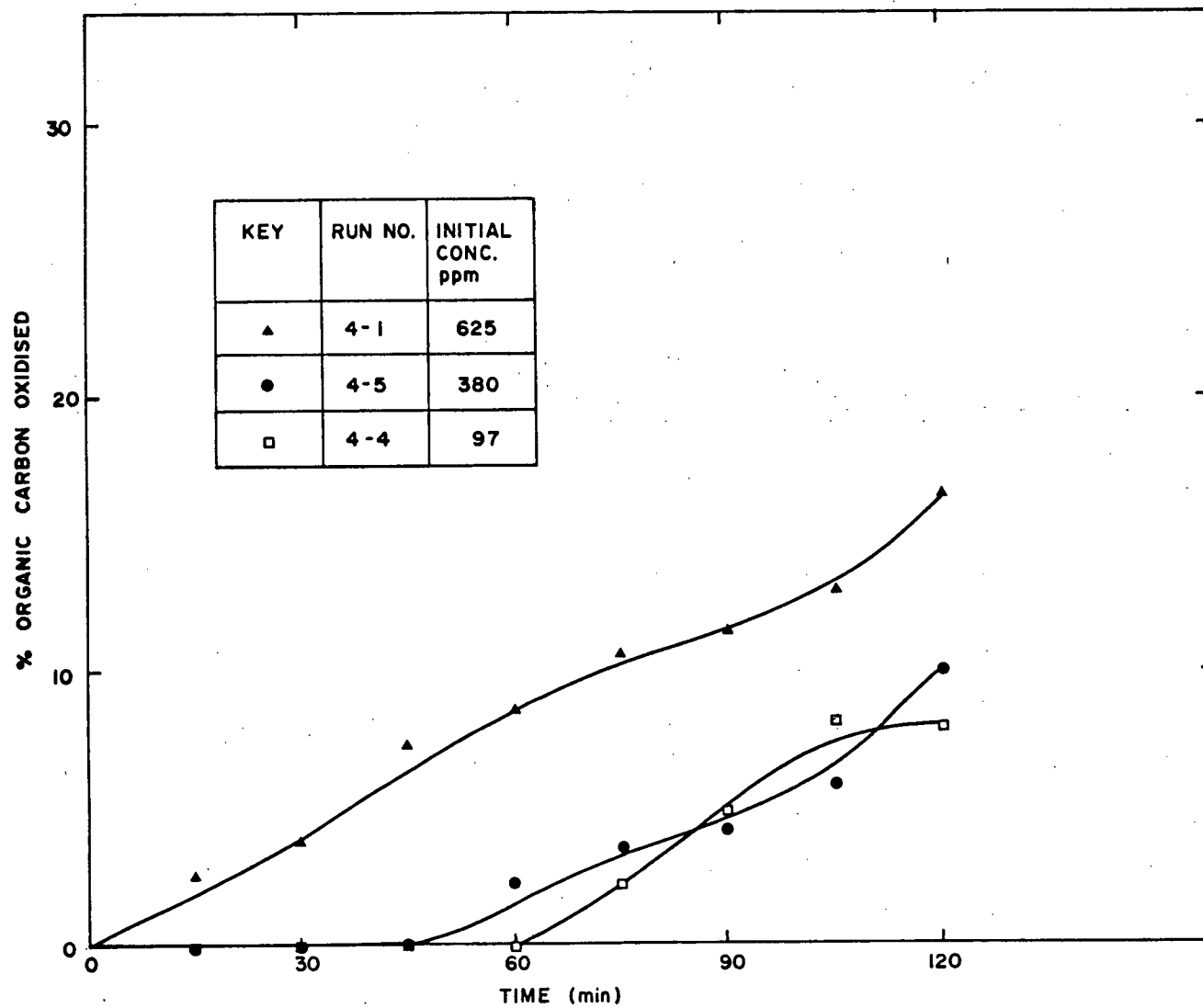


Fig. 18 Effect of conc. on rate of oxidation of organic carbon in 2,3-Xylenol at 10 A.

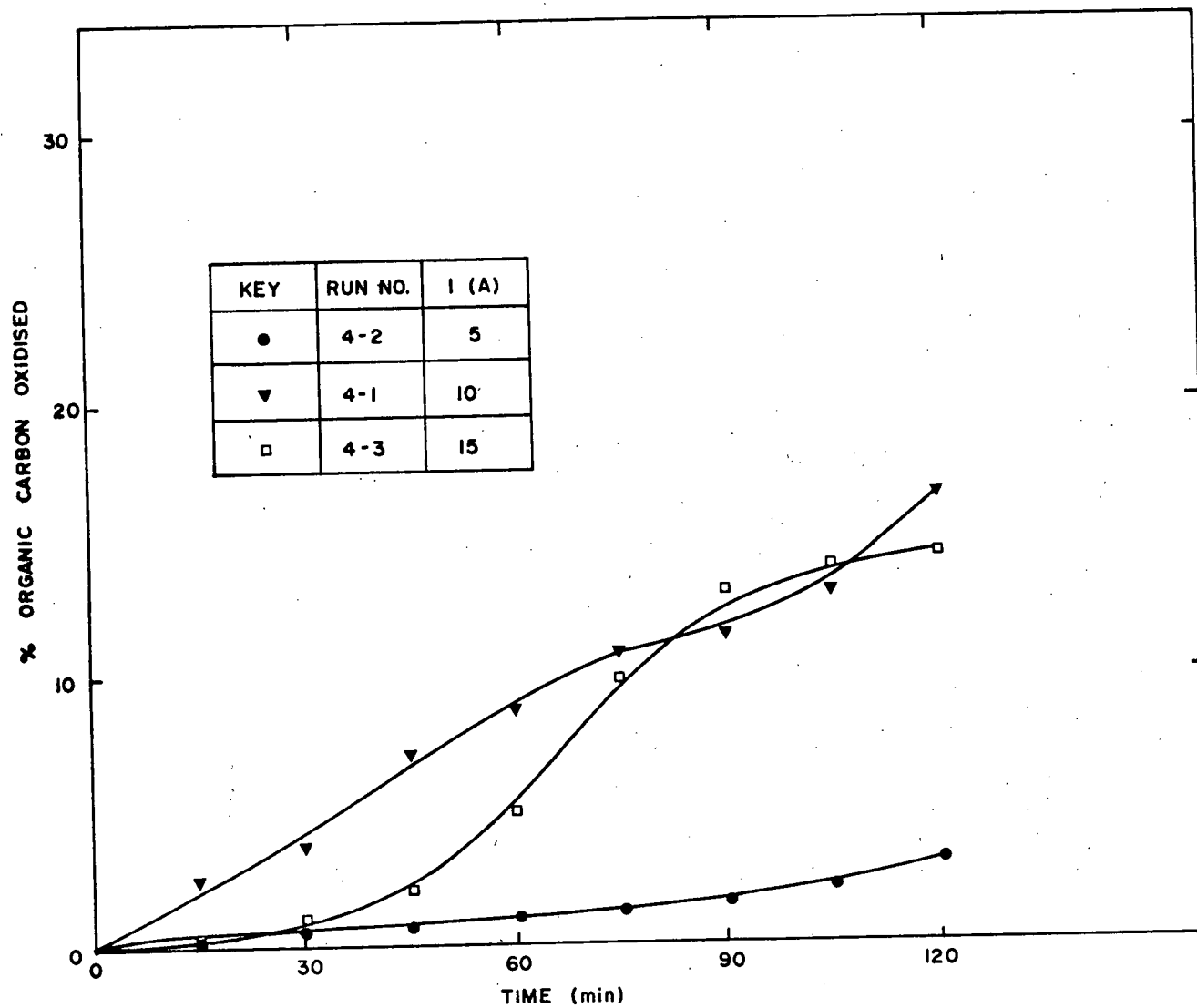


Fig. 19 Effect of current on rate of oxidation of organic carbon in 2,3-Xylenol (1 g/l runs)

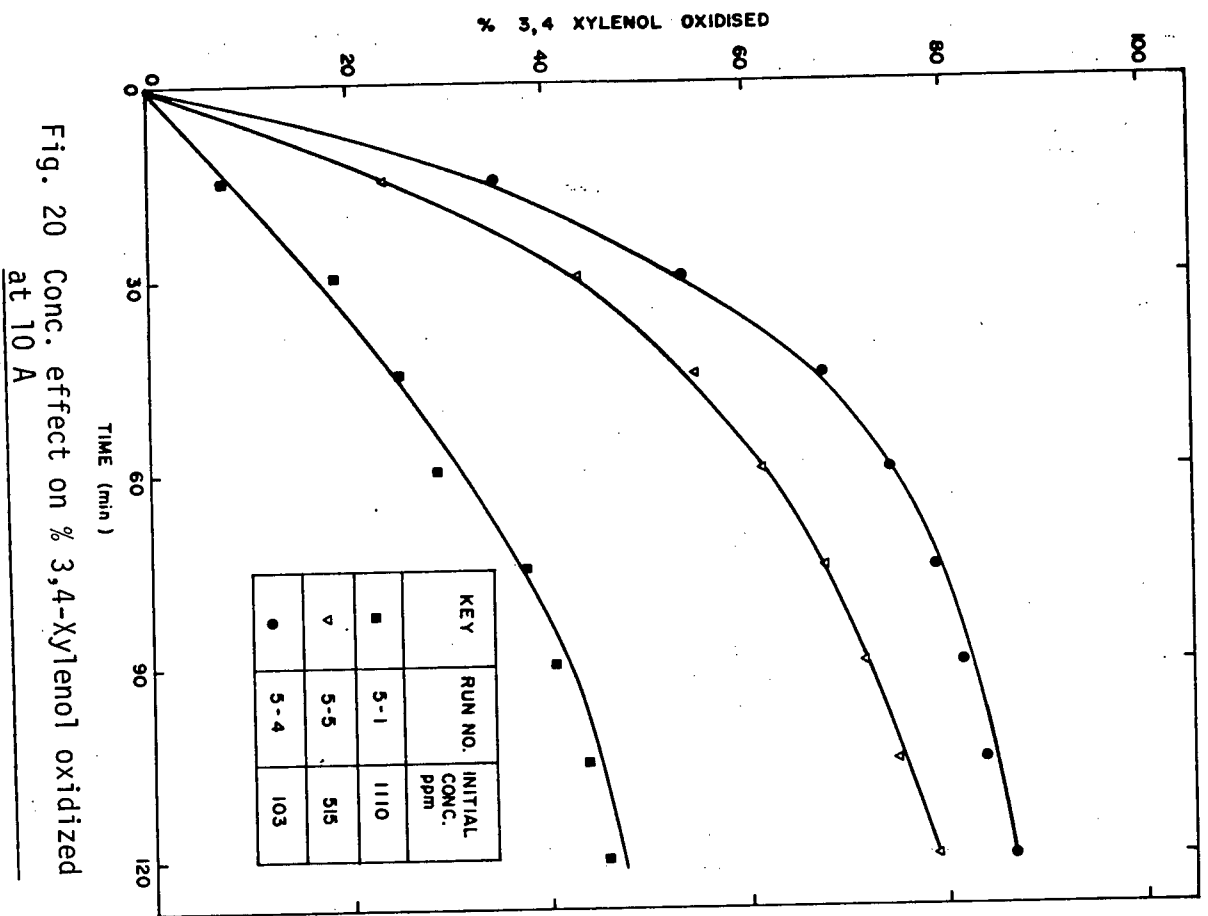


Fig. 20 Conc. effect on % 3,4-Xylenol oxidized at 10 A

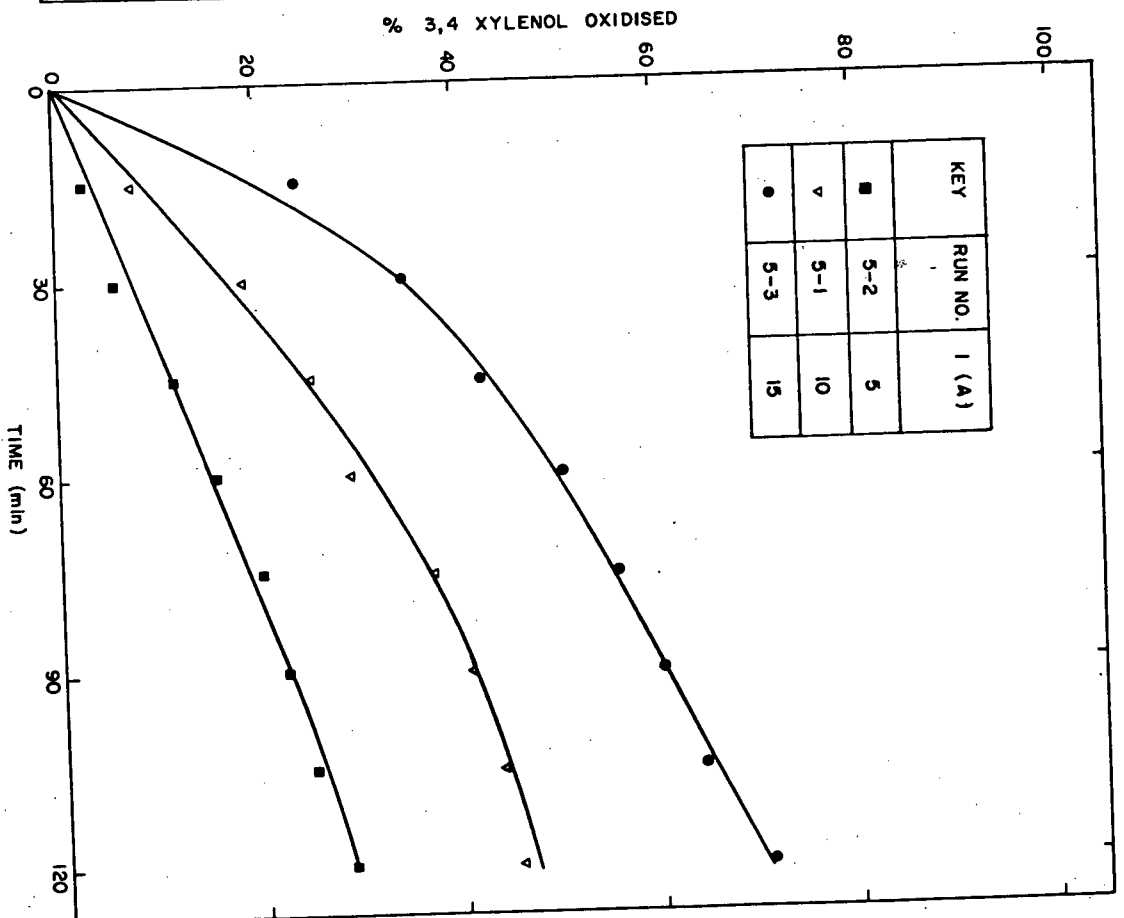
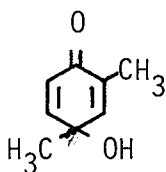


Fig. 21 Current effect on % 3,4-Xylenol oxidized (1 g/l runs)

The T.O.C. analysis showed that there was less than 5% oxidation of the organic carbon in all the runs and hence these results have not been reported.

The poor results obtained in the anodic oxidation of 3,4-Xylenol under the present conditions could be because of the low solubility of 3,4-Xylenol in water. A few insoluble oily droplets were noted in the electrolyte which also could have affected the whole process. The fact that there is no measurable decrease in T.O.C. further supports the observation that 3,4-Xylenol is resistant to anodic oxidation under the conditions used. The low oxidation of organic carbon could not be due to the formation of some non-oxidisable oxidation product because the only products that were identified in the treated solution were the starting compound, 3,4-Xylenol at 77.9%, and the following compound



4-hydroxy, 2,4-dimethyl,
2-5-cyclohexadiene-1-one at 22.1%

The above mentioned product was obtained from the oxidation of 2,3-Xylenol and has also been obtained [23] from the anodic oxidation of 2,4-Xylenol. Therefore it must have a stable configuration among the possible isomers of the oxidation products obtainable from various xylenols.

5.1.6 Oxidation of Resorcinol

Substitution of a hydroxyl group in the meta position of phenol decreases the half wave potential. Due to the electron donating nature

of the substituent, resorcinol should be more easily oxidized during anodic oxidation. This was found to be true. As seen from Fig. 22, resorcinol is destroyed completely in 60 minutes provided the initial concentration is lower than 500 mg/l. Increasing the initial concentration to 1200 mg/l has a well pronounced effect in decreasing the percentage oxidation in a given time.

The effect of current on the rate of oxidation (Fig. 23) follows the usual trend. Anodic oxidation of resorcinol is very interesting from the point of view of achieving carbon dioxide formation. Fig. 24 shows that with a decrease in initial concentration of resorcinol, there is an increase in % organic carbon oxidized. With an increase in applied current, although there is a slight increase in % organic carbon oxidized, the exact trend is unclear (Fig. 25).

As mentioned in section 4.3.5, none of the oxidation products of resorcinol could be identified by GC/MS analysis even when a solid probe was used. Thus no definite conclusion can be made about the reaction route in this case. However a few comments can be made based on the observations made during the runs.

In spite of the fact that there was an observable rate of oxidation of organic carbon, there was no foaming or noticeable gas evolution. This suggests that the foaming observed in the O-cresol runs and 2,3-Xylenol runs was perhaps due to the formation of some surface active compounds rather than being simply due to gas evolution.

During the resorcinol runs the electrolyte remained colourless for the first 30 minutes and became yellow thereafter. Also the samples collected at the beginning of the runs were yellow during collection and slowly became colourless in five minutes. This suggests that the reaction

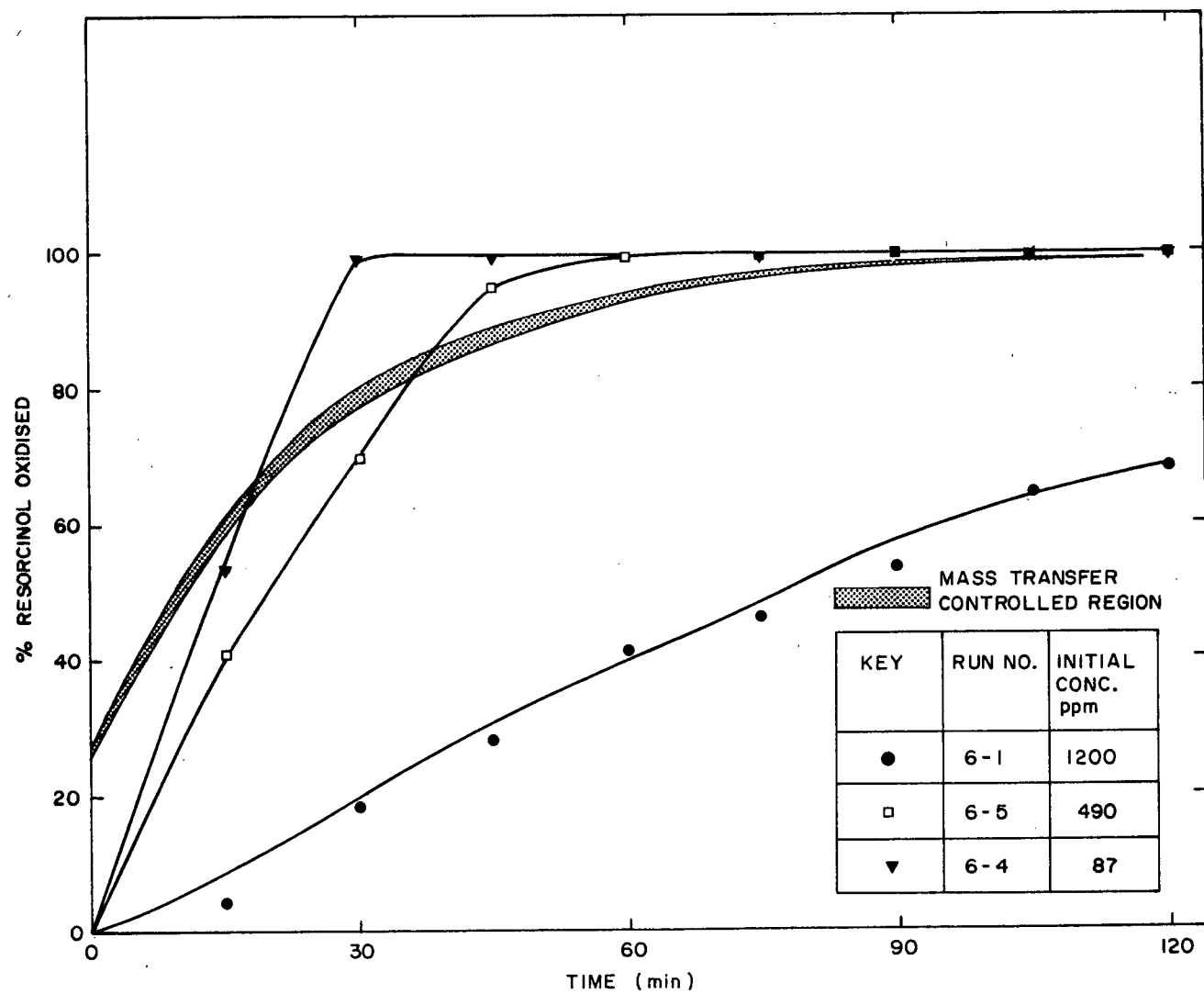


Fig. 22 Conc. effect on % resorcinol oxidized at 10 A

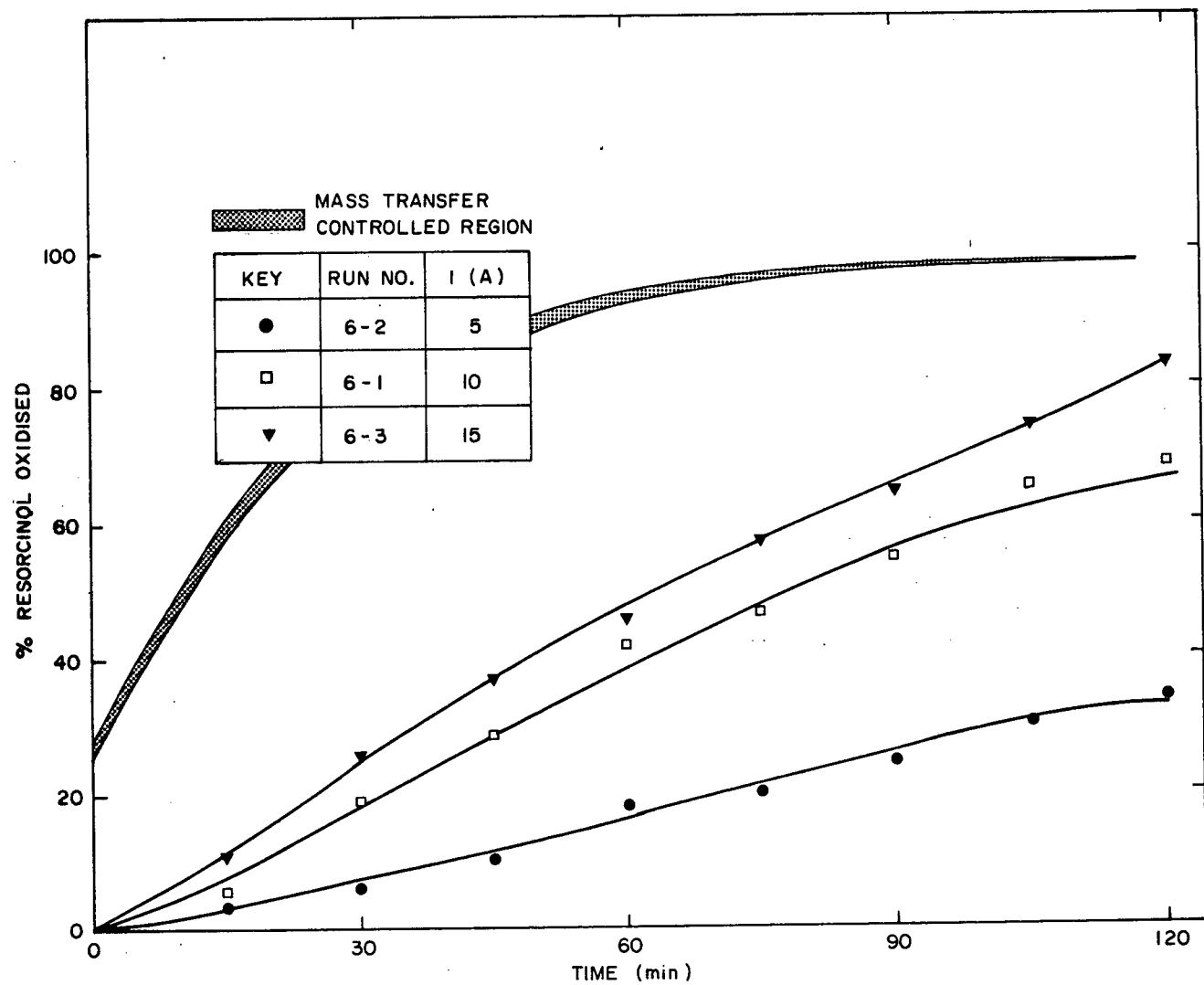


Fig. 23 Current effect on % resorcinol oxidized (1 g/l runs)

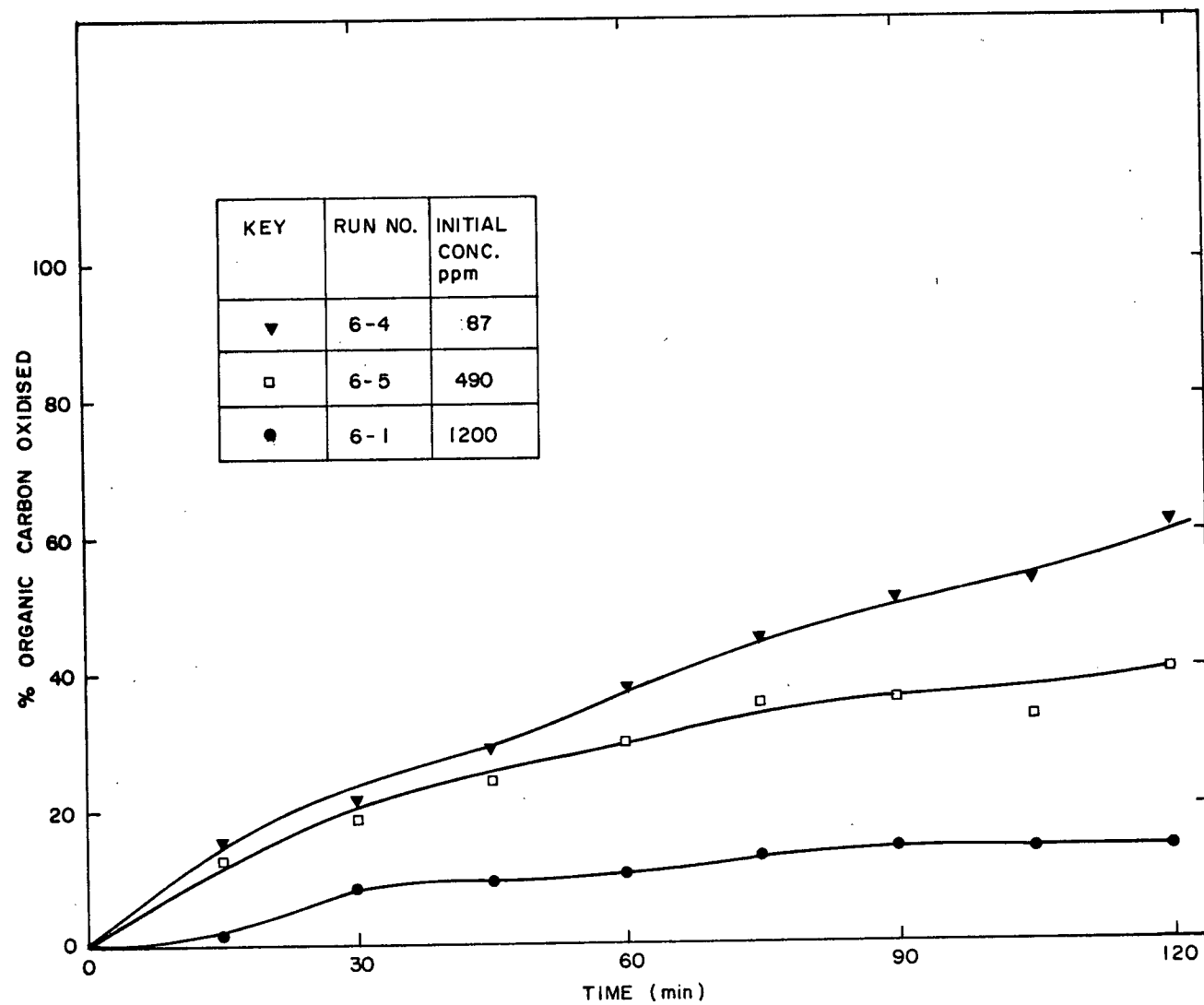


Fig. 24 Effect of conc. on rate of oxidation of organic carbon in resorcinol at 10 A

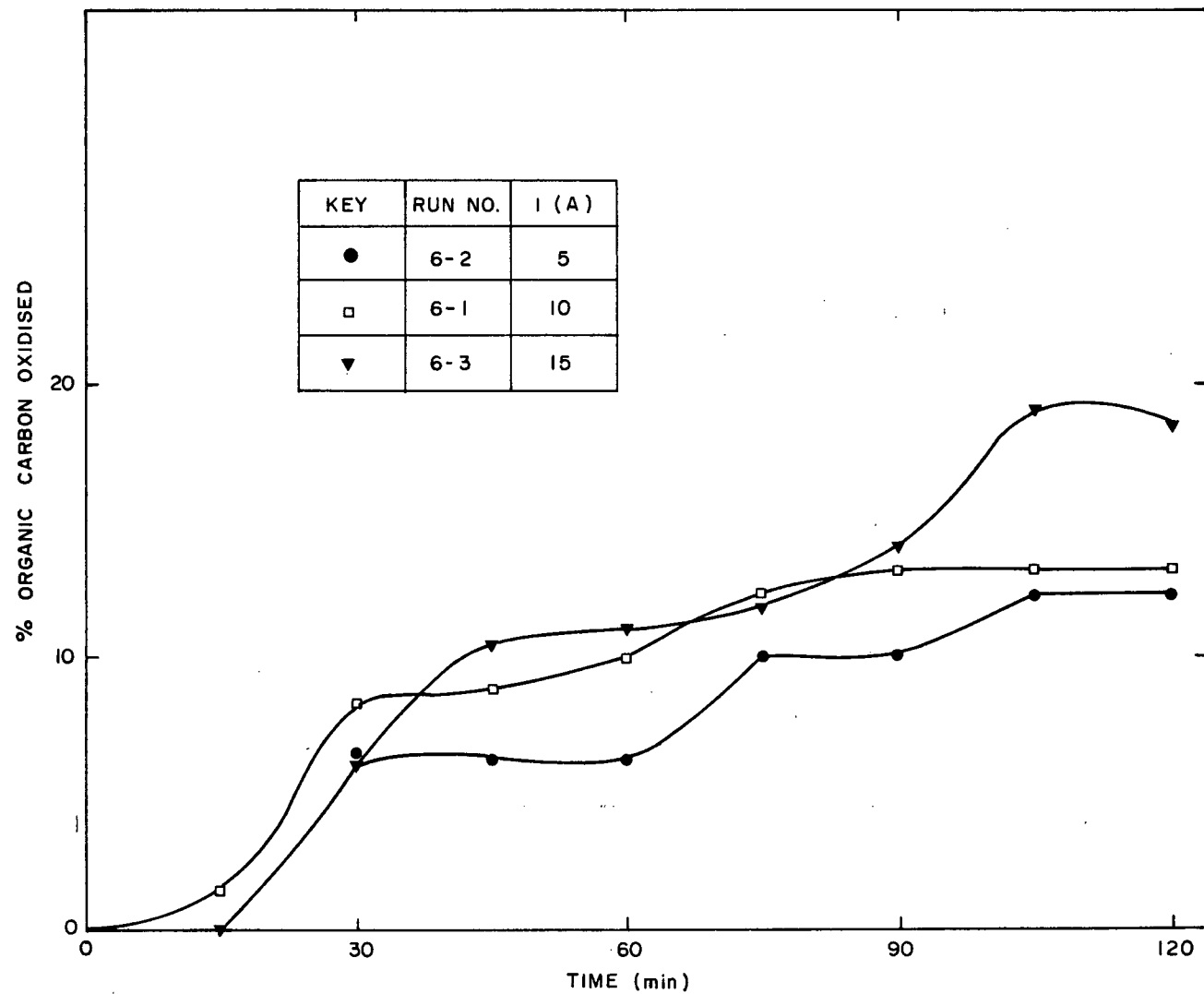


Fig. 25 Effect of current on rate of oxidation of organic carbon in resorcinol (1 g/l runs)

leading to the formation of the yellow oxidized product of resorcinol has its equilibrium shifted towards the forward reaction only at high concentrations of the initial oxidation product.

5.1.7 Oxidation of catechol

Anodic oxidation of catechol was found to be very vigorous as expected from its structure. Among the phenolics studied, catechol proved to be most susceptible to complete oxidation leading to the formation of carbon dioxide. The maximum oxidation of organic carbon (62.7%) was achieved in run 7-5 (Fig. 26). With higher initial concentrations of catechol (1000 mg/l), the curve levels off after 90 minutes of oxidation showing that probably an electro-inactive compound or a compound that is highly resistant to anodic oxidation under the present conditions is formed.* Besides, as expected [27] the catalytic effect of catechol described in Section 2.2.4 seems to be negligible under the low pH conditions of the experiment.

An increase in applied current does not quite seem to favour the oxidation of organic carbon because the trends followed in run 7-1 (10A) and 7-3 (15A) are similar (Fig. 27) although a lower rate of oxidation of organic carbon is observed in the case of 5A run.

As indicated earlier, (Chapter 4), the concentration of catechol in the runs could not be determined by the usual GC technique which was inapplicable for concentrations below 200 mg/l. However, under typical conditions (run 7-1, 1000 mg/l, initial conc., 10A), it was found by

* This is supported by the fact that the reaction appeared to be less vigorous, with less gas evolution and foaming after the first 90 minutes.

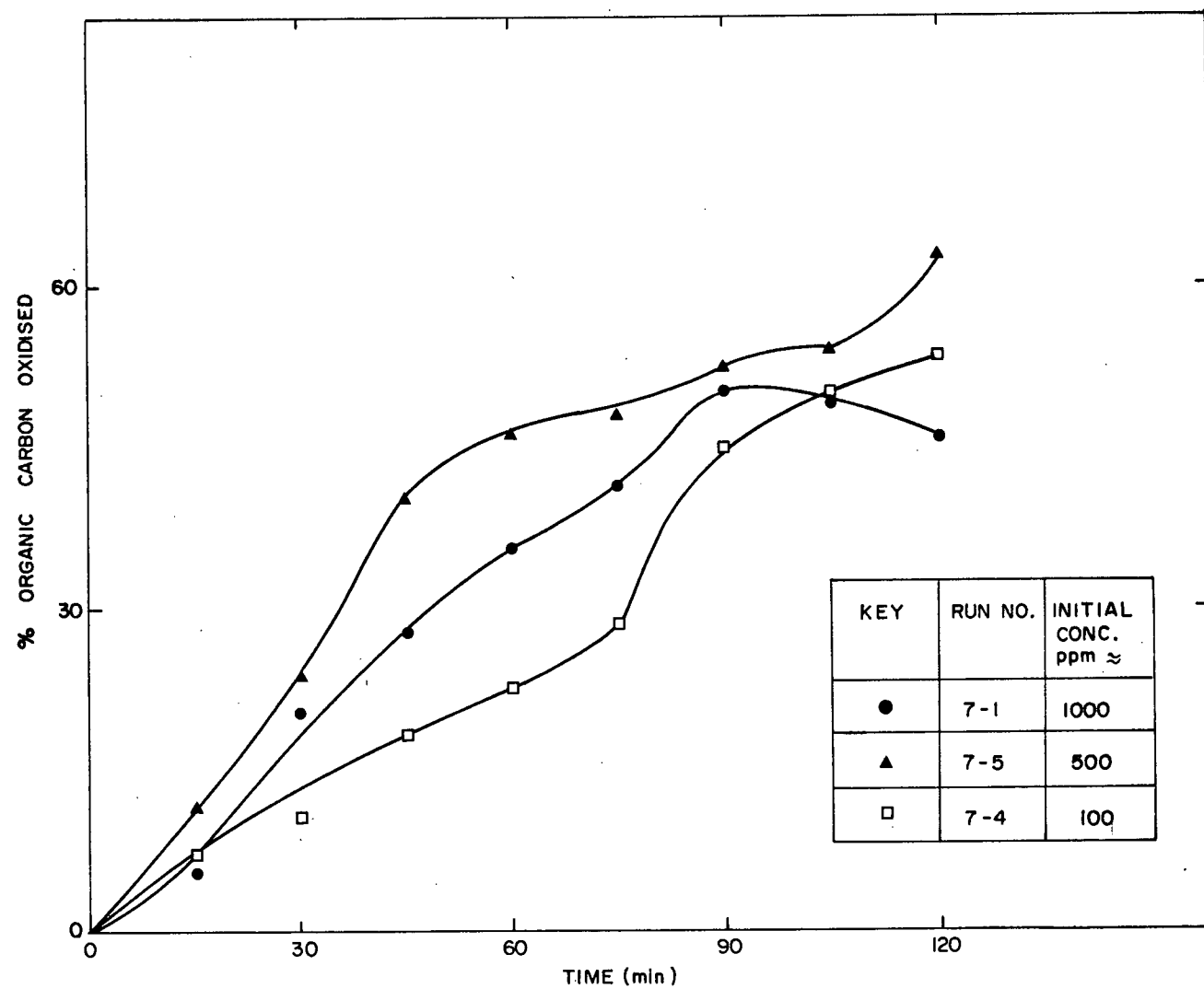


Fig. 26 Effect of conc. on rate of oxidation of organic carbon in catechol at 10 A

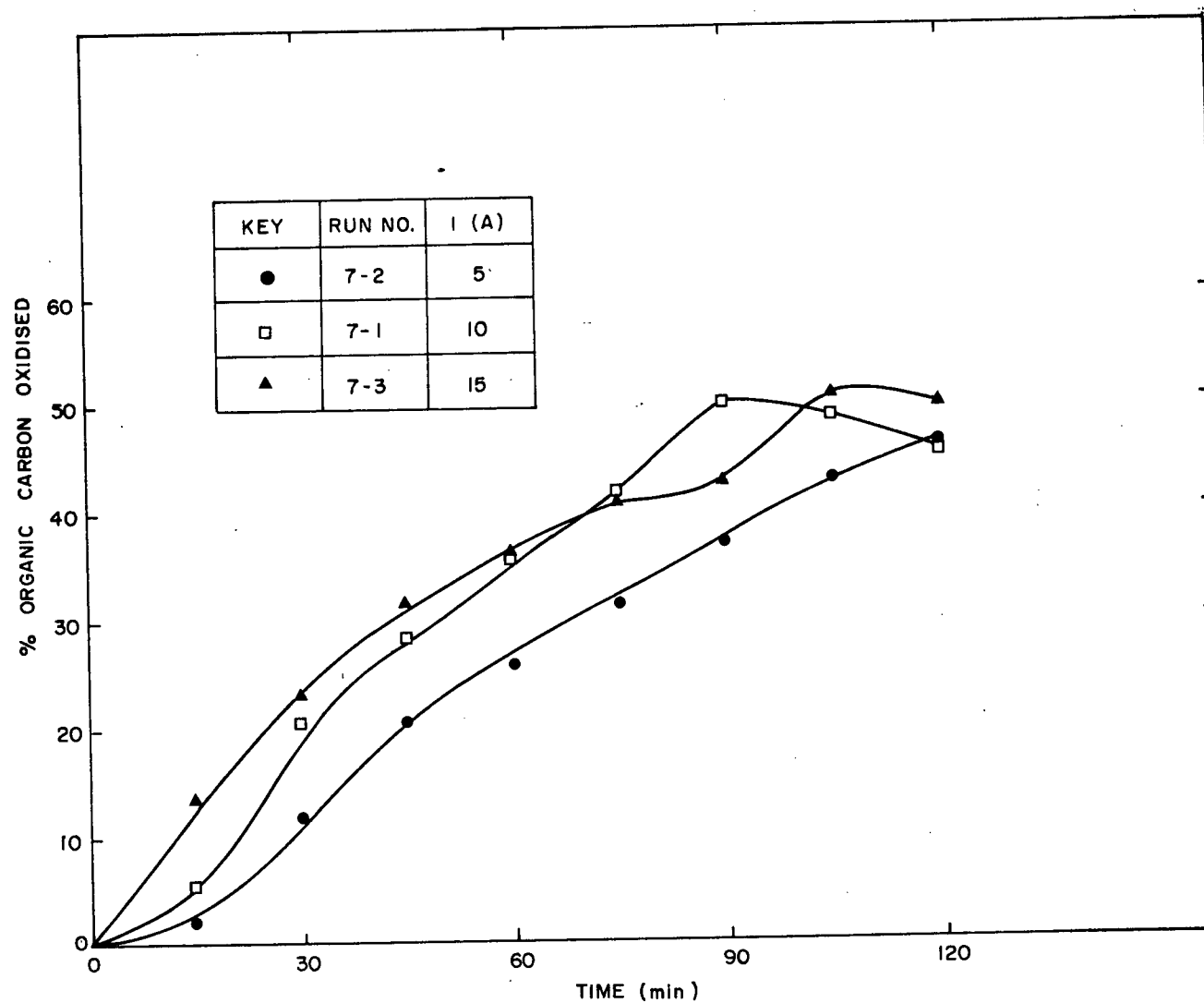


Fig. 27 Effect of current on rate of oxidation of organic carbon in catechol (1 g/l runs)

GC using the carbowax column that about 150 mg/l of catechol remained after 2 hours of anodic oxidation in which there was 45.6% oxidation of the organic carbon. A black product of polymerization was produced in all runs except in run (7-4) where the lowest (100 mg/l) initial concentration of catechol was used. Attempts to characterize the black precipitate were not successful.

The observations made in the catechol runs suggest that the initial two-electron process leading to the formation of O-quinone is followed immediately by its decomposition and condensation. The pale yellow solution collected in the initial stage of the process spontaneously formed the condensation product which precipitated out of the samples. Unfortunately, none of the products of oxidation could be identified in the GC/MS analysis.

In order to evaluate the anodic oxidation process from the point of view of effluent treatment of waste containing catechol, B.O.D. and C.O.D. results are reported. (Appendix 2, runs 7-2, 7-3). As expected, there is a larger % reduction in B.O.D. at a higher current. However between the two extreme values of current used (5A and 15A), there is only a small difference in reduction of B.O.D. achieved during the experiment. The treatment brings about 81% reduction in B.O.D. value at an applied current of 15A. The change in the C.O.D. values as a result of the oxidation is comparable with the % oxidation of organic carbon, but the effect of increase in the reduction of C.O.D. values with increase in current is more significant.

5.2 Comparison of performance of different phenolics

5.2.1 Effect of variation of initial concentration

An increase in the initial concentration of the phenolics studied is accompanied by a drop in the % of oxidation in 2 hours (Fig. 28). The phenol runs do not follow the trend due to the deposition of tars on the cathode surface in run 1-5 as mentioned earlier. 2,3-Xylenol was however oxidized completely at all the initial concentrations studied.

In order to discuss rates logically, controlled-potential electrolysis (cpe) carried out with a potentiostat should be performed rather than constant current experiments as the factor affecting the rate constant is the potential. In the present study, the calculation of the initial rate was based on the time interval during which % phenolic compound oxidized increased linearly with time. Except in the case of 2,3-Xylenol, the initial oxidation rates for all the phenolics go through a maximum value with increasing concentration (Fig. 29). This indicates that at an initial concentration of about 500 mg/l, the best rate of oxidation can be obtained. The actual values of the initial rates, however do not seem to have a direct correlation to the structure of the phenolics. This indicates that besides the nature of the substituents, other factors like diffusional effects, nature of the oxidation products, adsorption effects and optimum potential range can perhaps play a major role in the anodic process. An increase in the initial concentration seems to accelerate the rate of oxidation of 2,3-Xylenol in the concentration range studied.

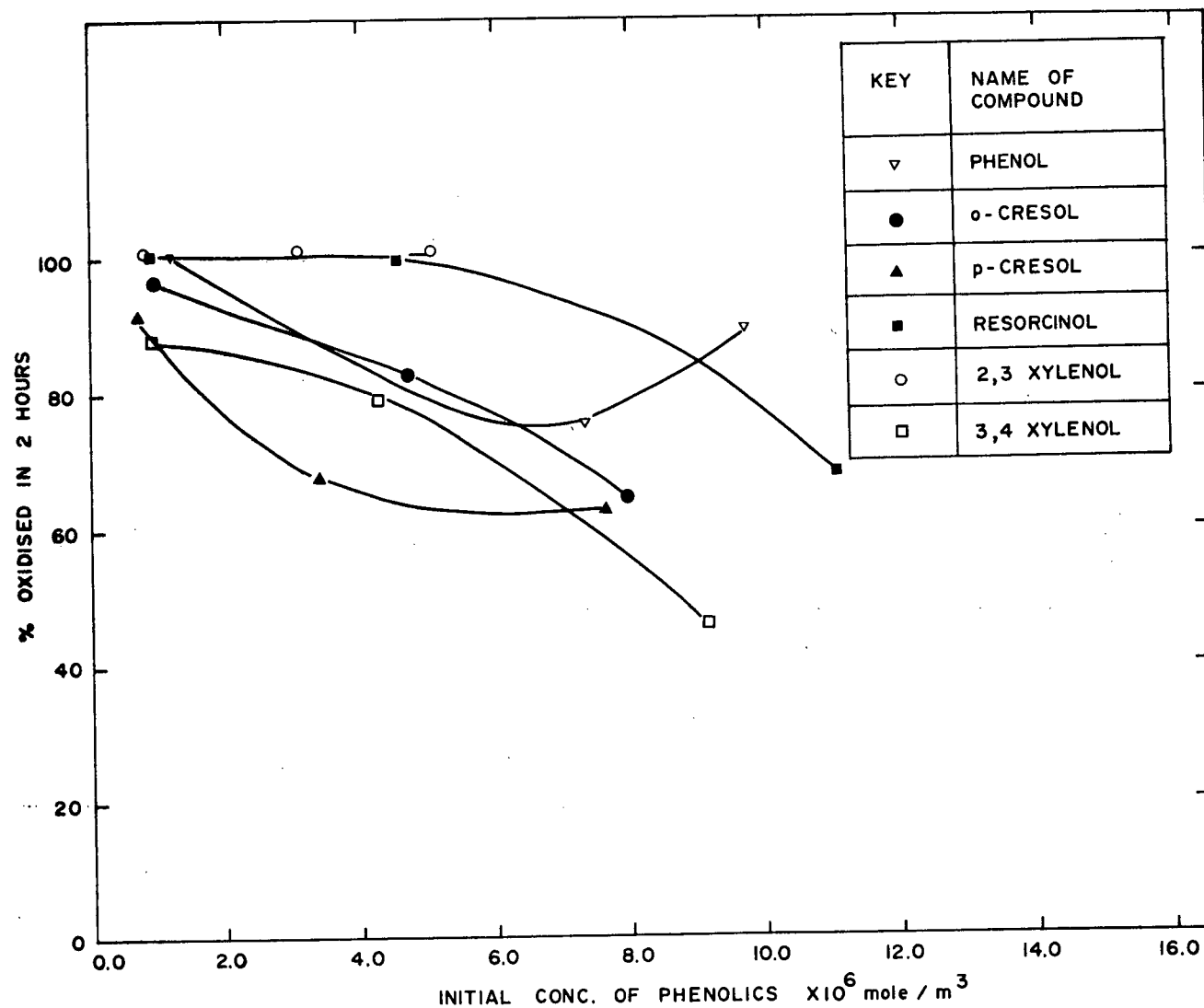


Fig. 28 Variation of final % oxidized with initial concentration of phenolics at 10 A

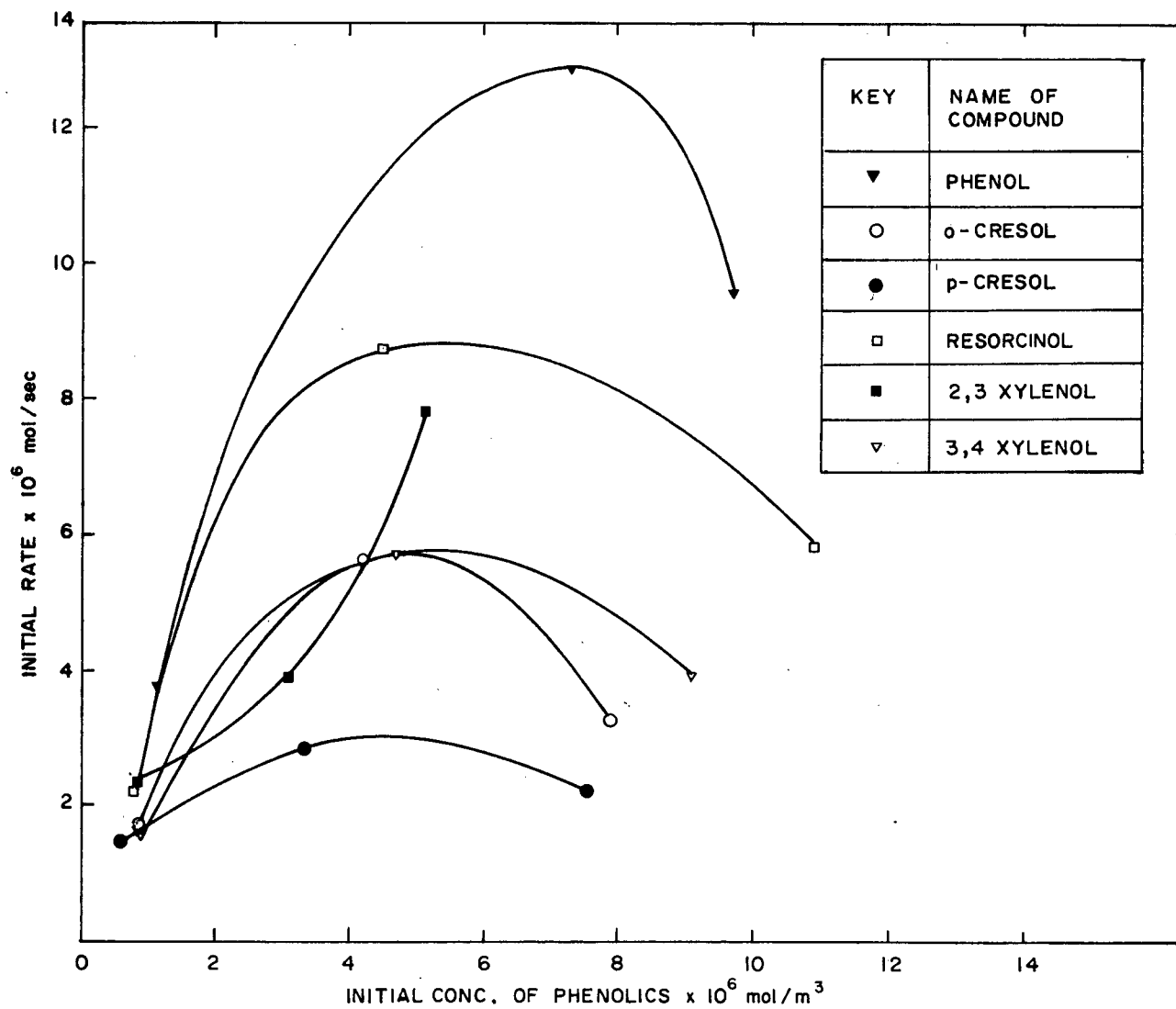


Fig. 29 Variation of initial rate with initial concentration at 10 A

5.2.2 Effect of variation of applied current

With an increase in applied current, there is an increase in the final % oxidation after 2 hours operation in all cases (Fig. 30). The final % of oxidation increases in the order 3,4-Xylenol, p-cresol, O-cresol, resorcinol, phenol, 2,3-Xylenol. This effect is more significant when the increase is between 5A and 10A than in the case of increase from 10A to 15A. The initial rate of oxidation (Fig. 31) increases with increase in applied current except in the case of p-cresol where the increase in rate between 5A and 10A is insignificant. In this study of the effect of applied current, the data obtained with different phenolics indicates that the trend followed with the initial rates is different from that obtained with the final % oxidized. This indicates that the kinetics and the transport phenomena associated with each process are complex and deserve further investigation.

5.2.3 Substituent effects

As referred earlier, (sections 2.2.2) most studies of substituent effects are based on shifts of half-wave potentials. However from the present study, it is obvious that there is no direct correlation between the half-wave potential values (Table II) and final % oxidized. The half-wave potential does take the diffusion and activity coefficients of the oxidized and reduced forms into account as shown by the following equation [41]

$$E_{1/2} = E^{\circ} - \frac{RT}{nF} \ln \left(\frac{D_{ox}}{D_{Red}} \right)^{1/2} - \frac{RT}{nF} \ln \frac{f_{Red}}{f_{ox}} \quad (10)$$

where D_{ox} and D_{Red} are the diffusion coefficients of the oxidized and

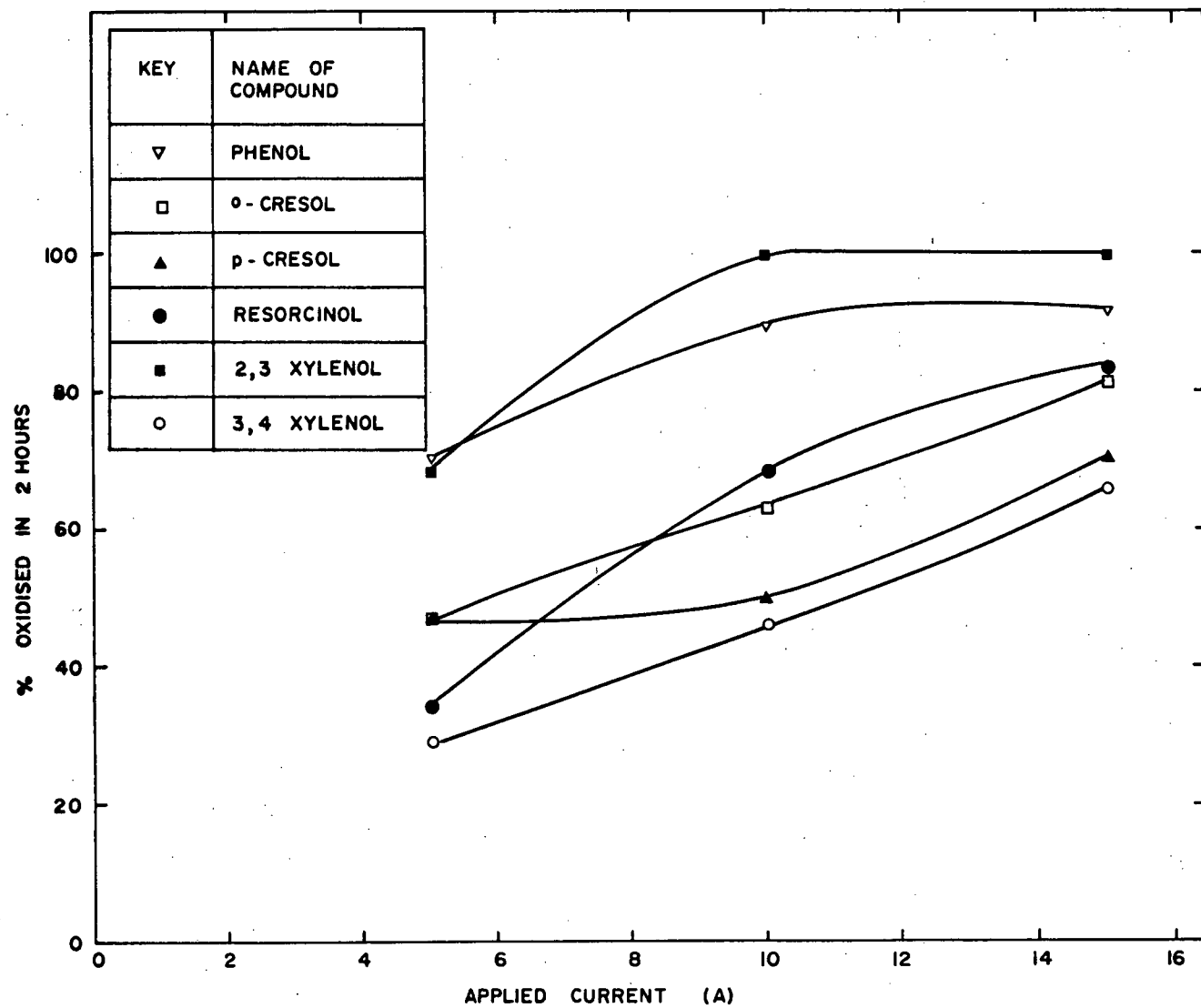


Fig. 30 Variation of final % oxidized with applied current
(1 g/l runs)

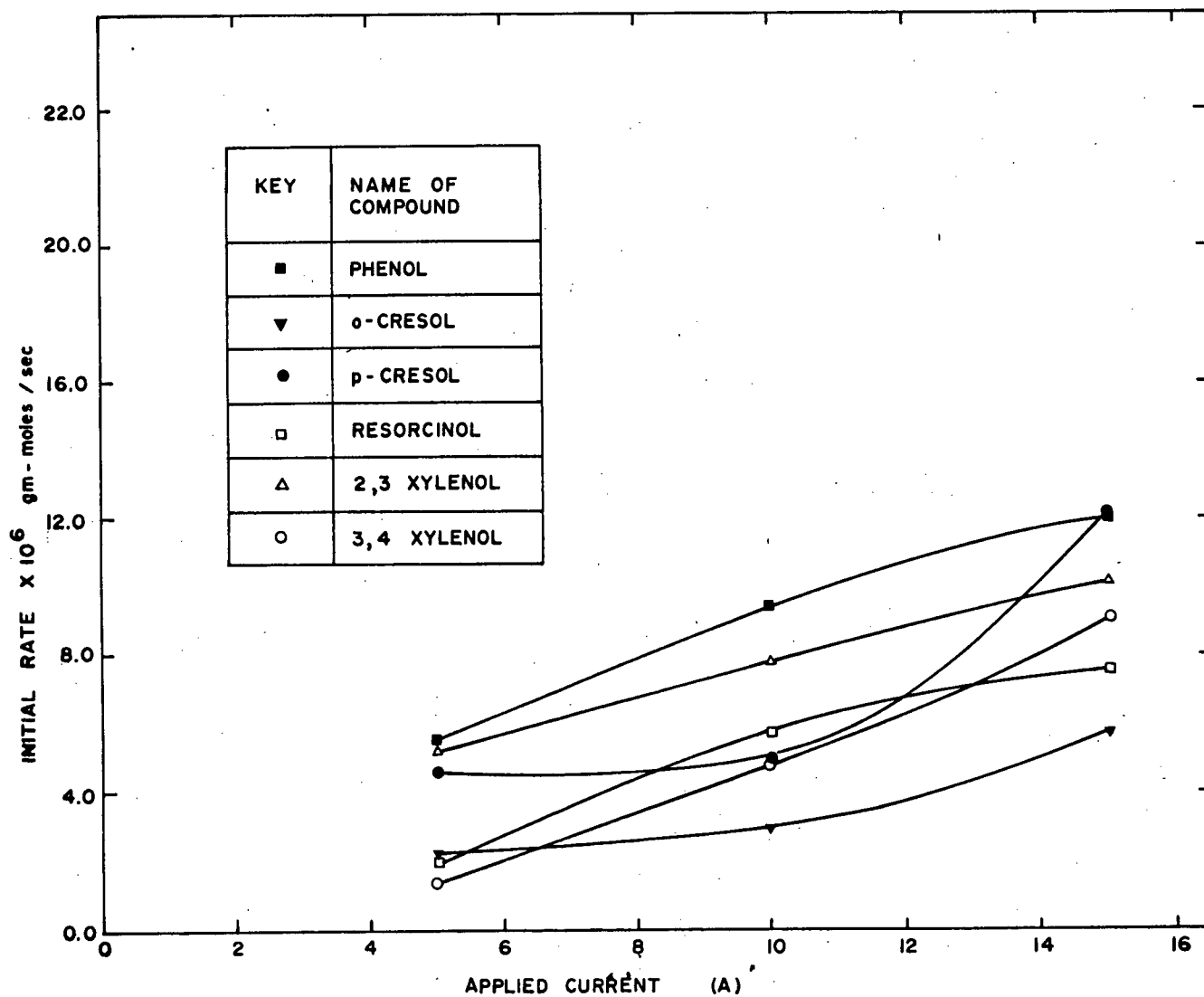


Fig. 31 Variation of initial rate of oxidation with applied current (1 g/l runs)

reduced forms, respectively, and f_{ox} and f_{Red} are the activity coefficients.

But the shift of the half-wave potential $(\Delta E_{1/2})_X$ caused by introducing the substituent X in to the parent molecule chosen as a reference compound, in which X = H is related [41] to the equilibrium constants for the reaction by eq. (11)

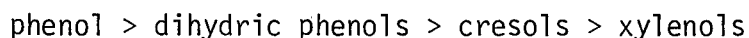
$$(\Delta E_{1/2})_X = \frac{2.3 RT}{nF} (\Delta \log K)_X \quad (11)$$

where K is the equilibrium constant of the reaction $O + ze \rightleftharpoons R$, and $\Delta \log K = \log K_X - \log K_D$, where K_D represents the value for the reference system for which X = H.

Although the shift in $E_{1/2}$ is related to the reaction kinetics, in the determination of half-wave potentials, it is assumed that the overall rate of the reaction is limited by the rate of diffusion of the reactant to the electrode, which may not be exactly true with the present cases. The overall rate of the reactions may be controlled by the processes occurring at the electrode surface. Besides, gas evolution, further oxidation of the intermediates and adsorption effects all of which need further investigation may play a role.

5.2.4 Effect of diffusivity

The theoretical diffusivity values (Appendix 4) have been presented in Table V. On the basis of diffusivity, if the reactions are controlled by the rate of mass transport of the phenolic molecules to the electrode, the ease of oxidation should be as follows.



In the present study, at an applied current of 10A, with an initial concentration of 1g/l of the phenolic compound, the initial rate of oxidation follows the order (Fig. 31).

phenol > 2,3-Xylenol > resorcinol > p-cresol > 3,4-Xylenol > O-cresol

TABLE V
DIFFUSIVITIES OF THE PHENOLIC COMPOUNDS IN WATER

Name of phenolic compound	Molal volume of the phenolic compound at its normal boiling point $\text{cm}^3/\text{g.mole}$	D^* cm^2/sec $\times 10^6 \text{ cm}^2/\text{s}$
Phenol	105	8.5
p-cresol	126	7.7
O-cresol	126	7.7
2,3-Xylenol	147	7.4
3,4-Xylenol	147	7.4
resorcinol	112	8.3
catechol	112	8.3

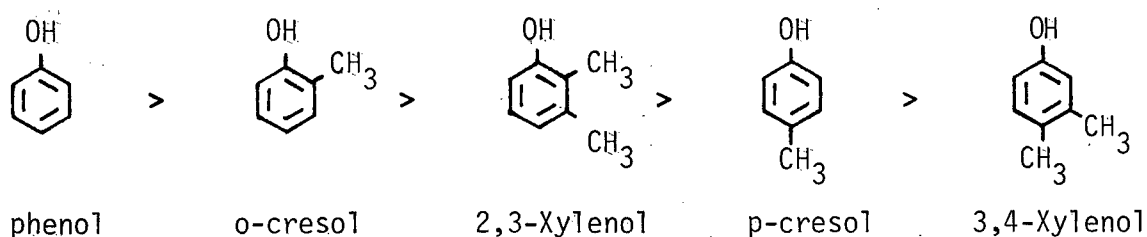
This trend conforms to the order expected from the diffusivity values except for 2,3-Xylenol which takes precedence over resorcinol and 3,4-Xylenol which has a higher initial rate than O-cresol. Considering the % oxidized in two hours (Fig. 30) under similar conditions the order seems to be different from above. Therefore, even though

* Calculation outlined in Appendix 4.

diffusivity might control the rate of oxidation in the initial stages of oxidations other factors which deserve further attention do play a role.

5.3 Oxidation of phenolic mixtures

When the monohydric phenolics are mixed in about the same concentrations as they are found in the wastewater of Table I, the extent to which the phenolics were oxidized in a given time decreased in the following order as shown in Fig. 32-34.



This leads us to the following conclusion.

- 1) Substitution of methyl (electron donating group) decreases the ease of oxidation.
- 2) Substitution in the ortho position is preferable to substitution in the para position.
- 3) No definite conclusion can be drawn about the preference of para position over meta.

Mass transfer effects would have also aided in the oxidation of phenol and o-cresol as their initial concentration is higher than the rest. The mixture oxidation runs (runs 8-1, 8-2, 8-3) prove that as the period of treatment is increased, better oxidations can be obtained. Even after 95.8% oxidation of the phenolic mixture (run 8-3), the curve did not flatten out showing that by increasing the period of oxidation or by using more optimal conditions, virtually complete oxidation might be obtained.

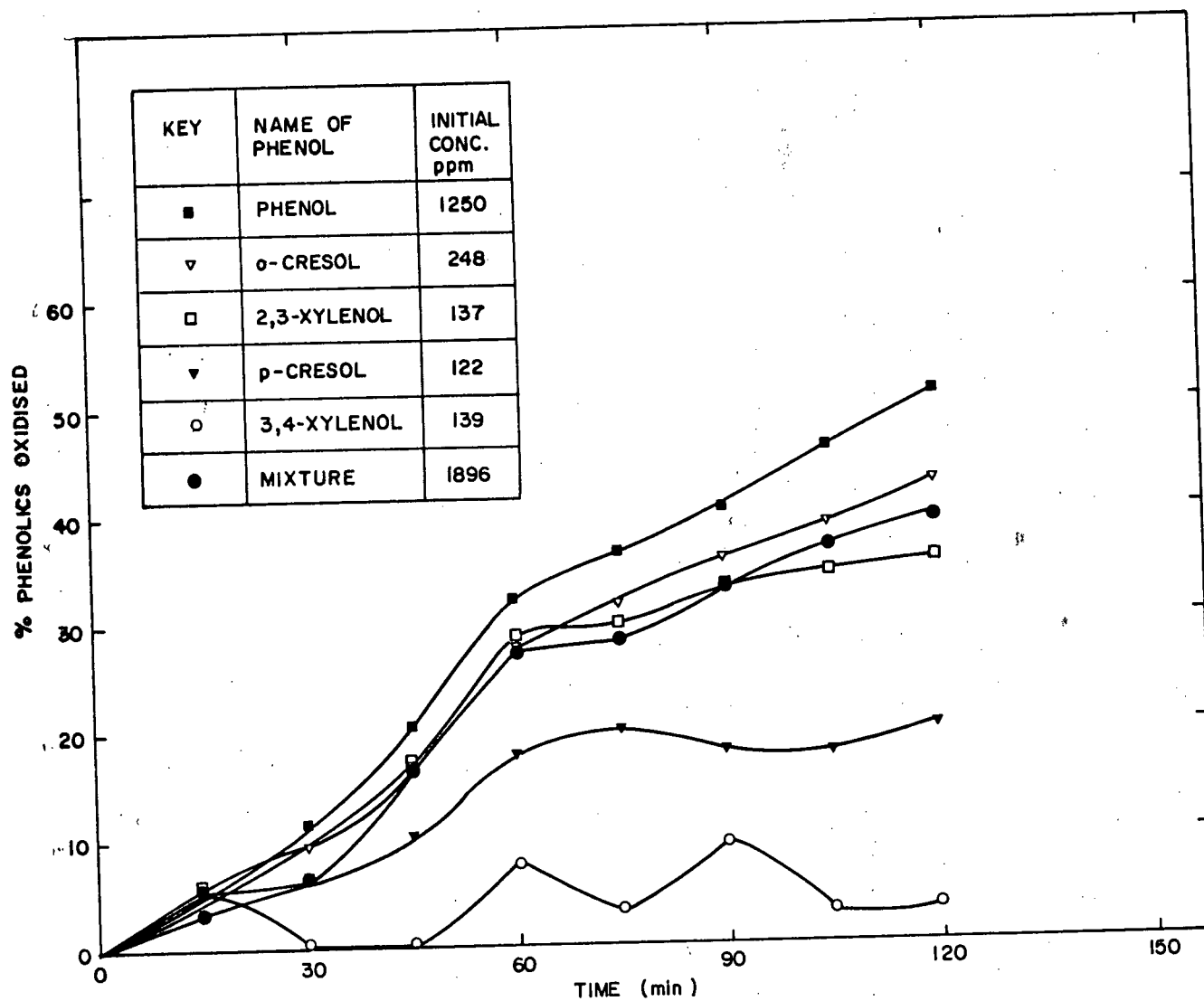


Fig. 32 Effect of nature of phenolics on % oxidation
(10A, 2 hrs; run 8-1)

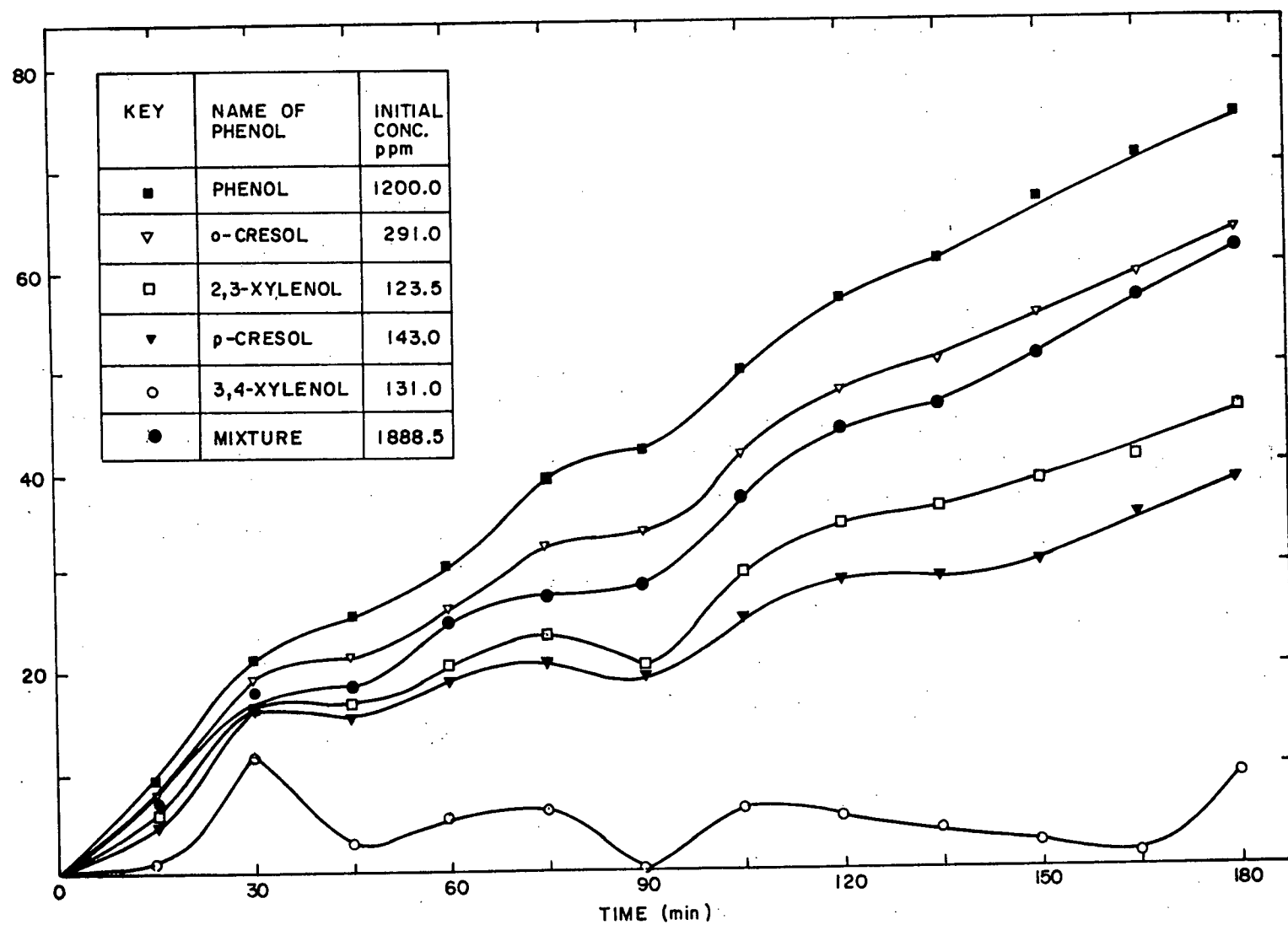


Fig. 33 Effect of nature of phenolics on % oxidation (10A, 3 hrs; run 8-2)

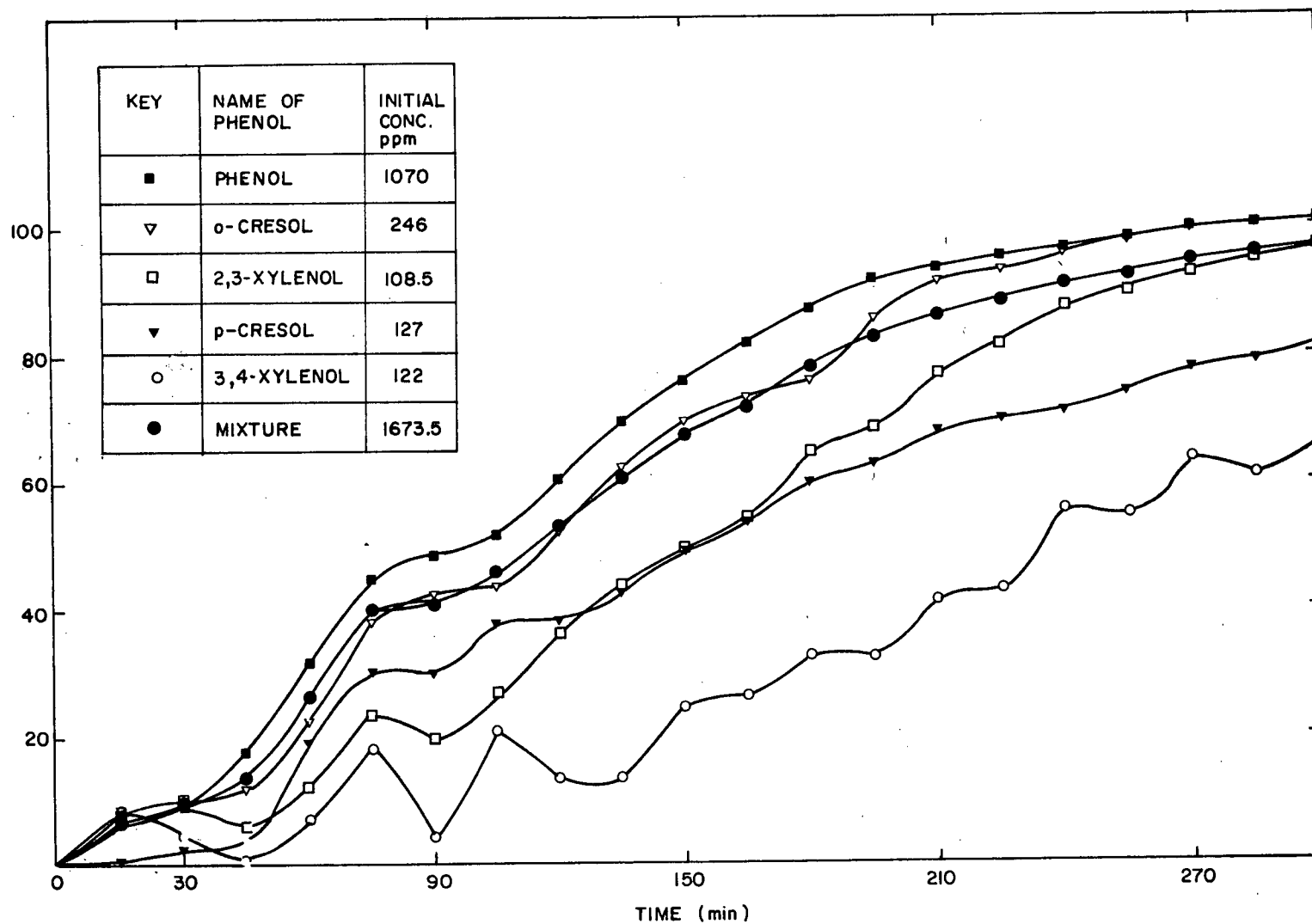


Fig. 34 Effect of nature of phenolics on % oxidation (10 A, 5 hrs; run 8-3)

From the GC/MS analysis of the treated solution, all the products obtained from the individual phenolic runs were identified. No product resulting from the interaction of the oxidation products of different phenolics was identified. This could be due to one of the following causes:

1) Conditions of the experiment were not favourable for the occurrence of any coupling reaction between the products.

2) Products of such interactions did not show up on the chromatograph either due to their different nature or due to their presence in negligible concentrations.

Although the phenolics maintain their individual behaviour even in the mixture, there is an irregular gradation in their rates of oxidation in all cases. This could be due to the different competing reactions taking place simultaneously.

A comparison is made between the T.O.C., B.O.D. and C.O.D. analysis of the initial and the treated sample from Run 8-3 in Table VI.

TABLE VI
RESULTS OBTAINED FROM THE OXIDATION OF MIXTURE
OF MONOHYDRIC PHENOLS (RUN 8-3) $i = 526 \text{ A/m}^{-2}$

Time min	T.O.C. mg/l	C.O.D. mg/l	B.O.D. mg/l
0	1480	4291	2783
300	1160	3502	1210
% Reduction	21.6	18.4	56.5

It can be noticed that the T.O.C. and C.O.D. reduction values are small and comparable whereas B.O.D. value is brought down to a value less than half the initial value. This B.O.D. reduction is comparable to the value obtained in biological treatment for five days [42].

5.4 Reaction efficiency for a typical run

It is apparent that the mechanism of anodic oxidation is complex. For example, consider the oxidation of phenol, run 9-1. The oxidation products reported are p-benzoquinone, hydroquinone and catechol. Besides about 4% of the organic carbon was converted into carbon dioxide and carbon monoxide. Benzoquinone is generated in the anode compartment with catechol, hydroquinone, carbon dioxide and oxygen, and it may be converted to hydroquinone at the cathode. If the process proceeds to produce only the above compounds, the sum of the current efficiencies for the formation of these products on the anode should be 1.0.

As gas analysis was not done, the fraction of carbon oxidized to CO and CO₂ is unknown, therefore current efficiency is reported assuming extreme values of the carbon monoxide to carbon dioxide ratios. The current efficiency (Appendix 4) is found to be 0.43 - 0.63 depending on the ratio of CO to CO₂ formed. Presumably there are other reactions occurring which account for the rest of the current. These reactions could be the formation of oxygen from water electrolysis or the formation of some other oxidation product that has not been identified.

Moreover, as no precaution has been taken to decrease the convection of benzoquinone to the cathode, reduction of benzoquinone to hydroquinone followed by the non-productive oxidation of that hydroquinone back to benzoquinone could account for a loss in current efficiency. However,

hydrogen evolution at the cathode would compete with the thermodynamically favoured reduction of benzoquinone at the cathode.

From the carbon balance, it can be seen that 21% of the carbon has not shown up in the products identified. Presumably there are other unidentified products which account for this discrepancy. Carbon loss could have also occurred due to deposition of tar products on the electrodes during the process.

5.5 Cell voltage

The cell voltage V is given by

$$\Delta V = V_{\min} + \eta_a + |\eta_c| + V_{\text{ohm}} \quad (12)$$

The variation between V_{initial} and V_{final} may be particularly dependent on V_{ohm} for a constant applied current. The potential drop across the packed bed should have been ideally measured by using probes at various points in the bed. However this drop was found to be very small in similar experiments when the potential profile was measured in a packed bed copper electrode under the conditions of constant current electrolysis [43].

V_{ohm} (Appendix 4) increases with the applied current. It is difficult to compare the change in cell voltage at different applied currents for a particular phenolic compound on the basis of V_{ohm} at different currents because η_a and η_c in eq. 12 will change with applied current. From Table VII it can be seen that the cell voltage increases during the anodic oxidation of 2,3-Xylenol, 3,4-Xylenol and catechol. With 2,3-Xylenol and catechol there was an excessive foaming and gas evolution. This would decrease the effective electrolyte conductivity according to the following equation

TABLE VII
VARIATION OF ΔV

Name of phenolic compound (Initial conc. 1 gpl)	5A runs		10A runs		15A runs	
	Initial ΔV volts	Final ΔV volts	Initial ΔV volts	Final ΔV volts	Initial ΔV volts	Final ΔV volts
Phenol	6.15	6.0	7.1	7.1	12.7	10.7
p-Cresol	5.4	5.4	7.9	7.5	12.4	10.8
O-Cresol	6.0	5.9	9.2	8.0	11.3	9.1
2,3-Xylenol	5.0	5.9	6.5	8.3	8.6	10.6
3,4-Xylenol	4.4	4.8	5.9	6.3	7.4	7.5
resorcinol	5.5	5.2	7.4	6.7	10.8	9.7
catechol	3.8	4.4	5.3	6.2	6.9	7.0

$$K_{eg} = K_e (1 - f)^{3/2} \quad (13)$$

where f is the fraction of gas in the electrolyte. It has been reported that depending on the gas loading, the effective conductivity of the electrolyte in the fixed bed can be lowered from 10-90% [44]. Therefore the ohmic drop would increase considerably and the cell voltage thus shows a distinct increase in these cases. The presence of the screen and water electrolysis increase this effect. With 3,4-Xylenol a similar increase in resistance is expected as indicated earlier (section 5.1.5).

A decrease in cell voltage is observed in several cases. This may be attributed to one of the following effects which can counteract the effect of gas evolution.

- 1) Increase in conductivity of the electrolyte due to either heating in the cell or due to the nature of the products formed. The conductivity of the electrolyte was found to increase in similar experiments [31].
- 2) An intermediate cathode reaction for example cathodic reduction of p-benzoquinone in phenol runs can occur at a high cathodic potential thus decreasing the effective cell voltage.
- 3) Physical changes may occur in the current feeders or the bed particles.

5.6 Comparison of experimental results with mathematical models

To test whether mass transfer of the phenolic compound from the bulk electrolyte to the surface of the electrode controls the rate of disappearance of the phenolic compound, calculations were performed with

2,3-Xylenol and resorcinol runs, in a manner similar to the calculations of Sucre [31].

Fractional conversion of the phenolic compound X was related with mass transfer groups (Appendix 3) by the following equation

$$X = 1 - \exp \left[\left\{ \exp \left(\frac{k_m aL}{u} \right) - 1 \right\} \frac{t}{t_m} - \frac{k_m aL}{u} \right] \quad (14)$$

The sample calculations (Tables A-1 and A-2) are represented as a band of conversion vs time in Figs. 16, 17, 22 and 23.

In Fig. 16, it can be seen that the curve corresponding to the lowest initial concentration (97 mg/l) approaches the mass transfer-controlled region in 15 minutes. Between 30 and 45 minutes, the theoretical and experimental curves coincide in this case, while with the initial concentration of 625 mg/l, the curve almost coincides with the theoretical region after 60 minutes. Thus in the case of 2,3-Xylenol runs where enhancement of mass transport by foaming may be expected as described by Nanis et al [45], the rate of oxidation seems to be controlled by mass transfer at initial concentrations in the range of 0.1 g/l. In fact in run 4.4 (initial concentration 97 mg/l), in about 45 minutes the experimental curve exceeds the theoretical region. At this point, it is hard to conclude whether this can be attributed to the excessive gas evolution, although it seems likely from Fig. 17 where the curve representing the rate of oxidation at an applied current of 5A is far below the mass transfer controlled region. It may be recalled that in this particular run, gas evolution was not distinct. At the highest applied current (15A) the experimental curve approaches the theoretical region only after 90 minutes with higher initial concentrations (1 g/l).

Considering the effect of increasing the initial concentration in

the runs with resorcinol (group 6) Fig. 22 where there was no foaming or noticeable gas evolution the experimental curves are closer to the mass transfer controlled region. It should be remembered, however that the diffusivity of resorcinol molecules is larger than that of 2,3-Xylenol although the change in diffusivity has been taken into account in calculating the theoretical mass transfer region.

Fig. 23 leads again to the suspicion about the role of gas evolution in mass transfer. It can be observed that at higher initial concentration of resorcinol, unlike the observation made with 2,3-Xylenol the experimental curve is far below the theoretical region even at the highest applied current (Run 6-3).

Any discussion of the above effects depends on the accuracy or applicability of the mass transfer coefficient correlation used. Although the equation of Pickett and Stanmore [46] used in Ref. 31 has been modified to improve its applicability to present case by considering the correction with a double layer of packed bed based on the suggestions in Ref. 10, pg.161, it is still a poor correlation for a gas evolving, randomly packed bed electrode. The equations used in the present study to determine k_m are

$$Sh = 0.66 Re^{0.56} Sc^{0.33} \quad (15)$$

$$Sh = 0.62 Re^{0.56} Sc^{0.33} \quad (16)$$

There are correlations [47] relating the volume of gas evolved to mass transfer coefficient which show that when there is hydrogen or oxygen evolution, the rate of mass transfer increases. Correlations are also

available for electrochemical processes involving gaseous reactants [48]. The overall capacity coefficient for mass transfer in the present set up can be calculated from equations of the type

$$k_o a = k_m a (1 + V_g)^n \quad (17)$$

where V_g , the volume of gas evolved would be needed. As the pressure drop was not measured, a more accurate calculation of mass transfer coefficient has not been attempted.

CHAPTER 6

CONCLUSIONS

An investigation was made of the anodic oxidation of major phenolics in coal processing waste from the point of view of effluent treatment. Experiments were performed with phenol, O-cresol, p-cresol, 2,3-Xylenol, 3,4-Xylenol, resorcinol, catechol and mixtures of the five monohydric phenols.

1. Generally, the percentage oxidation of the phenolics in a given time was favoured by increasing the applied current and decreasing the initial concentration of the phenolics.

2. Complete oxidation of the organic carbon under present conditions of 5 l of phenolic solution with concentration range 0.1 g/l to 1 g/l of phenolic compound recirculated for a two hour period, occurred to a significant extent only in the case of 2,3-Xylenol, resorcinol and catechol.

3. From the comparison of the performance of different phenolics, there is no simple correlation of the rates of oxidation with the structure and diffusivity of the phenolic compounds. The observed order of decreasing reaction rate at an applied current of 10A with an initial concentration of 1 g/l of the phenolic compounds was phenol, 2,3-Xylenol, resorcinol, p-cresol, 3,4-Xylenol, o-cresol.

4. When the synthetic mixture of five monohydric phenols present at concentrations corresponding to a typical coal conversion waste was oxidized, about 96% of the phenolics were oxidized in 5 hours. The ease with which the phenolics were oxidized was as follows

phenol > O-cresol > 2,3-Xylenol > p-cresol > 3,4-Xylenol

As a result of the treatment, T.O.C. and C.O.D. were reduced by about 20% while the reduction in the B.O.D. value was about 56%.

5. The products of the oxidation process were identified for typical runs of the individual phenolics and phenolic mixture. From the nature of the products and observations made in the runs, possible routes for the oxidations were proposed in most cases. Most of the oxidation products were in the form of quinones or hydroquinones. None of these oxidation products have been included [49] in the EPA list of organic priority pollutants.

6. Comparison of the experimental results from two different sets of runs with a mass transfer model indicated that the depletion of phenolics is controlled by mass transfer when the concentration of the phenolic compound is low.

CHAPTER 7

FURTHER WORK

Further investigation of the electrochemical treatment of coal conversion effluents would contribute the establishment of the technical feasibility of the process. To obtain a complete understanding of the process, the following recommendation are made on the basis of this study.

1. Routine analysis of the gaseous products by Orsat or gas chromatographic analysis should be attempted. The oxidation products should be monitored periodically and a complete GC/MS analysis should be performed on all the samples. This would lead to

- a) Presentation of a complete study on the effect of current density [50] and % current efficiency utilized in the formation of different anodic oxidation products.
- b) Formation of definite conclusions about effluent quality under different operating conditions.

2. Electrode potential variations should be determined by using reference electrodes located at certain points in the bed. This would assist with the modelling of the process.

3. The rotating disc electrode can be used with all of the above phenolics to elucidate the kinetics of electrooxidation under different operating conditions.

4. For future experiments with the packed bed a series of filters provided with valves should be added to the recycle loop of the equipment to prevent the buildup of the suspended condensation product during prolonged periods of operation.

5. The work should be extended to the study of treatment of all the chemicals in coal processing effluents and hence the actual effluent.

6. As an electrochemical process has several advantages over chemical oxidation process [51] the present process should be scaled up for continuous runs. As a part of the water purification system for industrial wastes, a larger cell assembly with a multiplicity of treating zones would be required.

7. Studies should be performed to test the application of anodic oxidation as a final polishing step after biological or any other treatment that is not capable of destroying the phenolics completely. A packed bed, if sufficiently long and appropriately polarized, can possibly function as an electrochemical filter which will reduce the concentration of all electrochemically oxidisable species to a level that can be desirably low for optimum biological treatment. This suggests the possibility of use of anodic oxidation as a prior step to any other treatment.

NOMENCLATURE

		<u>Typical units</u>
a	specific surface area of the bed	m^2/m^3
i	current density referred to the surface area of the feeder plate	A/m^2
C.E	current efficiency	
C_O	concentration of the oxidized form at the point of discharge	mg/l
CA_b	concentration of reactant in the bulk of solution	mg/l
CA_s	concentration of reactant at the surface of the electrode	mg/l
Cr	concentration of the reduced form at the point of discharge	mg/l
dp	average particle diameter	m
D	diffusivity of the phenolic compound in water	m^2/s
D_{Ox}, D_{Red}	diffusion coefficients	
E	half wave potential	V
ΔE	shift in half wave potential	
F	Faraday's constant	coul/g equiv.
f_{ox}, f_{Red}	activity coefficients	
I	applied current	A
k_r	electrochemical reaction rate constant	m/s
k_m	mass transfer coefficient	m/s
k_{Oa}	overall capacity coefficient	
Keg	effective electrolyte conductivity	$(\Omega\text{m})^{-1}$
K	equilibrium constant	

		<u>Typical units</u>
L	length of the cell	m
N	electrolyte flow rate	m ³ /s
R	universal gas constant	kJ/k mol °K
Re _{dp}	Reynolds number based on particle diameter	
Sc	Schmidt number	
S	thickness of the bed (in the direction of current)	m
T	temperature	°K
t	time of electrolysis	S
t [*]	dimensionless time	
t _m	residence time in the mixing tank	S
u	superficial velocity	m/s
V _a [*]	anode potential	V
V _c [*]	cathode potential	V
V _{min}	minimum cell voltage	V
ΔV	total cell voltage	V
V _{ohm}	ir drop in electrolyte	V
W	width of the bed	m
X	phenol fractional conversion	
y	variable length of the bed	m
z	number of electrons associated with the anodic oxidation	

Greek Letters

α	transfer coefficient	
Ø	experimental flow rate of electrolyte	m ³ /sec

Typical units

ϵ	voidage of the bed	
ξ	shape factor for the particles	
θ	$\frac{k_m a L}{u}$ dimensionless mass transfer group	
ν	kinematic viscosity of water	(cm ² /s)
η_a	overpotential for the anodic reactions	V
η_c	overpotential for the cathodic reactions	V
ϕ_x	association parameter of solvent	
μ	viscosity	cp

BIBLIOGRAPHY

1. Lanouette, K. "Treatment of phenolic wastes." Chem. Eng. 84, 99 (Oct. 1977).
2. "Control technology assessment." Environmental review of synthetic fuels 2, 3 (May 1979).
3. Assessment of coal conversion wastewaters: Characterization and preliminary biotreatability, PB-294338, EPA-600/7-78-181, 94 (Sept. 1978).
4. Throop, M.W. "Alternative methods of phenol waste water control." Journal of Hazardous Materials 1, 319 (1975/77).
5. Katzer, J., Sadana, A., and Ficke, H. "Aqueous phase catalytic oxidation as a waste water treatment technique." Eng. Ext. Series 145, 29 (1974).
6. Kazuo, S., Kazuto, T., and Satoru, T. "Degradation of aqueous phenol solutions by gamma irradiation." Environmental Science and Technology 12, No. 9, 1043 (1978).
7. Zeff, J. "UV. ox. process for the effective removal of organics in waste water." A.I.Ch.E. Symposium Series 73, No. 167, 206 (1976).
8. Surflett, B. "Electrolytic destruction of industrial effluents." The Electricity Council Research Centre. Report No. 204 (Oct. 1969).
9. Smith De Sucre, V., and Watkinson, A.P. "Anodic oxidation of phenol for waste water treatment." Can. J. Chem. Eng. 59, 52 (1981).
10. Pickett, D.J. Electrochemical reactor design. Elsevier, Amsterdam (1977).
11. Sherwood, T.K., Pigford, R.L., and Wilke, C.R. Mass Transfer. McGraw Hill, New York (1975).
12. Fichter, F. "Electrochemical oxidation of aromatic hydrocarbons." Trans Amer. Electrochem. Soc. 45, 107 (1924).
13. Fichter, F., and Stocker, R. "Electrochemical oxidation of aromatic hydrocarbons and phenols." Chem. Abstr. 8, 3037 (1914).
14. Fichter, F., and Brunner, E. "New products of the electrochemical oxidation of phenol." Chem. Abstr. 10, 2873 (1916).

15. Gladisheva, A.I., and Lavrenchuck, V.I. "Electrochemical oxidation of phenol." (original title in Russian). Uch. Zap. Tsent. Nauch. Issled. Inst. Glovyan. Prom, No. 1, 68 (1966); Chem. Abstr. 67, 28639X (1967).
16. Tarjanji, M. et al. "Decreasing the phenolic content of liquids by an electrochemical technique." U.S. Pat. 3,730,864 (May 1, 1973).
17. Covitz, F. "Electrochemical oxidation of phenol." U.S. Pat. 3,509,031. (Apr. 28, 1970).
18. Jones, G.C., et al. "Electrolytic oxidation of phenol at lead thallium anodes." U.S. Pat. 4,035,253 (July 12, 1977).
19. Jones, G.C., and Payne, D.A. "Electrochemical oxidation of phenol." U.S. Pat. 3,994,788. (Nov. 30, 1976).
20. Fioshin, M.Y., et al. "Electrochemical oxidation of phenol to quinone." Elektrokhimiya 13, No. 3, 381 (1977).
21. Swanton, J.C., Synder, R.E., and Clark, R.O. "Voltammetric studies of phenol and aniline ring substitution." Anal. Chem. 33, 1894 (1961).
22. Ross, D.S., Finkelstein, M., Rudd, J.E. Anodic Oxidation. Academic Press, New York (1975).
23. Nilson, A., Ronlan, A., and Parker, V. "Anodic oxidation of phenolic compounds." Journal Chem. Soc. Perkin trans. I 20, 2337 (1973); Chem. Abstr. 80, 115431k (1974).
24. Ronlan, A. "Phenols." Encyclopaedia of electrochemistry of the elements. M. Dekkar, New York, Vol. XI, 270 (1978).
25. Nash, R.A., Skauen, D.M., and Purdy, W.C. "The polarographic behaviour of certain antioxidants at the wax impregnated graphite electrode." J. Amer. Pharm. Ass. 47, 433 (1958).
26. Elwing, P.J., and Krivis, A.F. "Voltammetric studies with the graphite indicating electrode." Anal. Chem. 30, 1645 (1958).
27. Sivaramiah, G., and Krishnan, V.R. "Kinetics and mechanism of controlled potential coulometric oxidation of catechol." Indian J. Chem. 4, 541 (1966).
28. Dawson, C.R., and Nelson, J.M. "The influence of catechol on the stability of O-benzoquinone in aqueous solutions." J. Amer. Chem. Soc. 60, 245 (1938).
29. Wagreich, H., and Nelson, J.M. "On the mechanism of the catechol-tyrosinase reaction." J. Amer. Chem. Soc. 60, 1545 (1938).

30. Sakelliaropoulos, P.G. "Criteria for selective path promotion in electrochemical reaction sequences." *AIChE Journal*, 25, No. 5, 781 (1979).
31. Sucre, V.S. "Electrochemical oxidation of phenol for waste water treatment." M.A.Sc. thesis. The University of British Columbia (Aug. 1979).
32. Chu, A.K.P., Fleischmann, M., and Hills, G.J. "Packed bed electrodes. I. The electrochemical extraction of copper ions from dilute aqueous solutions." *J. App. Electrochem.* 4, 323 (1974).
33. Carr, J.P., and Hampson, N.A. "The lead dioxide electrode." *Chem. Rev.* 72, No. 6, 679 (1972).
34. Ronlan, A., "Phenols." Encyclopaedia of electrochemistry of the elements. M. Dekkar, New York, Vol. XI, 242 (1978).
35. Rifi, M.R., and Covitz, F.H. Introduction to organic electrochemistry. M. Dekkar, New York (1974).
36. Shields, J.R., and Coull, J. "Rate studies in the electrochemical oxidation of phenol." *Trans. Am. Electrochem. Soc.* 80, 113 (1941).
37. Vladimir, K. "Analysis of dihydric phenols by gas chromatography." *J. Chromatogr.* 57, 132 (1971).
38. Wesley, W. Water quality engineering for practicing engineers. Barnes & Noble, New York, (1970).
39. Standard methods for the examination of water and waste water. Thirteenth edition, APHA.AWWA.WPCF (1971).
40. Papouchado, L., et al. "Anodic oxidation pathways of phenolic compounds, Part 2 Stepwise electron transfers and coupled hydro-oxylations." *J. Electroanal. Chem.* 65, 275 (1975).
41. Zuman, P. The elucidation of organic electrode processes. Academic Press, New York (1969).
42. Singer, P.C., et al. Report Summary: Treatability and assessment of coal conversion wastewaters: Phase 1, EPA-600/7-79-248 (June 1980).
43. Yoshizawa, S., et al. "Cathodic reduction of nitrobenzene on the packed bed copper electrode." *Bulletin of the Chemical Society of Japan*, 49, No. 11, 2889 (1976).
44. Neale, G.H., and Nader, W.K. "Prediction of transport processes within porous media: Diffusive flow processes within an homogeneous swarm of spherical particles." *A.I.Ch.E. Journal*, 19, 112 (1973).

45. Nanis, L., and McLaren, F. "Rapid mass transport to electrodes in foamed electrolyte." J. Electrochem. Soc. 117, 1527 (1970).
46. Pickett, D.J., and Stanmore, B.R. "An experimental study of a single layer packed bed cathode in an electrochemical flow reactor." J. App. Electrochem. 5, 95 (1975).
47. Sedahmed, G.H. "Mass transfer behaviour of gas evolving particulate-bed electrode." J. App. Electrochem. 9, 37 (1979).
48. Oloman, C. "Trickle bed electrochemical reactors." J. Electrochem. Soc. 126, No. 11, 1885 (1979).
49. Patterson, J.W., and Kodukala, P.S. "Biodegradation of hazardous organic pollutants." CEP, 77, No. 4, 48 (1981).
50. Oloman, C. "Electro-oxidation of benzene in a fixed bed reactor." J. App. Electrochem. 10, 553 (1980).
51. Weinberg, N.L., and Weinberg, H.R. "Electrochemical oxidation of organic compounds." Chem. Rev. 68, No. 4, 445 (1968).
52. Li, K.Y., Kuo, C.H., and Weeks, J.L. "Kinetic study of ozone-phenol reaction in aqueous solutions." A.I.Ch.E. Journal, 25, No. 4, 583 (1979).
53. Brockmann, H.E., and Oke, T.O. "Gas chromatography of barbiturates, phenolic alkaloids and xanthene bases, flash heater methylation by means of trimethyl anilinium hydroxide." J. of Pharm. Sci. 58, 370 (1969).
54. Perry, R.H., and Chilton, C.H. Chemical engineers handbook. Fifth edition, McGraw Hill, New York (1973).
55. Reid, C.R., and Sherwood, T.K. The properties of gases and liquids. Second edition, McGraw Hill, New York (1966).
56. Hayduk, W., and Laudie, H. "Prediction of diffusion coefficients for nonelectrolytes in dilute aqueous solutions." A.I.Ch.E. Journal 20, 611 (1974).

APPENDIX 1

Specification of Auxilliary Equipment and Materials

Power supply

Sorenson DCR 4D-25B

Voltmeter range: 0-40V

Ammeter range: 0-30A (smallest division = 1 A)

Voltmeter

Central Sceintific Co., D.C. Voltmeter

Scales: 0-1.5 Volts (smallest division = .010 V)

0-15 Volts (smallest division = .10 V)

Rotameter

Brooks, full view indicating rotameter

Type: 7-1110

Tube No.: R-7M-25-1

Float: 316 stainless steel

Max. flow: 1400 cc/min (s.g. = 1)

Scale: 0-100% linear

Gas liquid separators

2.5 cm I.D. and 60 cm long glass tube. Liquid outlet located at 40 cm from the bottom (except for group VII where the inlet and outlet were interchanged) bed: 2 mm diameter glass beads.

Filter

3.0 cm I.D. and 15 cm long glass tube filled with glass wool (Merck).

Pressure gauge

Marsh-type 3-100-SS with 316 stainless steel tube scale 0-30 psi ($\frac{1}{4}$ psi/div)

Pump

Barrish Pumps Co., N.Y.

Model type: 12A-60-316

Flow data: 21 G.P.H. at 40 psid, 29 G.P.H. at 0 psid.

(psid indicates differential pressure)

Pump preset at 45 psid.

pH meter

Corning, Model 701A/digital ionalyzer (accuracy ± 0.01 pH)

Electrode: BJC-combination electrode

Tubings

1. Imperial Eastman "Poly Flo" 66-P-3/8".
2. PVC $\frac{1}{2}$ " schedule 40 piping.

Valves

1. Whitey, forged body regulating, 316 S.S. 3/8" connections.
2. PVC- $\frac{1}{2}$ " valve (chemline plastic).

Fittings

Swagelok compression tubing fitting

316 S.S. 3/8"

Plastic screen

Supplied by Chicopee Manufacturing Co., Georgia

Saran type

Max. operating temperature = 125°F

Chemical resistance: good resistance to acids and most alkalis

top layer, style 6100900, weight/sq.yd. = 7 oz.

bottom layer, style 61010XX, weight/sq.yd. = 10.6 oz.

Analytic equipment and operating conditions specifications

a) Gas chromatography specifications

Gas chromatograph

Manufacturer: Varian Aerograph

Model: 1440 series, single column model

Detection: H₂ flame ionization detector

Chromatographic columns

Supplier: Western Chromatography Supplies, New Westminster, B.C.

Material: glass

1. Column used for analysis of monohydric phenols

Dimensions: 2 mm I.D., 6.4 mm O.D., 6 feet long

Packing: 10% SP-2100 on 100/120 Supelcoport (details of the packing

are given in Bulletin 742D by Supelco, Inc.).

Operating conditions

Injector port temperature 150°C

Column temperature 130°C (brought to 115°C for analysis of phenolic mixtures)

Detector temperature 175°C

Carrier gas N₂ or He

Carrier gas flow 30 ml/min

Air flow 300 ml/min

H₂ flow 30 ml/min

Attenuation - varied for different concentrations

Recorder

Model: Sargent SRG-GC, Serial number 237 0073

Response 1 mV full scale

2. Column used for analysis of dihydric phenols

Dimensions: 2 mm I.D., 6.4 mm O.D., 1 m long

Packing: Porapak P (80/100 mesh) - support

Carbonax 20 M - stationary phase

Operating conditions

Injector port temperature 260°C

Column temperature 220°C

Detector temperature 280°C

Carrier gas He (oxygen content under 10 p.p.m)

Carrier gas flow 22 ml/min

Air flow 300 ml/min

H₂ flow 37 ml/min

Recorder

Model: Watanabe MC 641, Serial number 575283

Response 1 mV full scale

3. Column attempted for catechol analysis [52,53]

Dimensions: 2 mm I.D., 6.4 mm O.D., 1 m long

Packing: 3% OV-17 on chromosorb W (HP) 80/100 mesh

Operating conditions

Injection port temperature 300°C

Column temperature 140°C

Detector temperature 300°C

Carrier gas He

Carrier gas flow 40 ml/min

Air flow 300 ml/min

H₂ flow 40 ml/min

Recorder

Model: hp 17505 A

Range 0.1-100 MV

Syringe

Supplier: Unimetrics

Sample size: 1 µl

b) T.O.C. analysis specifications

Model: Beckman 915 total organic carbon

Analyzer: Beckman 865 infrared analyzer

Operating Conditions

Temperature of the total carbon channel 1000°C

Oxygen flow 250 ml/min

Syringe

Hamilton with automatic plunger

Sample size 50 μ l

Recorder

Model: Hewlett Packard 7127A

Response: 1 mV full scale

Chart speed: 1 cm/min

c) GC/MS Analysis specifications

Manufacturer: Hewlett-Packard

Model: 5985B (Quadrupole mass spectrometer)

Fully interactive data system

HP-1000 series computer

Chromatographic column

Supplier: Hewlett-Packard

Material: Fused silica capillary

Dimensions: 0.32 mm I.D. 25 metres long

Liquid phase: SE-54 (Silicone gum)

Operating conditions

Injection port temperature 260°C

Temperature program 30°C to 260°C at 8°C/min

Carrier gas He

Linear velocity: 50-80 cm/sec

Mass spectrometer conditions

Mode of ionization: Electron Impact (70 eV)

Ion source temperature: 200°C

Electron multiplier: 1600-2000 V

- (1) Run time 40
- (2,3,4) Start, stop masses 41,500 amv
- (6) A/D Measurements per datum point [3.0]i
- (7) Threshold 40 min
- (8) Scan start delay i
- (14) Ion source temperature [202.0]

Solid Probe Inlet conditions

Temperature program: 30°C to 250°C at 25°C/min

Reagents

Phenol - loose crystals, reagent grade

Matheson Coleman & Bell

p-Benzoquinone - Practical

Matheson Coleman & Bell

Silver Nitrate - Fine reagent

MBW Chemicals

Sodium Sulfate - Anhydrous, granular, Analytical grade

Mallinckrodt

Sodium Hydroxide - pellets, reagent

American Scientific and Chemical

Sulfuric acid - reagent A.C.S.

Allied Chemical

Buffer - Fisher Scientific (2 ± 0.02)

p-cresol, o-cresol - crystalline

BDH Laboratory Chemicals group

Resorcinol - laboratory grade

Fisher Scientific Company

Catechol - Pyrocatechin (resublimed)

Fisher Scientific Company

2,3-Dimethyl phenol
3,4-Dimethyl phenol - laboratory grade

Fisher Scientific Company

Magnesium Sulfate - Anhydrous, powder, Analytical reagent

Mallinckrodt

Methylene chloride - Dow Chemical of Canada Ltd.

Methylating agent (Methelute)

Pierce Chemicals Co. Rockford

Water for solutions - Laboratory, single distilled water

APPENDIX 2

Experimental Data

Characteristics for all experiments

a) Mode of operation:

Batch experiments using undivided cell

b) Cell description:

Cathode: stainless steel 316 plate

Anode: PbO_2 electrodeposited on graphite feeder plate

Particles: electrodeposited PbO_2 crushed and sized (obtained from
Pacific Engineering and Production Co., Nevada)

Size: $0.7 < d_p < 1.1 \text{ mm}$

Weight: 250 gm

$$\text{Volume: } \frac{250}{11.337 \text{ g/c.c.}} = 22 \text{ cm}^3 \quad [54]$$

$$\text{Void fraction } (\epsilon) = \frac{54-22}{54} = 0.59$$

Separation: two layers of saran screen between cathodic plate and
 PbO_2 particles. Electroplaters tape used for adhesion
where necessary.

Group I	Anodic oxidation of Phenol
Group II	Anodic oxidation of p-Cresol
Group III	Anodic oxidation of o-Cresol
Group IV	Anodic oxidation of 2,3-Xylenol
Group V	Anodic oxidation of 3,4-Xylenol
Group VI	Anodic oxidation of Resorcinol

Group VII Anodic oxidation of catechol

Group VIII Anodic oxidation of mixture of monohydric phenolics of interest

Group IX Anodic oxidations for GC/MS analysis

Temperatures

All experiments were set up at a temperature of 22-24°C with the use of heat exchanger except in the groups IV, V and VIII which were carried out at 40-45°C.

Anodization

Before each experiment the anode was treated with 20% H_2SO_4 at 10 A (2.5-3.5 Volts) for 1 hour.

RUN 1-1

Electrolyte	I(A)	$i(A/m^{-2})$	ϕ (c.c/min)	Initial pH
5 g/l Na_2SO_4 0.44 g/l H_2SO_4 1 gm/l phenol	10	526.3	770	1.9

t (min)	ΔV (volts)	phenol mg/l	% oxidized
0	7.10	910	0
15	7.10	750	17.6
30	7.10	635	30.2
45	7.10	480	47.3
60	7.10	350	61.5
75	7.10	300	67.0
90	7.10	200	78.0
105	7.10	140	84.6
120	7.10	95	89.6

Comment: The net change in T.O.C. was practically undetectable due to the high amount of carbon present in solution.

RUN 1-2

Electrolyte	I(A)	$i(\text{A/m}^{-2})$	ϕ (c.c/min)	Initial pH
5 g/l Na_2SO_4 0.44 g/l H_2SO_4 1 g/l phenol	5	263.2	719.25	2.16

t (min)	ΔV (volts)	phenol mg/l	% oxidized
0	6.15	970	0
15	6.15	875	9.8
30	6.15	750	22.7
45	6.10	670	30.9
60	6.10	595	38.7
75	6.05	533	45.1
90	6.00	432	55.5
105	6.00	330	66.0
120	6.00	291	70.0

RUN 1-3

Electrolyte	I(A)	$i(\text{A/m}^{-2})$	ϕ (c.c/min)	Initial pH
5 g/l Na_2SO_4 0.44 g/l H_2SO_4 1 g/l phenol	15	789.5	679	2.11

t (min)	ΔV (volts)	phenol mg/l	% oxidized
0	12.70	1010	0
15	12.70	805	20.3
30	12.65	545	46.0
45	11.50	480	52.5
60	11.30	350	65.4
75	11.00	265	73.8
90	11.00	195	80.7
105	10.60	130	87.1
120	10.70	80	92.1

RUN 1-4

Electrolyte	I(A)	$i(A/m^{-2})$	ϕ (c.c/min)	Initial pH
5 g/l Na_2SO_4 0.44 g/l H_2SO_4 0.1 g/l phenol	10	526.3	770	2.33

t (min)	ΔV (volts)	phenol mg/l	% oxidized	T.O.C. mg/l	% oxidized
0	7.40	108	0	84.5	0
15	7.20	46	57.4	82.0	3.0
30	6.90	12	88.9	79.0	6.0
45	6.65	2	98.2	78.0	7.0
60	6.60	0	100.0	73.5	13.0
75	6.50			72.0	14.0
90	6.50			70.3	17.0
105	6.40			69.0	18.0
120	6.40			66.0	22.0

Comment: T.O.C. reported is actually the total carbon because the concentration of inorganic carbon and its variation was negligible in all cases.

RUN 1-5

Electrolyte	I(A)	$i(\text{A/m}^{-2})$	ϕ (c.c/min)	Initial pH
5 g/l Na_2SO_4 0.44 g/l H_2SO_4 0.5 g/l phenol	10	526.3	784	2.56

t (min)	ΔV (volts)	phenol mg/l	% oxidized	T.O.C. mg/l	% oxidized
0	8.40	683	0	555	0
15	8.35	467	31.6	535	4.0
30	8.40	305	55.3	525	6.0
45	8.40	208	69.6	520	7.0
60	8.60	168	75.4	508	9.4
75	8.65	160	76.6	498	11.4
90	8.70	168	75.4	485	14.0
105	8.70	168	75.4	475	16.0
120	8.70	168	75.4	455	18.0

RUN 2-1

Electrolyte	I(A)	$i(\text{A/m}^{-2})$	ϕ (c.c/min)	Initial pH
5 g/l Na_2SO_4 0.44 g/l H_2SO_4 1 g/l p-cresol	10	526.3	623	2.3

t (min)	ΔV (volts)	p-cresol mg/l	% oxidized
0	7.9	823	0
15	8.20	780	5.2
30	8.00	625	24.1
45	7.80	540	34.4
60	8.30	485	41.1
75	8.15	433	47.4
90	7.50	390	52.6
105	7.70	355	56.9
120	7.50	305	62.9

RUN 2-2

Electrolyte	I(A)	$i(\text{A/m}^{-2})$	ϕ (c.c/min)	Initial pH
5 g/l Na_2SO_4 0.44 g/l H_2SO_4 1 g/l p-cresol	5	263.2	64.1	2.1

t (min)	ΔV (volts)	p-cresol mg/l	% oxidized
0	5.40	1100	0
15	5.60	960	12.7
30	5.45	920	16.4
45	5.45	860	21.8
60	5.50	740	32.7
75	5.45	720	34.6
90	5.45	710	35.5
105	5.45	640	41.8
120	5.40	590	46.4

RUN 2-3

Electrolyte	I(A)	$i(\text{A/m}^{-2})$	ϕ (c.c/min)	Initial pH
5 g/l Na_2SO_4 0.44 g/l H_2SO_4 1 g/l p-cresol	15	789.5	616	2.40

t (min)	ΔV (volts)	p-cresol mg/l	% oxidized
0	12.4	1100	0
15	11.6	775	29.6
30	11.1	625	43.2
45	11.1	545	50.5
60	11.0	535	51.4
75	10.9	470	57.3
90	11.0	450	59.1
105	10.8	365	66.8
120	10.8	325	70.5

RUN 2-4

Electrolyte	I(A)	$i(\text{A/m}^{-2})$	ϕ (c.c/min)	Initial pH
5 g/l Na_2SO_4 0.44 g/l H_2SO_4 0.1 g/l p-cresol	10	526.3	672	1.74

t (min)	ΔV (volts)	p-cresol mg/l	% oxidized	T.O.C. mg/l	% oxidized
0	8.00	69	0	72.0	0
15	7.50	40	41.3	70.2	2.5
30	7.40	26	61.6	69.3	3.8
45	7.30	19	72.5	68.4	5.0
60	7.20	15	79.0	68.1	5.4
75	7.30	11	84.8	66.7	7.4
90	7.40	9	87.0	62.9	12.6
105	7.50	8	88.4	61.1	15.2
120	7.50	6	91.3	60.1	16.6

RUN 2-5

Electrolyte	I(A)	$i(\text{A/m}^{-2})$	ϕ (c.c/min)	Initial pH
5 g/l Na_2SO_4 0.44 g/l H_2SO_4 0.5 g/l p-cresol	10	526.3	668.5	2.36

t (min)	ΔV (volts)	p-cresol mg/l	% oxidized	T.O.C. mg/l	% oxidized
0	8.7	355	0	300	0
15	8.5	300	15.5	300	0
30	8.3	223	37.2	300	0
45	8.0	208	41.4	300	0
60	7.9	193	45.6	300	0
75	7.8	168	52.7	300	0
90	7.5	140	60.6	300	0
105	7.7	125	64.8	299	0.3
120	7.6	115	67.6	292	2.7

RUN 3-1

Electrolyte	I(A)	$i(A/m^{-2})$	ϕ (c.c/min)	Initial pH
5 g/l Na_2SO_4 0.44 g/l H_2SO_4 1 g/l 0-cresol	10	526.3	658	2.34

t (min)	ΔV (volts)	0-cresol mg/l	% oxidized
0	9.2	853	0
15	8.6	790	7.4
30	8.0	735	13.8
45	7.9	600	29.7
60	8.0	555	34.9
75	8.0	470	44.9
90	8.0	405	52.5
105	8.0	368	56.9
120	8.0	300	64.8

RUN 3-2

Electrolyte	I(A)	$i(\text{A/m}^{-2})$	ϕ (c.c/min)	Initial pH
5 g/l Na_2SO_4 0.44 g/l H_2SO_4 1 g/l 0-cresol	5	263.2	658	2.43

t (min)	ΔV (volts)	0-cresol mg/l	% oxidized
0	6.0	995	0
15	5.9	978	1.7
30	6.0	905	9.1
45	6.0	770	22.6
60	6.0	742	25.4
75	5.9	715	28.1
90	5.9	620	37.7
105	5.9	572	42.5
120	5.9	535	46.2

RUN 3-3

Electrolyte	I(A)	$i(A/m^{-2})$	ϕ (c.c/min)	Initial pH
5 g/l Na_2SO_4 0.44 g/l H_2SO_4 1 g/l 0-cresol	15	789.5	630	2.61

t (min)	ΔV (volts)	0-cresol mg/l	% oxidized
0	11.3	905	0
15	10.0	855	5.5
30	9.5	657	25.4
45	9.3	585	35.4
60	9.1	515	43.1
75	9.0	400	55.8
90	9.0	310	65.8
105	9.0	220	75.7
120	9.1	170	81.2

RUN 3-4

Electrolyte	I(A)	$i(\text{A/m}^{-2})$	ϕ (c.c/min)	Initial pH
5 g/l Na_2SO_4 0.44 g/l H_2SO_4 0.1 g/l 0-cresol	10	526.3	686	2.35

t (min)	ΔV (volts)	0-cresol mg/l	% oxidized	T.O.C. mg/l	% oxidized
0	8.0	95	0	90	0
15	7.8	65	31.6	85	5.6
30	7.6	33	65.3	83	7.8
45	7.5	17	82.1	83	7.8
60	7.5	13	86.3	-	-
75	7.5	7	92.6	82	8.9
90	7.5	5	94.7	81	10.0
105	7.7	3	96.8	80	11.1
120	7.7	3	96.8	80	11.0

RUN 3-5

Electrolyte	I(A)	$i(A/m^{-2})$	ϕ (c.c/min)	Initial pH
5 g/l Na_2SO_4 0.44 g/l H_2SO_4 0.5 g/l O-cresol	10	526.3	669	2.48

t (min)	ΔV (volts)	O-cresol mg/l	% oxidized	T.O.C. mg/l	% oxidized
0	8.1	505	0	570	0
15	7.7	395	21.8	545	4.39
30	7.5	320	36.6	545	4.39
45	7.3	265	47.5	545	4.39
60	7.3	238	52.9	545	4.39
75	7.2	198	60.8	545	4.39
90	7.2	165	67.3	545	4.39
105	7.2	115	77.2	528	7.37
120	7.2	88	82.6	520	8.77

RUN 4-1

Electrolyte	I(A)	$i(\text{A/m}^{-2})$	ϕ (c.c/min)	Initial pH
5 g/l Na_2SO_4 0.44 g/l H_2SO_4 1 g/l 2,3-Xylenol	10	526.3	784	2.54

t (min)	ΔV (volts)	2,3-Xylenol mg/l	% oxidized	T.O.C. mg/l	% oxidized
0	6.5	625	0	578	0
15	6.6	455	27.2	560	3.1
30	6.8	325	48.0	550	4.8
45	7.3	205	67.2	525	9.2
60	7.7	140	77.6	515	10.9
75	7.9	75	88.0	500	13.5
90	8.1	22	96.5	495	14.4
105	8.2	0	100.0	483	16.4
120	8.3	0	100.0	458	20.8

RUN 4-2

Electrolyte	I(A)	$i(\text{A/m}^{-2})$	ϕ (c.c/min)	Initial pH
5 g/l Na_2SO_4 0.44 g/l H_2SO_4 1 g/l 2,3-Xylenol	5	263.2	777	2.5

t (min)	ΔV (volts)	2,3-Xylenol mg/l	% oxidized	T.O.C. mg/l	% oxidized
0	5.0	830	0	714	0
15	5.1	712	14.2	712	0.4
30	5.2	625	24.7	710	0.7
45	5.3	595	28.3	707	1.1
60	5.4	515	38.0	705	1.4
75	5.5	450	45.8	702	1.8
90	5.6	375	54.8	700	2.1
105	5.7	310	62.7	695	2.8
120	5.9	260	68.7	687	3.9

RUN 4-3

Electrolyte	I(A)	$i(\text{A/m}^{-2})$	ϕ (c.c/min)	Initial pH
5 g/l Na_2SO_4 0.44 g/l H_2SO_4 1 g/l 2,3-Xylenol	15	789.5	791	2.58

t (min)	ΔV (volts)	2,3-Xylenol		T.O.C.	
		mg/l	% oxidized	mg/l	% oxidized
0	8.6	780	0	707	0
15	8.9	555	28.9	705	0.3
30	9.7	380	51.3	697	1.4
45	10.3	235	69.9	686	2.7
60	10.6	155	80.1	663	6.2
75	10.7	95	87.8	620	12.3
90	10.7	50	93.6	592	16.3
105	10.7	30	96.2	585	17.3
120	10.6	0	100.0	580	18.0

RUN 4-4

Electrolyte	I(A)	$i(\text{A/m}^{-2})$	ϕ (c.c/min)	Initial pH
5 g/l Na_2SO_4 0.44 g/l H_2SO_4 1 g/l 2,3-Xylenol	10	526.3	791	2.36

t (min)	ΔV (volts)	2,3-Xylenol mg/l	% oxidized	T.O.C. mg/l	% oxidized
0	7.0	97	0	73.5	0
15	6.8	46	52.6	73.5	0
30	7.0	24	75.8	73.5	0
45	7.3	15	84.5	73.5	0
60	7.4	6	93.8	73.5	0
75	7.4	0	100.0	71.3	3.1
90	7.4	0	100.0	69.0	6.1
105	7.4	0	100.0	66.0	10.2
120	7.4	0	100.0	66.0	10.2

RUN 4-5

Electrolyte	I(A)	$i(A/m^{-2})$	ϕ (c.c/min)	Initial pH
5 g/l Na_2SO_4 0.44 g/l H_2SO_4 0.5 g/l 2,3- Xylenol	10	526.3	864.5	2.3

t (min)	ΔV (volts)	2,3-Xylenol		T.O.C.	
		mg/l	% oxidized	mg/l	% oxidized
0	7.4	380	0	251.3	0
15	7.2	295	22.4	251.3	0
30	7.9	160	57.9	251.3	0
45	8.5	82	78.4	251.3	0
60	8.8	33	91.3	243.8	3.0
75	8.9	17	95.5	240.0	4.5
90	8.7	5	98.7	237.8	5.4
105	8.5	0	100.0	232.5	7.5
120	8.4	0	100.0	219.0	12.8

RUN 5-1

Electrolyte	I(A)	$i(\text{A/m}^{-2})$	ϕ (c.c/min)	Initial pH
5 g/l Na_2SO_4 0.44 g/l H_2SO_4 1.2 g/l 3,4- Xylenol	10	526.3	819	2.32

t (min)	ΔV (volts)	3,4-Xylenol mg/l	% oxidized
0	5.9	1110	0
15	6.5	1025	7.7
30	6.5	900	18.9
45	6.5	825	25.7
60	6.5	785	29.3
75	6.4	690	37.8
90	6.4	655	41.0
105	6.3	623	43.9
120	6.3	600	46.0

RUN 5-2

Electrolyte	I(A)	$i(\text{A/m}^{-2})$	ϕ (c.c/min)	Initial pH
5 g/l Na_2SO_4 0.44 g/l H_2SO_4 1.2 g/l 3,4- Xylenol	5	263.2	805	2.34

t (min)	ΔV (volts)	3,4-Xylenol mg/l	% oxidized
0	4.4	1290	0
15	4.7	1250	3.1
30	4.8	1218	5.6
45	4.8	1140	11.6
60	4.8	1085	15.9
75	4.8	1030	20.2
90	4.8	1000	22.5
105	4.8	965	25.2
120	4.8	915	29.1

RUN 5-3

Electrolyte	I(A)	$i(\text{A/m}^{-2})$	ϕ (c.c/min)	Initial pH
5 g/l Na_2SO_4 0.44 g/l H_2SO_4 1.2 g/l 3,4- Xylenol	15	789.5	805	2.25

t (min)	ΔV (volts)	3,4-Xylenol mg/l	% oxidized
0	7.4	1175	0
15	7.8	890	24.3
30	7.7	765	34.9
45	7.6	675	42.6
60	7.6	581	50.6
75	7.6	515	56.2
90	7.6	465	60.4
105	7.6	423	64.0
120	7.5	395	66.4

RUN 5-4

Electrolyte	I(A)	$i(A/m^{-2})$	ϕ (c.c/min)	Initial pH
5 g/l Na_2SO_4 0.44 g/l H_2SO_4 0.1 g/l 3,4- Xylenol	10	526.3	819	2.33

t (min)	ΔV (volts)	3,4-Xylenol mg/l	% oxidized
0	6.6	103	0
15	6.3	67	35.4
30	6.3	48	53.9
45	6.4	33	68.0
60	6.4	27	73.8
75	6.4	22	79.1
90	6.4	19	81.6
105	6.4	17	83.8
120	6.3	14	86.9

RUN 5-5

Electrolyte	I(A)	$i(A/m^{-2})$	ϕ (c.c/min)	Initial pH
5 g/l Na_2SO_4 0.44 g/l H_2SO_4 0.5 g/l 3,4- Xylenol	10	526.3	784	2.32

t (min)	ΔV (volts)	3,4-Xylenol mg/l	% oxidized
0	6.6	515	0
15	6.4	393	23.7
30	6.2	290	43.7
45	6.1	230	55.3
60	6.1	196	61.9
75	6.1	165	68.0
90	6.0	143	72.2
105	5.9	130	74.8
120	6.0	108	79.0

RUN 6-1

Electrolyte	I(A)	$i(\text{A/m}^{-2})$	ϕ (c.c/min)	Initial pH
5 g/l Na_2SO_4 0.44 g/l H_2SO_4 1 g/l Resorcinol	10	526.3	805	2.16

t (min)	ΔV (volts)	Resorcinol mg/l	% oxidized	T.O.C. mg/l	% oxidized
0	7.4	1200	0	725	0
15	7.2	1130	5.8	715	1.4
30	7.2	970	19.2	665	8.3
45	7.0	855	28.8	660	9.0
60	7.0	695	42.1	653	9.9
75	7.0	635	47.1	635	12.4
90	7.0	545	54.6	625	13.8
105	6.9	420	65.0	625	13.8
120	6.7	380	68.3	625	13.8

RUN 6-2

Electrolyte	I(A)	$i(\text{A/m}^{-2})$	ϕ (c.c/min)	Initial pH
5 g/l Na_2SO_4 0.44 g/l H_2SO_4 1 g/l Resorcinol	5	263.2	763	2.3

t (min)	ΔV (volts)	Resorcinol		T.O.C.	
		mg/l	% oxidized	mg/l	% oxidized
0	5.5	1230	0	750	0
15	5.5	1190	3.3	750	0
30	5.4	1150	6.5	700	6.7
45	5.3	1105	10.2	700	6.7
60	5.3	1000	18.7	700	6.7
75	5.3	980	20.3	675	10.0
90	5.2	930	24.4	675	10.0
105	5.3	855	30.5	658	12.3
120	5.2	810	34.2	658	12.3

RUN 6-3

Electrolyte	I(A)	$i(A/m^{-2})$	ϕ (c.c/min)	Initial pH
5 g/l Na_2SO_4 0.44 g/l H_2SO_4 1 g/l Resorcinol	15	789.5	784	2.23

t (min)	ΔV (volts)	Resorcinol		T.O.C.	
		mg/l	% oxidized	mg/l	% oxidized
0	10.8	1205	0	715	0
15	9.9	1070	11.2	715	0
30	9.3	890	26.1	670	6.3
45	9.3	755	37.3	640	10.5
60	9.0	650	46.1	635	11.2
75	9.3	510	57.7	630	11.9
90	9.4	425	64.7	615	14.0
105	9.5	310	74.3	578	19.2
120	9.7	200	83.4	585	18.2

RUN 6-4

Electrolyte	I(A)	$i(A/m^{-2})$	ϕ (c.c/min)	Initial pH
5 g/l Na_2SO_4 0.44 g/l H_2SO_4 0.1 g/l Resorcinol	10	526.3	816	2.59

t (min)	ΔV (volts)	Resorcinol		T.O.C.	
		mg/l	% oxidized	mg/l	% oxidized
0	8.2	87	0	66	0
15	8.0	40	54.0	55	14.5
30	7.8	0	100.0	52	20.6
45	7.7	0	100.0	47	28.2
60	8.0	0	100.0	41	37.4
75	8.5	0	100.0	37	44.3
90	8.8	0	100.0	33	49.9
105	9.0	0	100.0	31	52.7
120	9.0	0	100.0	26	61.1

RUN 6-5

Electrolyte	I(A)	$i(A/m^{-2})$	ϕ (c.c/min)	Initial pH
5 g/l Na_2SO_4 0.44 g/l H_2SO_4 0.5 g/l Resorcinol	10	526.3	798	1.45

t (min)	ΔV (volts)	Resorcinol mg/l	% oxidized	T.O.C. mg/l	% oxidized
0	3.4	490	0	377	0
15	3.5	285	41.8	330	12.5
30	3.5	145	70.4	308	18.3
45	3.5	20	95.9	288	23.6
60	3.5	0	100.0	267	29.2
75	3.5	0	100.0	245	35.0
90	3.5	0	100.0	245	35.0
105	3.5	0	100.0	255	32.4
120	3.5	0	100.0	230	39.0

RUN 7-1

Electrolyte	I(A)	$i(A/m^{-2})$	ϕ (c.c/min)	Initial pH
5 g/l Na_2SO_4 0.44 g/l H_2SO_4 1 g/l Catechol	10	526.3	798	2.39

t (min)	ΔV (volts)	T.O.C. mg/l	% oxidized
0	5.3	800	0
15	6.5	755	5.6
30	6.6	635	20.6
45	6.5	575	28.1
60	6.5	515	35.6
75	6.4	468	41.5
90	6.3	400	50.0
105	6.2	410	48.8
120	6.2	435	45.6

Comment: All the samples were centrifuged and T.O.C. analysis was performed on the centrifugate in the case of catechol runs.

RUN 7-2

Electrolyte	I(A)	$i(\text{A/m}^{-2})$	ϕ (c.c/min)	Initial pH
5 g/l Na_2SO_4 0.44 g/l H_2SO_4 1 g/l Catechol	5	263.2	823	2.34

t (min)	ΔV (volts)	T.O.C. mg/l	% oxidized
0	3.8	720	0
15	4.3	705	2.1
30	4.5	635	11.8
45	4.6	570	20.8
60	4.6	535	25.7
75	4.5	495	31.3
90	4.5	455	36.8
105	4.4	410	43.1
120	4.4	390	45.8

RUN 7-3

Electrolyte	I(A)	i(A/min ⁻²)	ϕ (c.c/min)	Initial pH
5 g/l Na ₂ SO ₄ 0.44 g/l H ₂ SO ₄ 1 g/l Catechol	15	789.5	840	2.30

t (min)	ΔV (volts)	T.O.C. mg/l	% oxidized
0	6.9	535	0
15	7.2	463	13.5
30	7.4	410	23.4
45	7.3	365	31.8
60	7.2	343	35.9
75	7.1	318	40.6
90	7.1	308	42.4
105	7.0	263	50.8
120	7.0	270	49.5

RUN 7-4

Electrolyte	I(A)	$i(A/m^{-2})$	ϕ (c.c/min)	Initial pH
5 g/l Na_2SO_4 0.44 g/l H_2SO_4 0.1 g/l Catechol	10	526.3	84.4	2.34

t (min)	ΔV (volts)	T.O.C. mg/l	% oxidized
0	5.8	84	0
15	5.9	78	7.1
30	5.9	75	10.7
45	5.9	69	18.5
60	5.9	65	22.6
75	5.9	60	28.6
90	5.8	46	45.2
105	5.8	43	48.8
120	5.8	39	53.6

RUN 7-5

Electrolyte	I(A)	$i(\text{A/m}^{-2})$	ϕ (c.c/min)	Initial pH
5 g/l Na_2SO_4 0.44 g/l H_2SO_4 0.5 g/l Catechol	10	526.3	833	2.52

t (min)	ΔV (volts)	T.O.C. mg/l	% oxidized
0	5.5	335	0
15	5.8	295	11.9
30	5.9	255	23.9
45	5.8	200	40.3
60	5.7	180	46.3
75	5.7	175	47.8
90	5.6	160	52.2
105	5.6	155	53.7
120	5.6	125	62.7

B.O.D. Analysis (Runs 7-2, 7-3)

B.O.D. Analysis results Run 7-2 (5 amps)

B.O.D. (5 days at 20°C) ppm:

Initial sample (t = 0 min) 930

Final sample (t = 120 min) 240

% Reduction in B.O.D. 74

B.O.D. Analysis results Run 7-3 (15 amps)

B.O.D. (5 days at 20°C) ppm:

Initial sample (t = 0 min) 600

Final sample (t = 120 min) 117

% Reduction in B.O.D. 81

C.O.D. Analysis (Runs 7-2, 7-3)

Sample Description	Dilution (if any)	Titre-FAS (m.l)	Blank-Sample (m.l)	C.O.D. (mg/l)	Average C.O.D. mg/l
Initial sample (run 7-2) (t = 0 min)	20	23.90	2.85	2103.3	2103.3
	10	21.05	5.70	2103.3	
Final sample (run 7-2) (t = 120 min)	20	24.70	2.05	1512.9	1448.3
	10	23.00	3.75	1383.8	
<u>% Reduction in C.O.D. 31.1</u>					
Initial sample (run 7-3) (t = 0 min)	20	24.30	2.45	1884.5	1772.5
	10	22.25	4.50	1660.5	
Final sample (run 7-3) (t = 120 min)	20	25.4	1.35	996.3	950.2
	10	24.3	2.45	904.1	
<u>% Reduction in C.O.D. 46.4</u>					

COMPARISON OF PERFORMANCE OF DIFFERENT PHENOLICS

1. Variation of final % oxidized with initial concentration of phenolics at 10 A
2. Variation of initial rate with initial concentration at 10 A
3. Variation of final % oxidized with applied current (1 g/l runs)
4. Variation of initial rate of oxidation with applied current (1 g/l runs)

Name of Compound	Final % oxidized	Initial conc. ppm	Initial conc. mole/m ³ x 10 ⁶	Initial rate ppm/min	Initial rate g.mol/sec x 10 ⁶
Phenol	100.0	108	1.15	4.13	3.66
	75.4	683	7.26	14.40	12.75
	89.6	910	9.67	10.67	9.45
O-Cresol	96.8	95	0.88	2.00	1.54
	82.6	505	4.68	7.33	5.66
	64.8	853	7.90	4.20	3.24
p-Cresol	91.3	69	0.64	1.93	1.47
	67.6	355	3.29	3.67	2.83
	62.9	823	7.62	2.87	2.21
Resorcinol	100.0	87	0.78	2.90	2.20
	100.0	490	4.45	11.50	8.70
	68.3	1200	10.90	7.67	5.81
2,3-Xylenol	100.0	97	0.80	3.40	2.32
	100.0	380	3.12	5.67	3.87
	100.0	625	5.12	11.33	7.74
3,4-Xylenol	86.9	103	0.84	2.40	1.66
	79.0	515	4.22	8.13	5.55
	46.0	1110	9.10	5.67	3.87

Note: Similar data could not be obtained from catechol runs because concentrations of catechol samples were not determined.

.../cont'd

COMPARISON OF PERFORMANCE OF DIFFERENT PHENOLICS/cont'd

Name of Compound	Applied current (Amps)	Final % oxidized	Initial rate ppm/min	Initial rate g.mol/sec x 10 ⁶
Phenol	5	70.0	6.33	5.61
	10	89.6	10.67	9.45
	15	92.1	13.67	12.11
O-Cresol	5	46.2	3.00	2.32
	10	62.9	3.93	3.03
	15	81.2	7.67	5.92
p-Cresol	5	46.4	6.00	4.63
	10	50.0	6.60	5.09
	15	70.5	15.83	12.21
Resorcinol	5	34.2	2.78	2.10
	10	68.3	7.67	5.81
	15	83.4	10.00	7.57
2,3-Xylenol	5	68.7	7.87	5.38
	10	100.0	11.33	7.74
	15	100.0	15.00	10.25
3,4-Xylenol	5	29.1	2.40	1.64
	10	46.0	7.00	4.78
	15	66.4	13.67	9.34

Note: The rates were determined from the linear portion of the curves in all cases.

RUN 8-1

Electrolyte		I(A)	i(A/m ⁻²)	ϕ c.c/min	Initial pH
5 g/l Na ₂ SO ₄	0.16 g/l p-Cresol	10	526.3	823	2.48
0.44 g/l H ₂ SO ₄	0.20 g/l 2,3-Xylenol				
1.37 g/l phenol	0.17 g/l 3,4-Xylenol				
0.28 g/l O-cresol					

t (min)	ΔV (volts)	Phenol		O-Cresol		p-Cresol		2,3-Xylenol		3,4-Xylenol		Total mg/l	Total % oxidized
		mg/l	% oxidized	mg/l	% oxidized	mg/l	% oxidized	mg/l	% oxidized	mg/l	% oxidized		
0	5.5	1250	0	248	0	122	0	137	0	139	0	1896	0
15	5.6	1190	4.8	240	3.2	116	4.9	131	4.6	131	5.8	1808	4.6
30	5.8	1110	11.2	234	5.7	115	5.7	124	9.5	139	0	1722	9.2
45	5.9	998	20.2	208	16.1	110	9.8	115	16.1	139	0	1570	17.2
60	6.0	850	32.0	181	27.0	101	17.2	98	28.5	129	7.2	1359	28.3
75	6.0	798	36.2	179	27.8	98	19.7	97	29.2	134	3.6	1306	31.1
90	6.0	745	40.4	167	32.7	101	17.2	93	32.1	126	9.4	1232	35.0
105	6.0	678	45.8	158	36.3	101	17.2	90	34.3	134	3.6	1161	38.8
120	6.0	615	50.8	152	38.7	98	19.7	89	35.0	134	3.6	1088	42.6

RUN 8-2

Electrolyte		I (A)	c.d. (A/m ²)	Average flow rate c.c/min	Initial pH
5 g/l Na ₂ SO ₄	0.18 g/l p-cresol	10	526.3	793	2.36
0.44 g/l H ₂ SO ₄	0.16 g/l 2,3-Xylenol				
1.33 g/l phenol	0.17 g/l 3,4-Xylenol				
0.30 g/l O-cresol					

t (min)	ΔV (volts)	Phenol		O-cresol		p-Cresol		2,3-Xylenol		3,4-Xylenol		Total mg/l	Total % oxidized
		mg/l	% oxidized	mg/l	% oxidized	mg/l	% oxidized	mg/l	% oxidized	mg/l	% oxidized		
0	5.2	1200	0	291	0	143	0	124	0	131	0	1889	0
15	5.5	1093	8.9	269	7.6	137	4.2	117	5.7	130	0.8	1746	7.6
30	5.7	948	21.0	240	17.5	120	16.1	103	16.9	116	11.5	1527	19.2
45	5.8	898	25.2	238	18.2	121	15.4	103	16.9	128	2.3	1488	21.2
60	5.8	840	30.0	220	24.4	116	18.9	99	20.2	125	4.6	1401	25.8
75	5.8	735	38.8	212	27.2	114	20.3	95	23.4	123	6.1	1279	32.3
90	5.9	700	41.7	208	28.5	116	18.9	99	20.2	131	0	1254	33.6
105	5.9	605	49.6	184	36.8	108	24.5	87	29.8	123	6.1	1107	41.4
120	5.9	520	56.7	164	43.6	102	28.7	82	33.9	124	5.3	992	47.5
135	5.9	475	60.4	157	46.1	102	28.7	80	35.5	126	3.8	941	50.2
150	5.9	400	66.7	143	50.9	99	30.8	76	38.7	128	2.8	846	55.2
165	5.9	350	70.8	126	56.7	93	35.0	73	41.1	130	0.8	773	59.1
180	5.9	305	74.6	111	61.9	88	38.5	67	46.0	119	9.2	690	63.5

RUN 8-3

Electrolyte		I (A)	c.d (A/m ²)	Average flow rate c.c/min	Initial pH
5 g/l Na ₂ SO ₄	0.14 g/l p-cresol	10	526.3	794.5	2.38
0.44 g/l H ₂ SO ₄	0.14 g/l 2,3-Xylenol				
1.14 g/l phenol	0.14 g/l 3,4-Xylenol				
0.27 g/l O-cresol					

t (min)	ΔV (volts)	Phenol		O-Cresol		p-Cresol		2,3-Xylenol		3,4-Xylenol		Total mg/l	Total % oxidized
		mg/l	% oxidized	mg/l	% oxidized	mg/l	% oxidized	mg/l	% oxidized	mg/l	% oxidized		
0	5.2	1070	0	246	0	127	0	109	0	122	0	1674	0
15	5.4	1005	6.1	228	7.3	127	0	101	7.3	112	8.2	1573	6.0
30	5.5	970	9.4	223	9.4	125	1.6	99	9.2	117	4.1	1534	8.4
45	5.6	885	17.3	217	11.8	123	3.2	104	4.6	122	0	1451	13.3
60	5.7	735	31.3	192	22.0	103	18.9	96	11.9	114	6.6	1240	25.9
75	5.8	593	44.6	154	37.4	90	29.1	83	23.9	101	17.2	1013	39.5
90	5.8	563	47.4	143	41.9	90	29.1	88	19.3	118	3.3	1002	40.1
105	5.8	520	51.4	140	43.1	80	37.0	80	26.6	97	20.5	917	45.2
120	5.8	428	60.0	118	52.0	79	37.8	70	35.8	106	13.1	801	52.2

....cont'd

RUN 8-3/cont'd

t (min)	ΔV (volts)	Phenol		O-Cresol		p-Cresol		2,3-Xylenol		3,4-Xylenol		Total	Total
		mg/l	% oxidized	mg/l	% oxidized	mg/l	% oxidized	mg/l	% oxidized	mg/l	% oxidized	mg/l	% oxidized
135	5.8	332	69.0	94	61.8	73	42.5	62	43.1	106	13.1	667	60.2
150	5.7	260	75.7	76	69.1	65	48.8	55	49.5	93	23.8	549	67.2
165	5.7	198	81.5	69	72.0	60	52.8	50	54.1	91	25.4	468	72.0
180	5.6	142	86.7	61	75.2	52	59.1	39	64.2	83	32.0	377	77.5
195	5.6	95	91.1	36	85.4	48	62.2	35	67.9	83	32.0	297	82.3
210	5.6	78	92.7	21	91.5	42	66.9	25	77.1	72	41.0	238	85.8
225	5.6	55	94.9	18	92.7	39	69.3	21	80.7	70	42.6	203	87.9
240	5.6	43	96.0	9	96.3	38	70.1	14	87.2	54	55.7	158	90.6
255	5.6	28	97.4	7	97.2	34	73.2	12	89.0	56	54.1	137	91.8
270	5.6	10	99.1	4	98.4	29	77.2	9	91.7	45	63.1	97	94.2
285	5.6	0	100.0	0	100.0	28	78.0	7	93.6	48	60.7	83	95.0
300	5.6	0	100.0	0	100.0	24	81.1	4	96.3	43	65.2	71	95.8

T.O.C. Analysis results, Run 8-3

t (min)	mg/l	T.O.C. % oxidized
0	1480	0
60	1380	6.8
120	1320	10.8
180	1290	12.8
240	1260	14.9
300	1160	21.6

B.O.D. Analysis results, Run 8-3

B.O.D. (5 days at 20°C) ppm:

Initial sample (t = 0 min) 27.83

Final sample (t = 300 min) 12.10

% Reduction in B.O.D. 56.52

C.O.D. Analysis results, Run 8-3

Sample Description	Dilution (if any)	Titre-FAS (m.l)	Blank-Sample (m.l)	C.O.D. (mg/l)	Average C.O.D. mg/l
Initial sample (t = 0 min)	10	14.20	11.20	4310	4291
	10	14.30	11.10	4271	
Final Sample (t = 300 min)	10	16.20	9.20	3540	3502
	10	16.40	9.00	3463	
% Reduction in C.O.D. 18.4					

RUN 9-1

Electrolyte	I(A)	$i(A/m^{-2})$	ϕ (c.c/min)	Initial pH
5 g/l Na_2SO_4 0.44 g/l H_2SO_4 1 gm/l Phenol	10	526.3	760	2.34

t (min)	ΔV (Volts)	phenol mg/l	% oxidized
0	5.60	975	0
15	5.65	850	12.8
30	5.60	675	30.8
45	5.60	565	42.1
60	5.60	390	60.0
75	5.65	305	68.7
90	5.75	200	79.5
105	5.75	145	85.1
120	5.75	105	89.2

Other phenolic runs for GC/Ms analysis

1 g/l, $i = 526.3 \text{ A/m}^{-2}$ runs, 2 hours' oxidation

Run No.	Name of phenolic compound (and initial pH)	Initial voltage	Final voltage volts	ϕ c.c/min	Comments
9-2	O-Cresol (2.35)	6.2	6.55	826	Foaming-increasing as oxidation proceeded.
9-3	p-Cresol (2.38)	6.15	6.25	812	Foaming-increasing as oxidation proceeded.
9-4	2,3-Xylenol (2.31)	5.85	9.35	777	Excessive foaming, solution turned yellow.
9-5	3,4-Xylenol (2.34)	6.05	6.15	847	-
9-6	Resorcinol (2.39)	6.10	6.35	819	Clear, pale brown solution obtained.
9-7	Catechol (2.40)	5.75	6.5	840	Vigorous reaction, solution turned deep yellow, brown and black in 15 mins, foaming associated with formation of black precipitate.
9-8	Phenol-9gms O-Cresol-2gms p-Cresol-1gm 2,3-Xylenol-1gm 3,4-Xylenol-1gm (2.3)	5.35	5.85	630	Solution turned pale yellow with slight foaming towards the end.

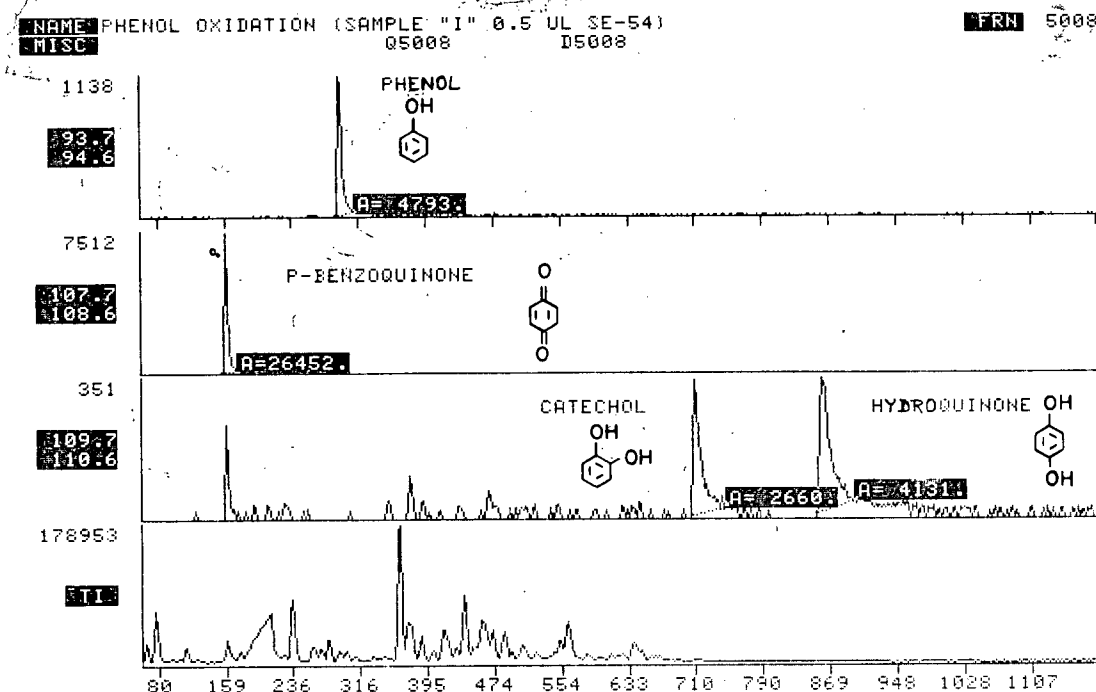


Fig. 35 GC/MS analysis of final product from phenol oxidation (run 9-1)

Area Table Entries: FRN 5008

Entry	Time	Mass	Area	%
1	4.8	94.0	4793.	12.6
2	3.6	108.0	26452.	69.5
3	8.8	110.0	2660.	7.0
4	10.1	110.0	4131.	10.9

NAME P-CRESOL OXIDATION (FINAL SAMPLE) SE-54 2UL
 MISC

FRN 5004

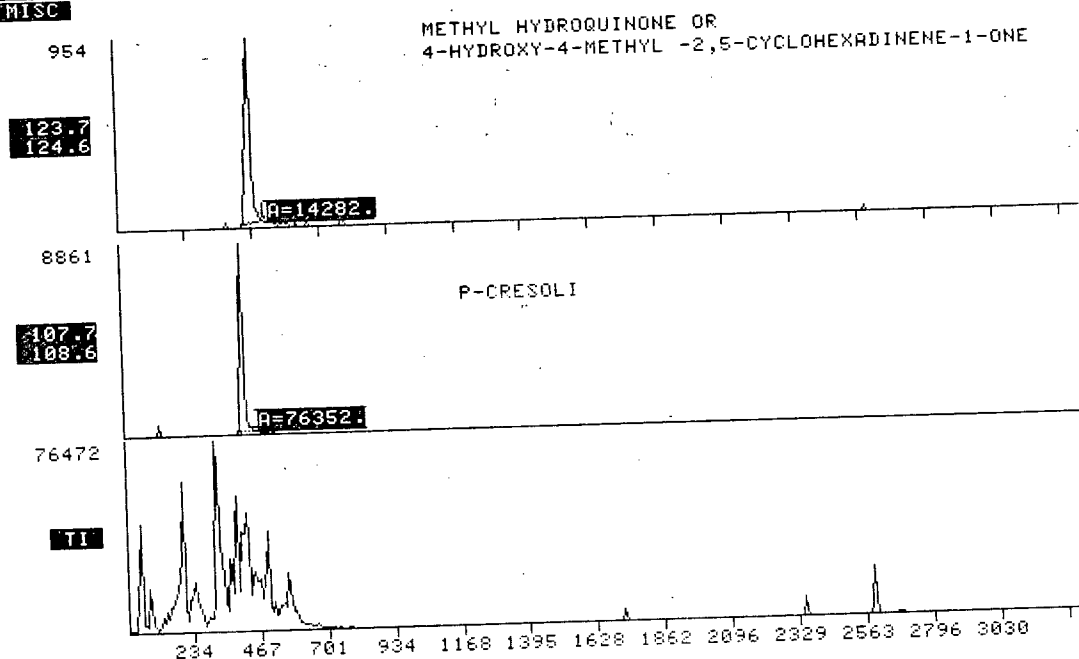


Fig. 36 GC/MS analysis of final product from p-cresol
 oxidation (run 9-3)

Area Table Entries: FRN 5004

Entry	Time	Mass	Area	%
1	6.9	124.0	14282.	15.8
2	6.5	108.0	76352.	84.2

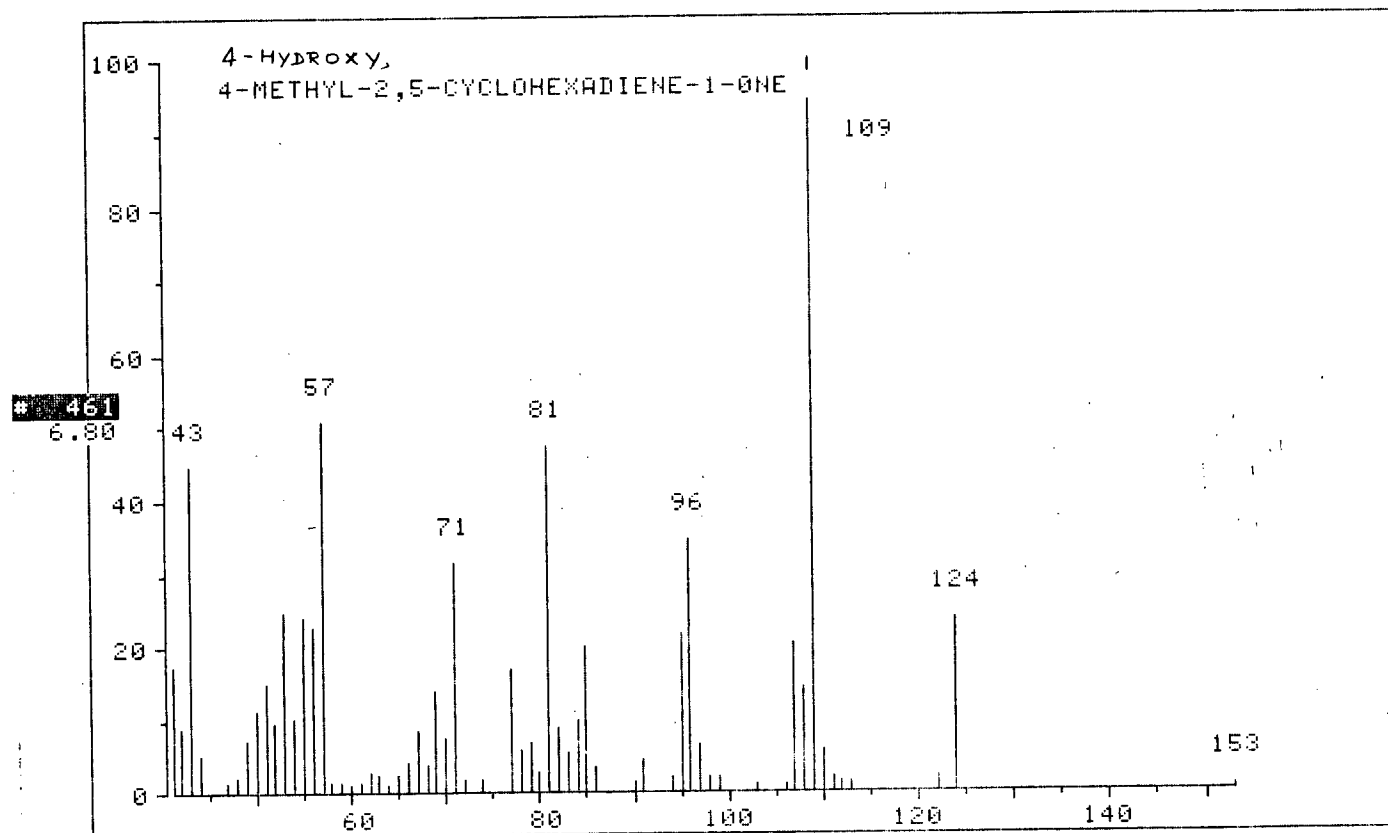


Fig. 37 Mass spectrum showing the presence of 4-Hydroxy-4-Methyl-
2,5-Cyclohexadiene-1-one

NAME O-CRESOL OXIDATION (SE-54 2UL)
 MISC 30 - 260 8C/MIN

FRN 5005

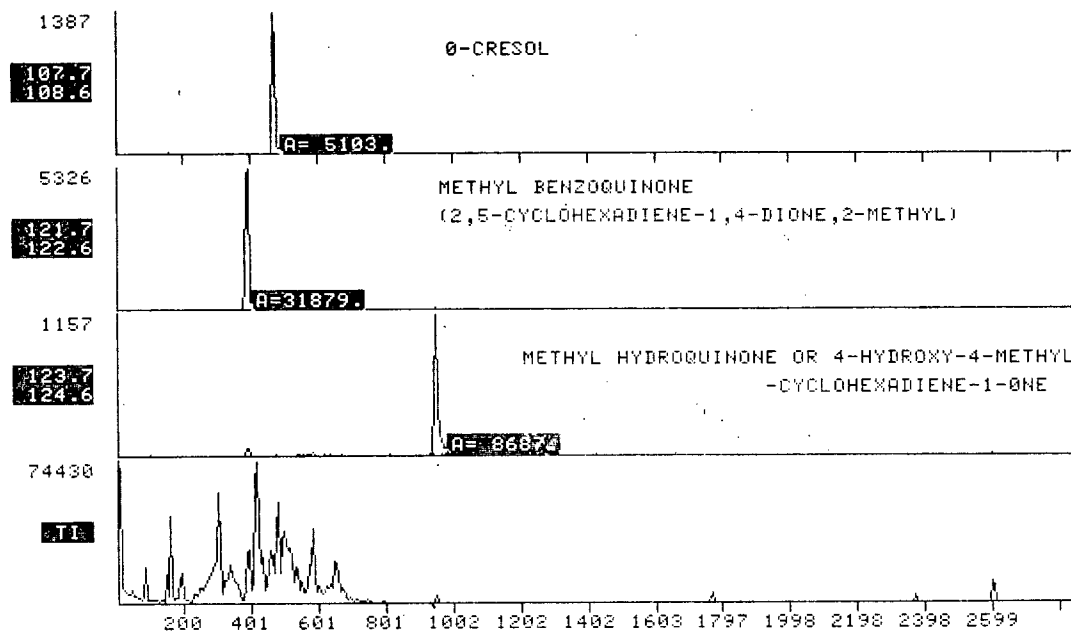


Fig. 38 GC/MS analysis of final product from
 o-cresol oxidation (run 9-2)

Area table entries: FRN 5005

Entry	Time	Mass	Area	%
1	6.0	108.0	5103	11.17
2	5.1	122.0	31879	69.80
3	11.2	124.0	8687	19.02

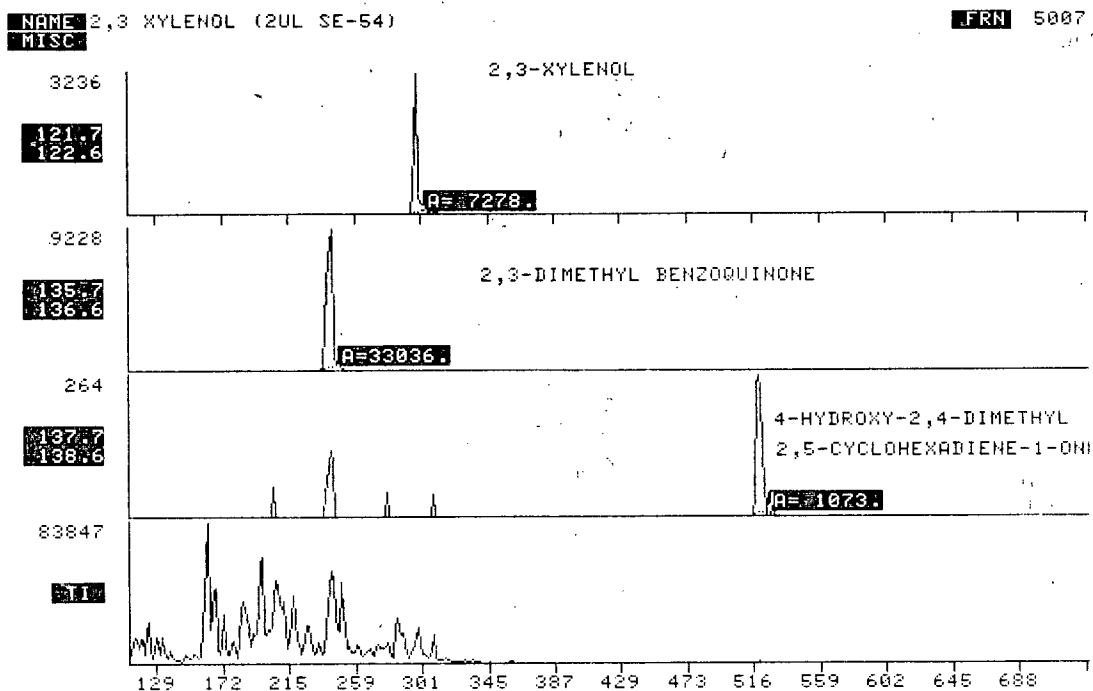


Fig. 39 GC/MS analysis of final product from
2,3-Xylenol oxidation (run 9-4)

Area table entries: FRN 5007

Entry	Time	Mass	Area	%
1	8.2	122.0	7423.	17.59
2	7.0	136.0	33709.	79.82
3	12.8	138.0	1021.	2.59

NAME 3,4XYLENOL OXIDATION (2UL SE-54)
MISC

FRN 5006

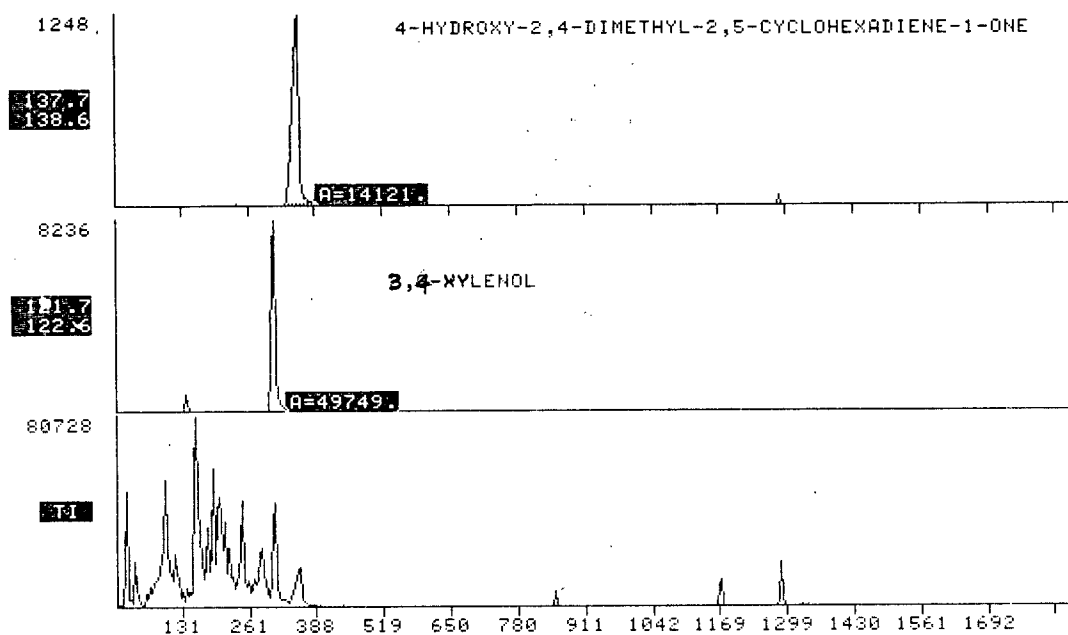


Fig. 40. GC/MS analysis of final product from
3,4-Xylenol oxidation (run 9-5)

Area table entries: FRN 5006

Entry	Time	Mass	Area	%
1	9.6	138.0	14121.	22.11
2	8.6	122.0	49749.	79.89

2,3 XYLENOL (2UL SE-54)

IRN 5007

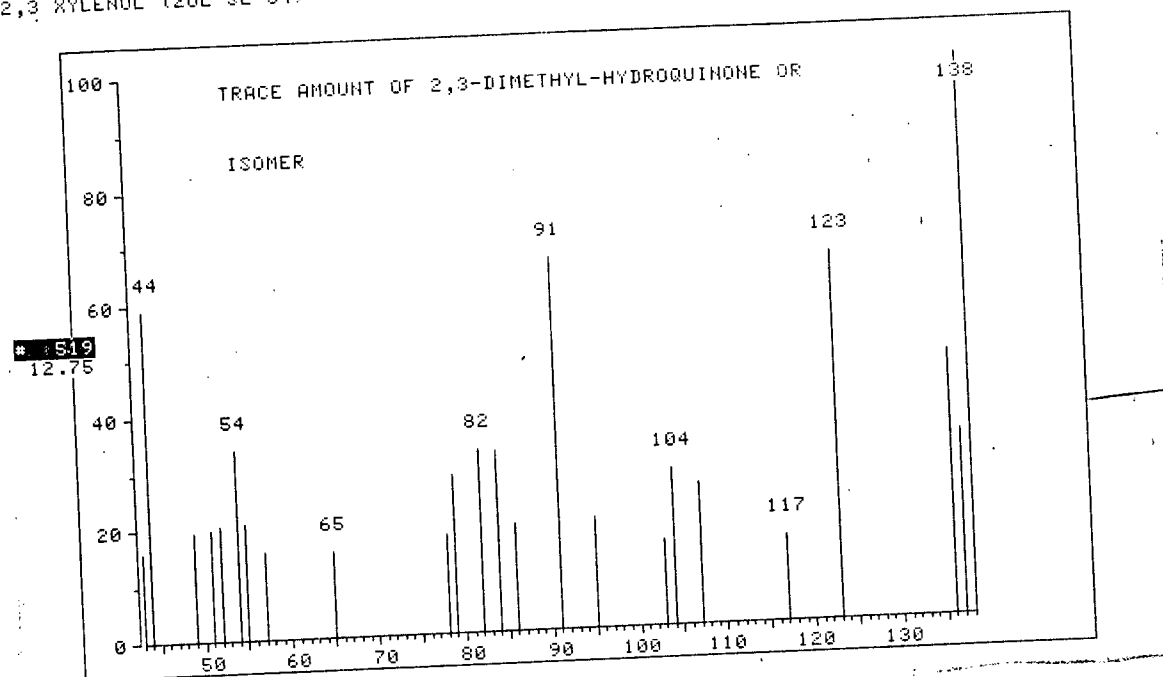
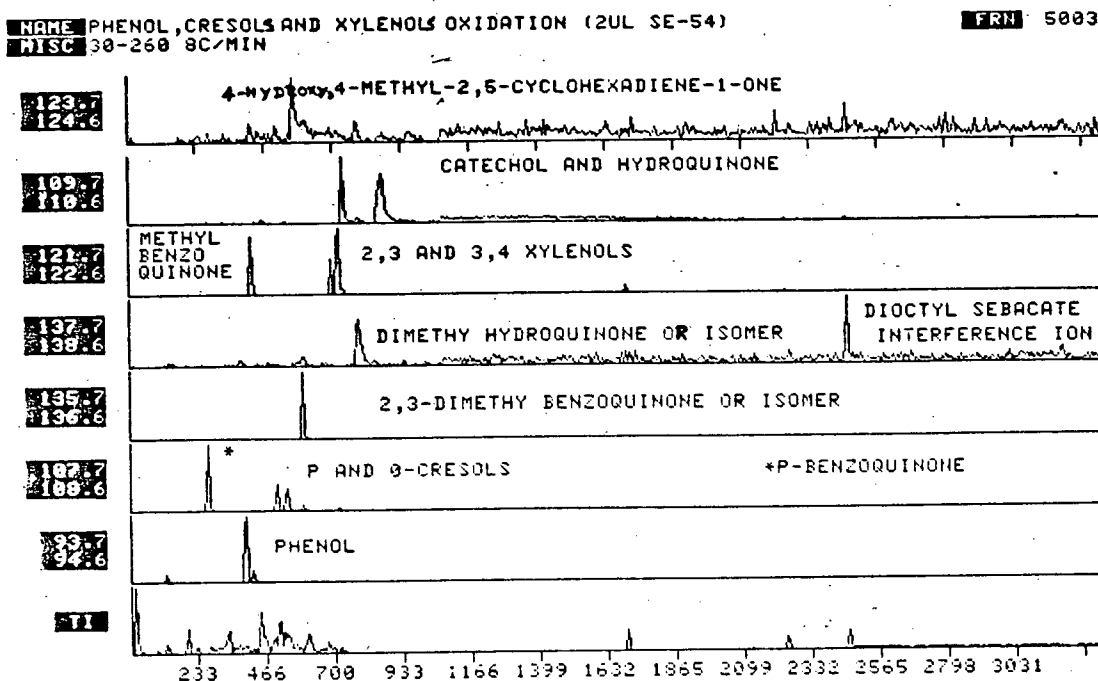


Fig. 41 MS confirmation of traces of 2,3-Dimethyl hydroquinone or isomer

Fig. 42 GC/MS analysis of final product of oxidation of mixture and Xylenols (run 9-8)

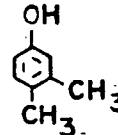
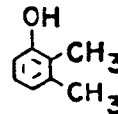
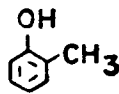


AREA TABLE ENTRIES: FRN 5003

Entry	Time	Mass	Area	%
1	7.0	124.0	2917.	1.0
2	10.2	110.0	37568.	13.4
3	8.7	110.0	14724.	5.2
4	5.1	122.0	22154.	7.9
5	8.2	122.0	13180.	4.7
6	8.5	122.0	31438.	11.2
7	9.3	138.0	3237.	1.2
8	7.0	136.0	9311.	3.5
9	3.4	108.0	31376.	11.2
10	6.4	108.0	17290.	6.2
11	6.0	108.0	16670.	5.9
12	4.9	94.0	30741.	23.7

CALCULATE % ON ENTRY #:

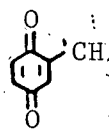
STARTING COMPOUNDS:



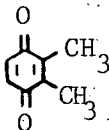
OXIDATION PRODUCTS:



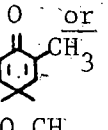
108



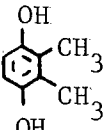
122



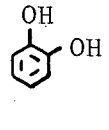
136



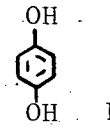
138



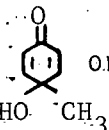
138



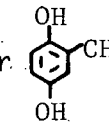
110



110



124



124

APPENDIX 3

Mathematical Model

In this study, a multiple-pass system is used in a fixed volume (5 l) of solution circulated continuously through the bed. Under these conditions, if the packed bed electrode is connected to a reservoir containing solution of volume V_m , the concentration of the phenolic compound decreases with the time of electro-oxidation.

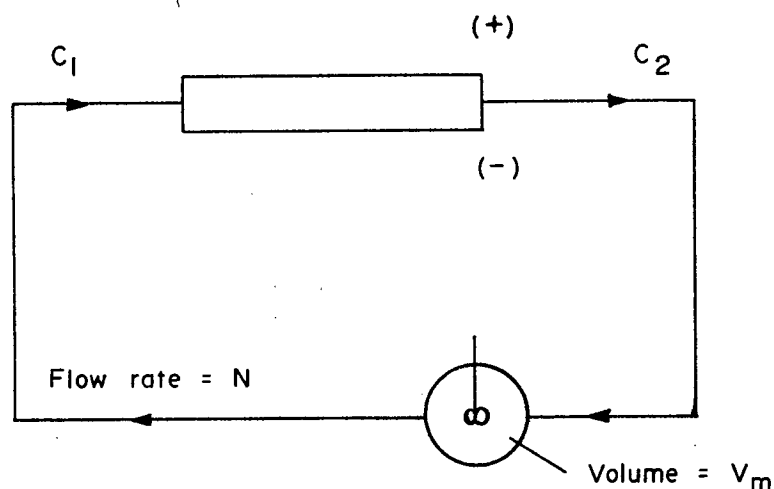


Fig. A-1 Schematic representation of a multiple-pass system

At any instant, the inlet concentration is C_1 and the outlet concentration is C_2 . As approached by Pickett Ref. 10, p. 178, for ideal limiting conditions, C_1 and C_2 can be related as follows

$$C_2 = C_1 \left[\exp \left(- \frac{k_m A_{min}}{N} \right) \right] \quad (A.1)$$

The anodic oxidation of the phenolic compound can be controlled by

mass transfer or the electrochemical reaction. An attempt to obtain a mathematical model when the reaction is controlled by the latter process would be very complicated because as C_1 and C_2 vary the electrode potential and k_r , the electrochemical reaction constant will vary too. Hence only a mass transfer controlled model has been treated here.

Following the approach made by Sucre [31], C_2 can be related to the initial phenol concentration C_0 as follows

$$C_2 = C_0 \exp \left[\left\{ \exp - \left(\frac{k_m a L}{u} \right) - 1 \right\} \frac{t}{t_m} - \frac{k_m a L}{u} \right] \quad (A.2)$$

Eq. A.2 can be simplified by using the following substitutions

$$t^* = \frac{t}{t_m} = \text{dimensionless time}$$

$$Q = \frac{k_m a L}{u} = \text{dimensionless mass transfer group}$$

$$X = \frac{C_0 - C_2}{C_0} = \text{fractional conversion}$$

whence:

$$X = 1 - \exp \left[\left\{ \exp (-Q) - 1 \right\} t^* - Q \right]$$

Estimation of mass transfer coefficient.

Due to the lack of proper correlations for mass transfer coefficients under the conditions of the present study, the approach made by Pickett and Stanmore using a single layer packed bed electrode has been used [46].

$$Sh = 0.83 Re^{0.56} Sc^{0.33} \quad (A.3)$$

It has been reported [10] that data by Stanmore on a double layer of regularly packed electrode indicated that values of k_m obtained were

about 20-25% lower than that given by eq. A.3. Thus calculations were based on the equation

$$Sh = a Re^{0.56} Sc^{0.33} \quad (A.4)$$

with upper and lower bounds of $a = 0.66$ and $a = 0.62$ respectively. A sample calculation is given below.

Calculation of theoretical fractional conversion if mass transfer controls

Specific surface area of the bed,

$$a = \frac{1}{S} + \frac{6 \times (1 - \epsilon)}{\xi dp} \quad (\text{A.5})$$

$$\xi = 0.59 \text{ (Appendix 2)}$$

Assume $\xi = 0.75$ [54]

$$\begin{aligned} a &= \frac{1}{0.3} + \frac{6(1 - 0.59)}{0.75 \times 0.09} \\ &= 9.41 \text{ c.m}^{-1} \end{aligned}$$

Superficial velocity of the liquid,

$$\begin{aligned} u &= \frac{0.8 \text{ l/min}}{5 \text{ l} \times 0.3 \text{ cm}^2} \times 10^3 \text{ cm}^3/\text{l} \times \frac{1 \text{ min}}{60 \text{ sec}} \\ &= 8.89 \text{ cm/s} \end{aligned}$$

$$D_{2,3\text{-Xylenol}} = 7.0 \times 10^{-6} \text{ cm}^2/\text{s} \quad [\text{Table V}]$$

$$D_{\text{resorcinol}} = 8.3 \times 10^{-6} \text{ cm}^2/\text{s} \quad [\text{Table V}]$$

(see Section 2, Appendix 4 for calculation of diffusivity values)

$$Re = \frac{Udp}{\nu} = \frac{8.89 \text{ cm/s} \times 0.09 \text{ cm}}{0.01 \text{ cm}^2/\text{s}} = 80$$

consider group-4

$$Sc = \frac{\nu}{D} = \frac{0.01 \text{ cm}^2/\text{s}}{7.0 \times 10^{-6} \text{ cm}^2/\text{s}} = 1429$$

expanding eq. A.4,

$$\frac{k_m dp}{D} = 0.66 \left[\frac{udp}{\nu} \right]^{0.56} \left[\frac{\nu}{D} \right]^{0.33}$$

$$\begin{aligned} k_m &= 0.66 \times \frac{7.0 \times 10^{-6}}{0.09} \times 80^{0.56} \times 1429^{0.33} \\ &= 6.61 \times 10^{-3} \text{ cm/s} \end{aligned}$$

The lower limit of k_m is obtained from eq. A.5 as follows

$$\begin{aligned} k_m &= 0.62 \times \frac{7.0 \times 10^{-6}}{0.09} \times 80^{0.56} \times 1429^{0.33} \\ &= 6.19 \times 10^{-3} \text{ cm/s} \end{aligned}$$

Therefore k_m ranges from $6.61 \times 10^{-3} \text{ cm/s}$ to $6.19 \times 10^{-3} \text{ cm/s}$

$$Q = \frac{k_m aL}{u} = \frac{k_m \cdot 9.41 \text{ cm}^{-1} \cdot 38 \text{ cm}}{8.89 \text{ cm/s}}$$

The extreme values of Q would therefore be

$$Q_1 = 0.25$$

$$Q_2 = 0.27$$

The 2,3-Xylenol fraction conversion for mass transfer is given by

$$X = 1 - \exp [\{ \exp (-Q) - 1 \} t^* - Q]$$

$$t^* = t/t_m$$

$$t_m = \frac{5 \text{ l}}{0.8 \text{ l/min}} = 6.250 \text{ min}$$

The range of theoretical fractional conversion for mass transfer control at various time intervals are shown in Table A-1.

TABLE A-1

Theoretical 2,3-Xylenol fractional conversion vs time for a mass transfer controlled batch system

t(min)	t [*]	X ₁	X ₂
0	0	0.22	0.24
15	2.4	0.54	0.57
30	4.8	0.73	0.76
45	7.2	0.84	0.86
60	9.6	0.91	0.92
75	12.0	0.94	0.96
90	14.4	0.97	0.98
105	16.8	0.98	0.99
120	19.2	0.99	0.99

Similar treatment for group 6 experiments

$$Sc = \frac{0.01 \text{ cm}^2/\text{s}}{8.3 \times 10^{-6} \text{ cm}^2/\text{s}} = 1204$$

$$k_m = 9.25 \times 10^{-3} \text{ cm/s}$$

$$Q_1 = 0.28$$

$$Q_2 = 0.30$$

The resorcinol fractional conversion for mass transfer control is shown in Table A-2.

TABLE A-2

Theoretical resorcinol fractional conversion vs time for a mass transfer controlled batch system

t(min)	t [*]	x ₁	x ₂
0	0	0.24	0.26
15	2.4	0.58	0.60
30	4.8	0.76	0.79
45	7.2	0.87	0.89
60	9.6	0.92	0.94
75	12.0	0.96	0.97
90	14.4	0.98	0.98
105	16.8	0.99	0.99
120	19.2	0.99	0.99

APPENDIX 4

Calculations1. C.O.D. analysis - sample calculations (run 8-3)

Sample Description	Dilution (if any)	Titre-FAS (ml)	Blank-Sample (ml)	COD (mg/l)	Average COD (mg/l)
Initial sample (t=0 min)	10	14.2	11.2	4310	4291
	10	14.3	11.1	4271	
Final sample (t=300 min)	10	16.2	9.2	3540	3502
	10	16.4	9.0	3463	

i.e. 18.4% reduction in C.O.D.

Titre-FAS (in ml) Values for the Blank and Standard Samples

	Blank Sample	Standard Sample
	25.45	26.00
	25.35	26.00
Average:	25.4	26.00

For the standard sample values,

$$N_{\text{FAS}} = \frac{2.5}{\text{Titre-FAS (ml)}} = \frac{2.5}{26.0} = 0.0961$$

$$\begin{aligned} \text{Factor} &= \frac{N_{\text{FAS}} \times 8000 \times \text{Dilution factor (if any)}}{\text{Sample volume (ml)}} \\ &= \frac{0.0962 \times 8000 \times 10}{20} = 384.8 \end{aligned}$$

$$\text{C.O.D. (mg/l)} = \text{Factor} \times \text{Blank-Sample}$$

2. Calculation of diffusivity of phenolics

The diffusivity of the phenolics were calculated by using the relationship of Wilke and Change [55]

$$D_{12}^0 = \frac{7.4 \times 10^{-8} (\phi M_2)^{\frac{1}{2}} T}{\mu_2 V_1^{0.6}}$$

where D_{12}^0 = mutual diffusion of solute 1 in solvent 2 at very low solute concentration, cm^2/sec

ϕ_x^* = "association parameter" of solvent [11]

M_2 = molecular weight of solvent

T = temperature, K

μ_2 = viscosity of solution (solvent), cp

V_1 = molal volume of the solute at its normal boiling point
in $\text{cm}^3/\text{g mole}$

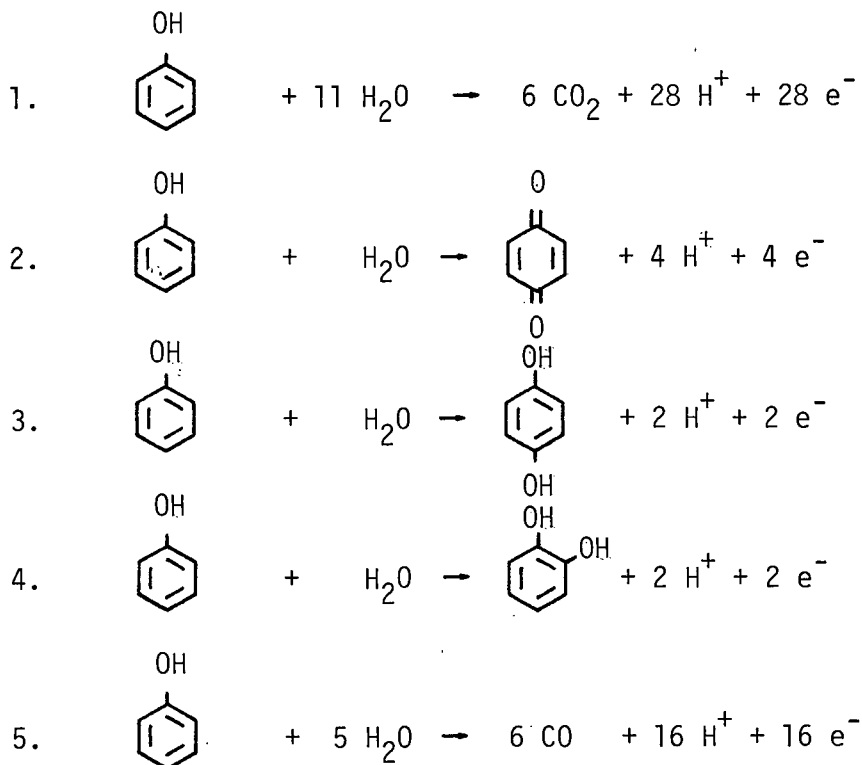
$$\begin{aligned} D_{12 \text{ phenol}}^0 &= \frac{7.4 \times 10^{-8} (2.26 \times 18)^{\frac{1}{2}} \times 297}{1 \times (105)^{0.6}} \quad (\text{refer to p. 87, ref. 55}) \\ &= 8.5 \times 10^{-6} \text{ cm}^2/\text{s} \end{aligned}$$

* Improved value of association parameter put forth by Hayduk and Laudie [56] has been used.

Note: D_{12}^0 Xylenols calculated at 40°C

3. Calculation of current efficiency for a typical phenol run

The stoichiometry of the predominant processes which occurs in the oxidation of phenol (run 9-1) are as follows



Consider a carbon balance.

Amount of phenol oxidized = (975-105) = 870 mg/l

Results from GC/MS analysis of final sample

	%
Phenol	12.6
Benzoquinone	69.5
Hydroquinone	10.9
Catechol	7.0

Actual quantity of phenol = 105 mg/l

Actual quantity of benzoquinone = 579.2 mg/l

Actual quantity of hydroquinone = 90.8 mg/l

Actual quantity of catechol = 58.3 mg/l

$$\begin{aligned}\text{Conc. of organic carbon in starting solution} &= \frac{71.4}{93.3} \times 975 \\ &= 746.1 \text{ mg/l}\end{aligned}$$

conc. of organic carbon in the products

$$\begin{aligned}&= 105 \times \frac{71.4}{93.3} + 579.2 \times \frac{71.4}{107.4} + (90.8 + 58.3) \frac{71.4}{109.4} \\ &= 562.7 \text{ mg/l}\end{aligned}$$

conc. of organic carbon that left the solution

(from T.O.C. analysis) = 29.8 mg/l

conc. of organic carbon unaccounted from carbon balance = 153.6 mg/l = (21%)

Calculation of current efficiency

% C.E.* for the formation of benzoquinone

$$\begin{aligned}&= \frac{579.2 \text{ mg/l} \times 5 \text{ l} \times \frac{1 \text{ g mole}}{107.4 \text{ g}} \times \frac{1 \text{ g}}{10^3 \text{ mg}} \times 96500 \text{ coul/eq} \times 4 \text{ eq/mole} \times 100}{10 \text{ A} \times 120 \text{ min} \times \frac{60 \text{ sec}}{\text{min}}} \\ &= 14.5\end{aligned}$$

% C.E. for formation of catechol and hydroquinone

$$\begin{aligned}&= \frac{149.1 \text{ mg/l} \times 5 \text{ l} \times \frac{1 \text{ g mole}}{109.4} \times \frac{1 \text{ g}}{10^3 \text{ mg}} \times 96500 \text{ coul/eq} \times 2 \text{ eq/mole} \times 100}{10 \text{ A} \times 120 \text{ min} \times \frac{60 \text{ sec}}{\text{min}}}\end{aligned}$$

$$* \% \text{ C.E.} = \frac{F Z (\text{moles oxidized}) \times 100}{It}$$

$$= 1.83$$

% C.E. for the formation of CO_2

[Assume 100% conversion to CO_2]

$$= \frac{29.8 \text{ mg/l} \times 5 \text{ l} \times \frac{1 \text{ g mole}}{12 \text{ g}} \times \frac{1 \text{ g}}{10^3 \text{ mg}} \times 96500 \text{ coul/eq} \times 28 \text{ eq/mole} \times 100}{10 \text{ A} \times 120 \text{ min} \times \frac{60 \text{ sec}}{\text{min}}}$$

$$= 46.6$$

% C.E. for the formation of CO

Assume 100 % conversion to CO

$$= \frac{29.8 \text{ mg/l} \times 5 \text{ l} \times \frac{1 \text{ g mole}}{12 \text{ g}} \times \frac{1 \text{ g}}{10^3 \text{ mg}} \times 96500 \text{ coul/eq} \times 16 \text{ eq/mole} \times 100}{10 \text{ A} \times 120 \text{ min} \times \frac{60 \text{ sec}}{\text{min}}}$$

$$= 26.6$$

Total current efficiency = 42.9 - 62.9

depending on $\text{CO}:\text{CO}_2^*$

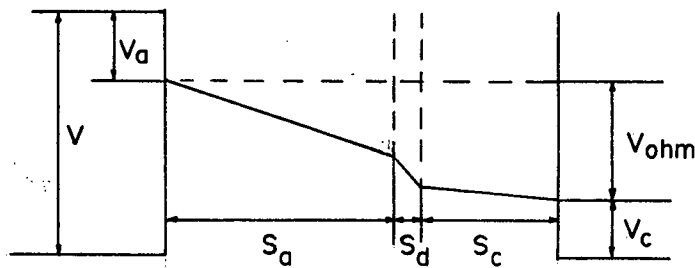
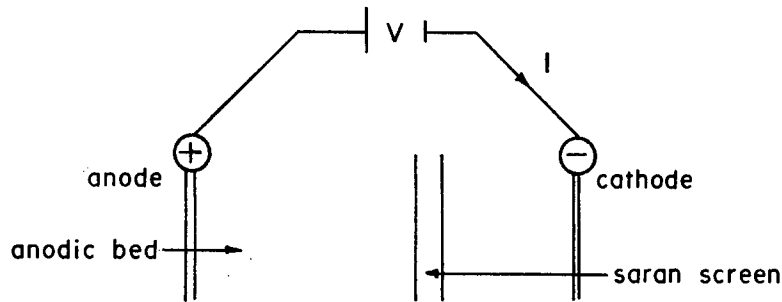
*Gas analysis by G.C. corresponding to the time of collection of the final sample was as follows: $\%\text{H}_2$, 68.42; $\%\text{CO}_2$, 6.54; $\%\text{O}_2$, 24.73; $\%\text{CO}$, 0.31

$\text{CO}:\text{CO}_2$ was found to vary as follows

1:7.4 (after 90 minutes of oxidation)

1:21.0 (after 120 minutes of oxidation)

4. Calculation of V_{ohm} in the electrolyte



$$V_{ohm} = i \cdot r_a \cdot S_a + i \cdot r_d \cdot S_d + i \cdot r_c \cdot S_c + V_L$$

where V_L is the liquid function potential

The last two factors are negligible. $i r_d S_d$ would depend on the quantity of gas evolved and type of screen.

Consider $i r_a S_a$ across the bed. It can be approximated as follows.

$$v_a = \frac{1}{K_{electrolyte}} + \frac{1}{K_{ebed}}$$

$$\frac{1}{K_{ebed}} \approx 0 \text{ (due to the high conductivity of bed)}$$

Average conductivity of the electrolyte [31] = $0.895(\Omega m)^{-1}$

$$\frac{1}{K_{electrolyte}} = 1.12 \text{ ohm.m}$$

$$\begin{aligned}V_{\text{ohm}} (5 \text{ A runs}) &= 263.2 \text{ A/m}^2 \times 1.12 \text{ ohm m} \times 0.003 \text{ m} \\&= 0.88 \text{ volts}\end{aligned}$$

$$\begin{aligned}V_{\text{ohm}} (10 \text{ A runs}) &= 526.3 \text{ A/m}^2 \times 1.12 \text{ ohm.m} \times 0.003 \text{ m} \\&= 1.77 \text{ volts}\end{aligned}$$

$$\begin{aligned}V_{\text{ohm}} (15 \text{ A runs}) &= 789.5 \text{ A/m}^2 \times 1.12 \text{ ohm.m} \times 0.003 \text{ m} \\&= 2.65 \text{ volts}\end{aligned}$$

APPENDIX 5

Relevant Physical dataACTUAL COMPOSITION OF SYNTHETIC COAL
CONVERSION WASTEWATER OUTLINED IN
TABLE I

<u>Compound</u>	<u>Concentration, mg/l</u>
1. Phenol	2000
2. Resorcinol	1000
3. Catechol	1000
4. Acetic Acid	400
5. o-Cresol	400
6. p-Cresol	250
7. 3,4-Xylenol	250
8. 2,3-Xylenol	250
9. Pyridine	120
10. Benzoic Acid	100
11. 4-Ethylpyridine	100
12. 4-Methylcatechol	100
13. Acetophenone	50
14. 2-Indanol	50
15. Indene	50
16. Indole	50
17. 5-Methylresorcinol	50
18. 2-Naphthol	50
19. 2,3,5-Trimethylphenol	50
20. 2,-Methylquinoline	40

<u>Compound</u>	<u>Concentration, mg/l</u>
21. 3,5-Xylenol	40
22. 3-Ethylphenol	30
23. Aniline	20
24. Hexanoic Acid	20
25. 1-Naphthol	20
26. Quinoline	10
27. Naphthalene	5
28. Anthracene	0.1
29. $\text{MgSO}_4 \cdot 7\text{H}_2\text{O}$	22.5
30. CaCl_2	27.5
31. FeNaEDTA	0.34
32. NH_4Cl	3820
33. Phosphate buffer:	
KH_2PO_4	170
K_2HPO_4	435
$\text{Na}_2\text{HPO}_4 \cdot 7\text{H}_2\text{O}$	668